Stellarator Experiments

T. Windisch

MPI for Plasma Physics, Greifswald

IPP summer university 2016

Force balance

MHD force balance

$$\nabla p = \mathbf{j} \times \mathbf{B}$$

$$\mathbf{B} \cdot \nabla p = 0$$

$$\mathbf{j} \cdot \nabla p = 0$$

∇B**-drifts** $\rightarrow$ **twisting the field**

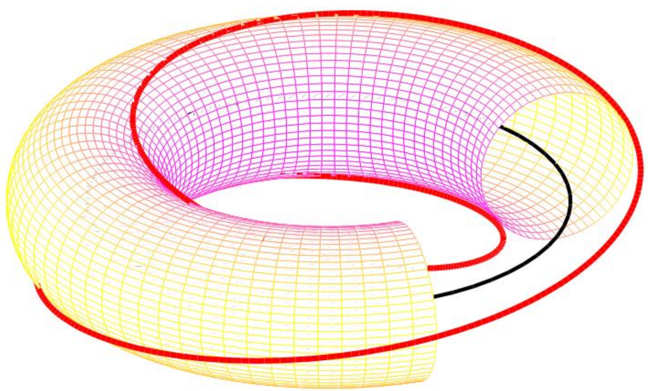

polodial projection: drift surfaces

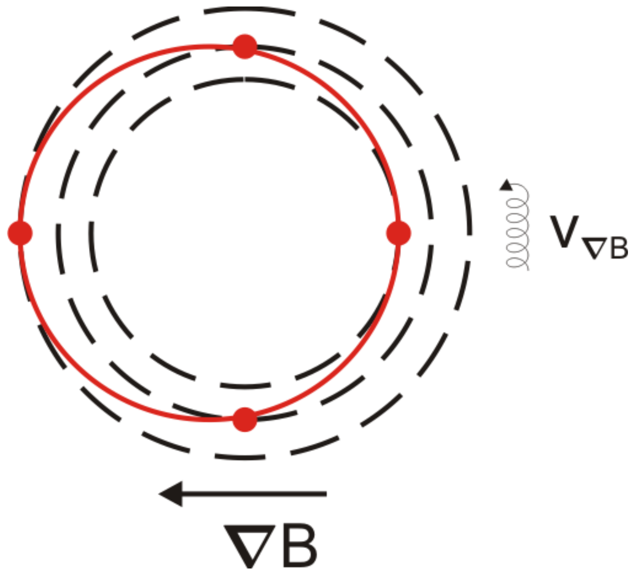

Rotational transform ι

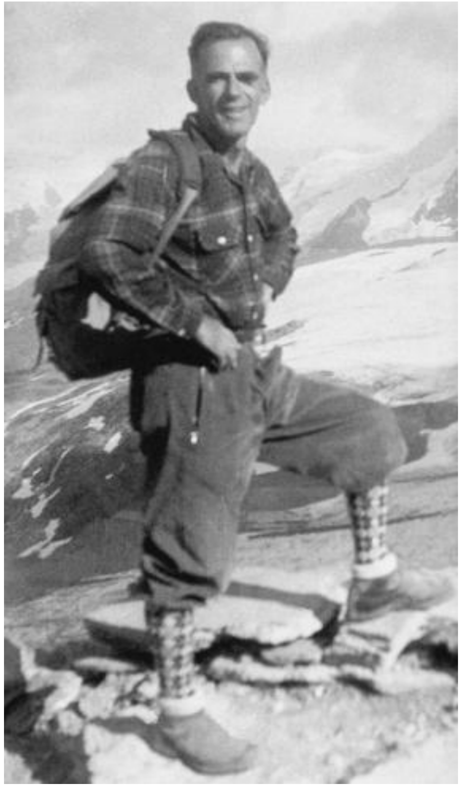

Lyman Spitzer Jr.

closed fieldline

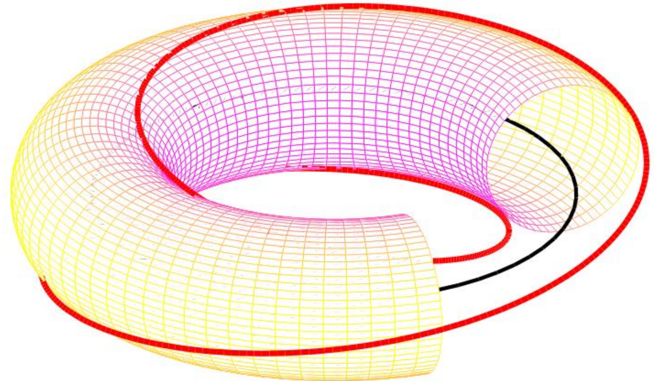

$$\frac{\iota}{2\pi} = \frac{1}{2}$$

ergodic coverage: flux surface

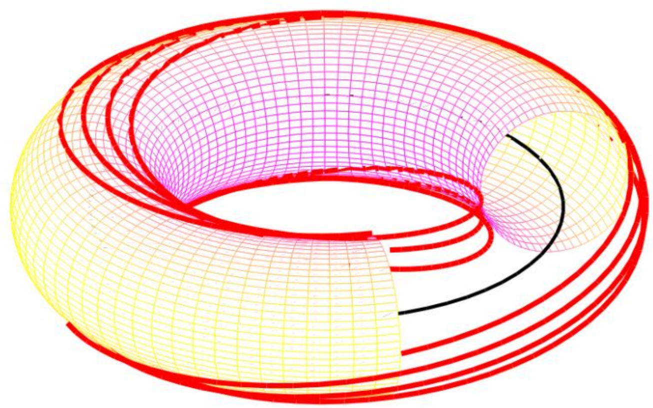

$$\frac{\iota}{2\pi} = \frac{1}{2.1}$$

Achieve the twist:

1. **non-planar magnetic axis**
2. **elongation and poloidal rotation of the flux surfaces (transverse magnetic field)**
3. **driving a toroidal current**

Figure-8 devices (PPPL)

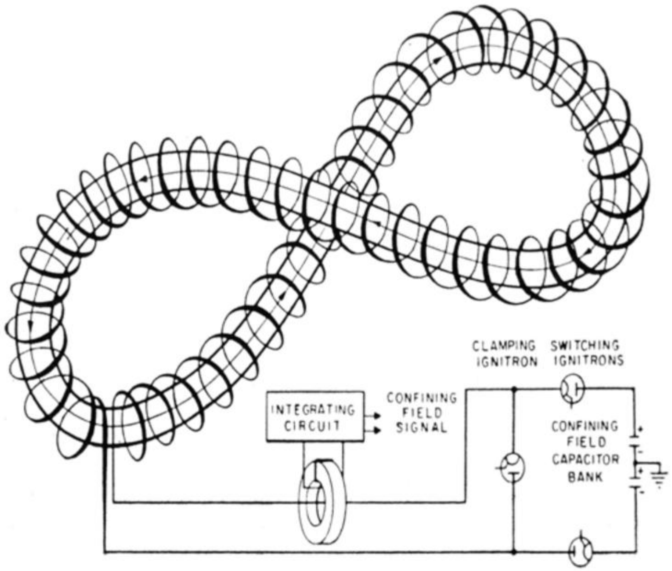

• **proposed by Spitzer (1951):** $\iota/2\pi = 0.5$

Model A Stellarator (*1953)

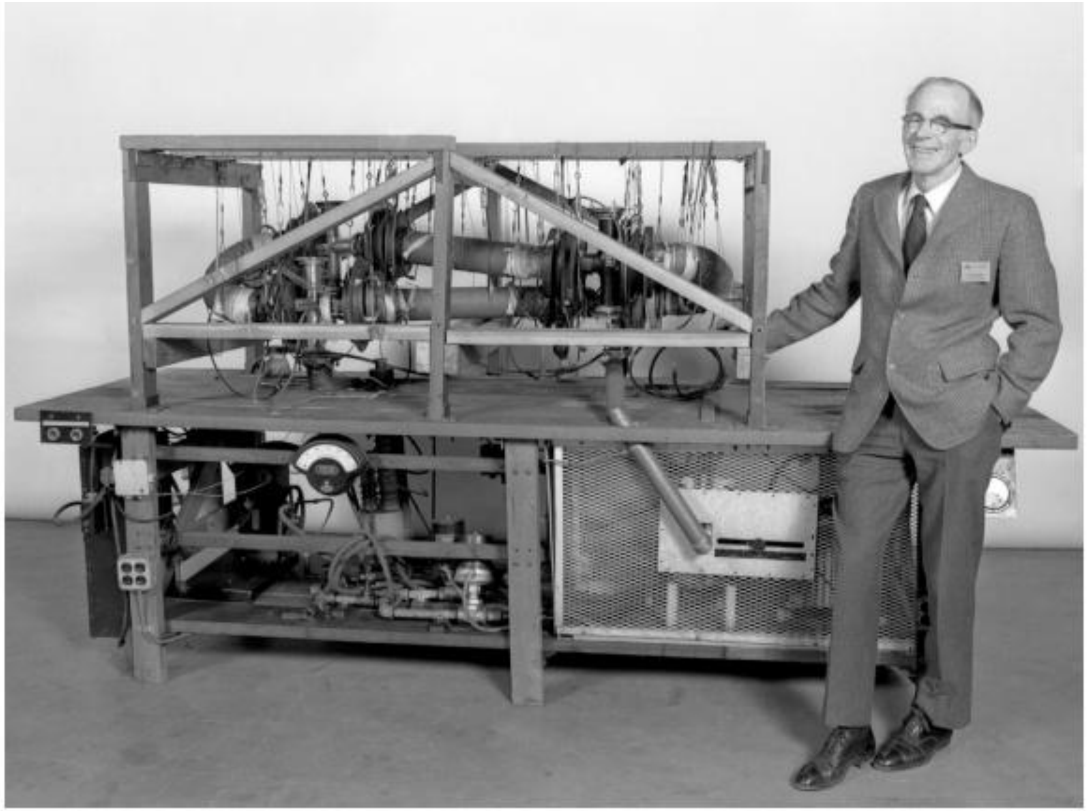

• **<u>but:</u> poor confinement**

Bohm diffusion $D \sim B^{-1}$

Classical l=2 stellarator

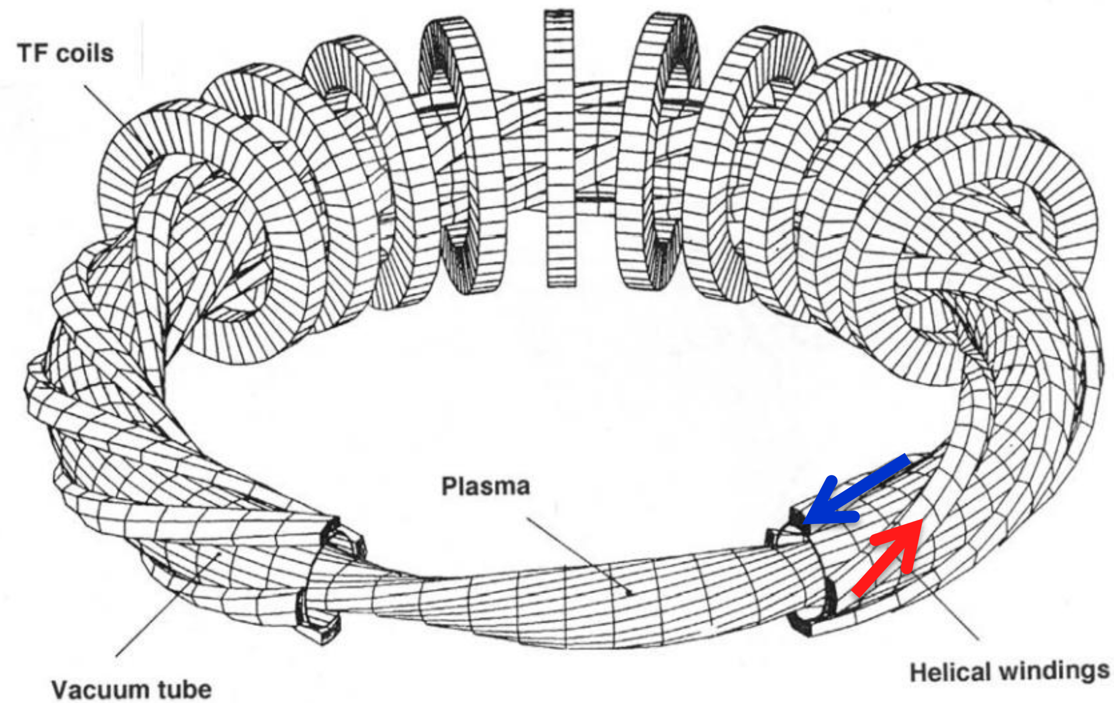

$$B/B_0 = 1 - \epsilon_t \cos\theta - \epsilon_h \cos(l\theta - M\phi)$$

- no net toroidal current in conductors
- no currents induced in the plasma
- strong forces between conductors may occur (size limit)

Classical l=2 stellarator

W2-B: R=0.5 m, a=0.09 m, M=5

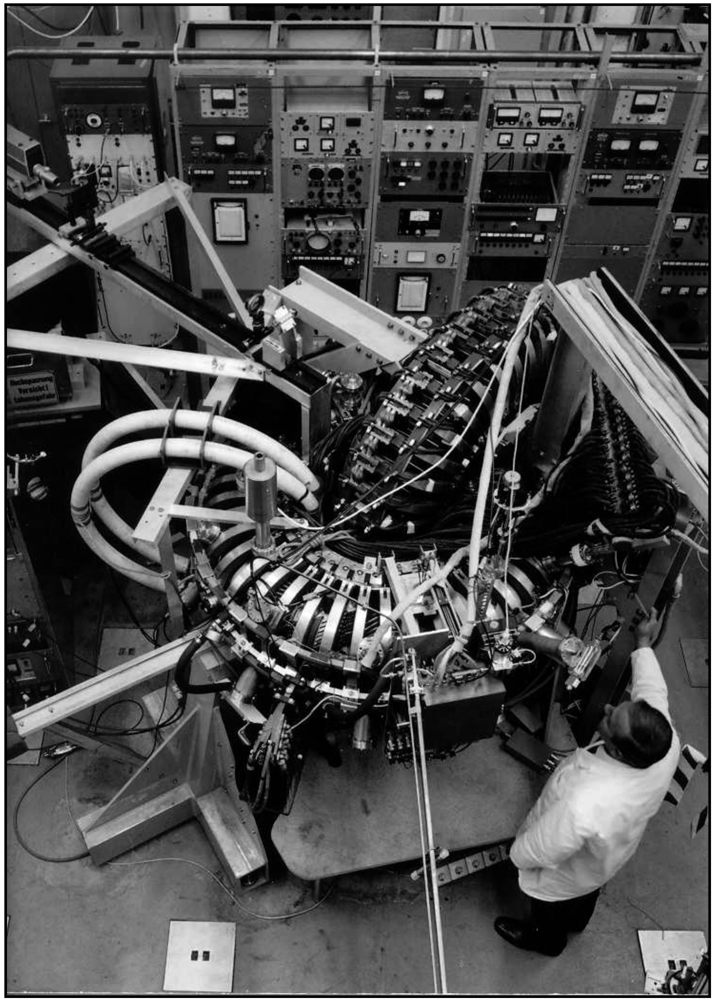

W7-A: R=2 m, a=0.1 m, M=5

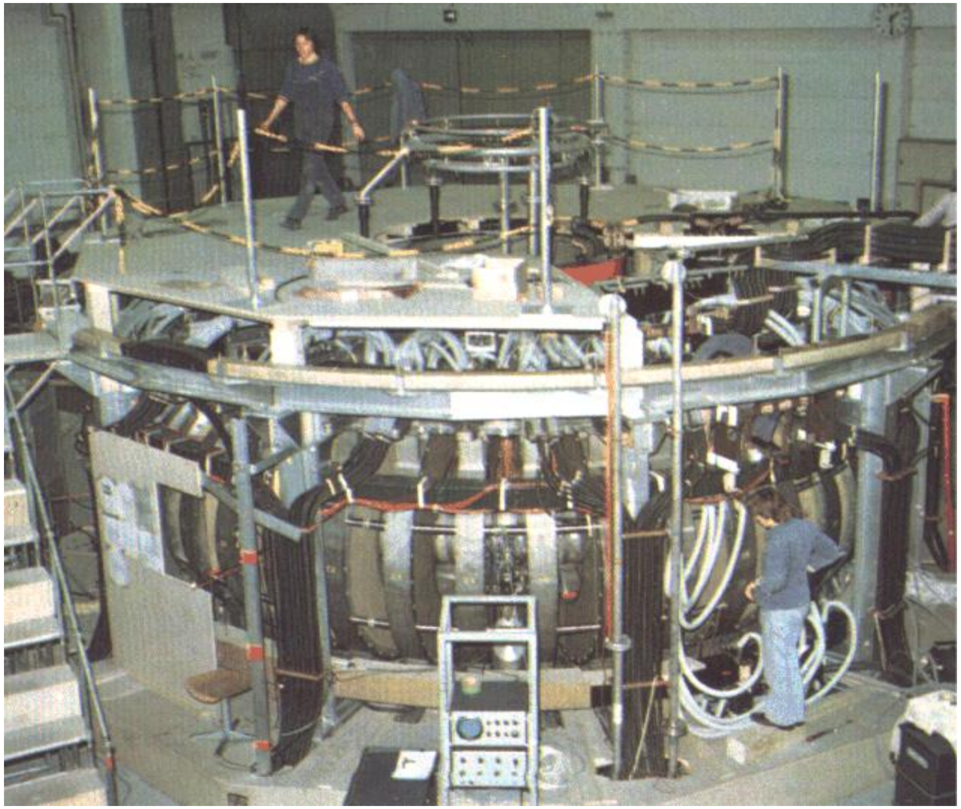

$T_e \leq 300\,\mathrm{eV}$

Heliotron / Torsatron

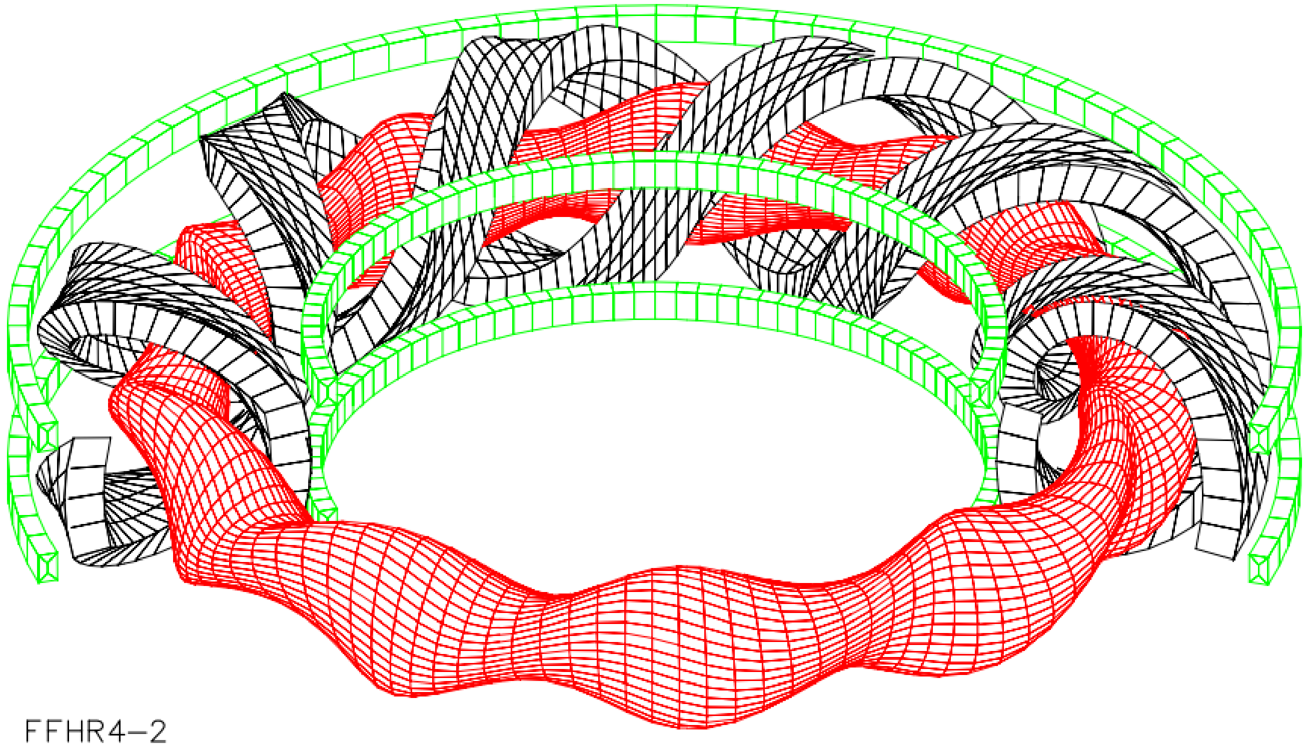

- l helical windings produce poloidal and toroidal field
- unidirectional currents
- vertical field due net toroidal current needs compensation

Heliotron LHD

- superconducting,
- magnetic axis can be shifted radially

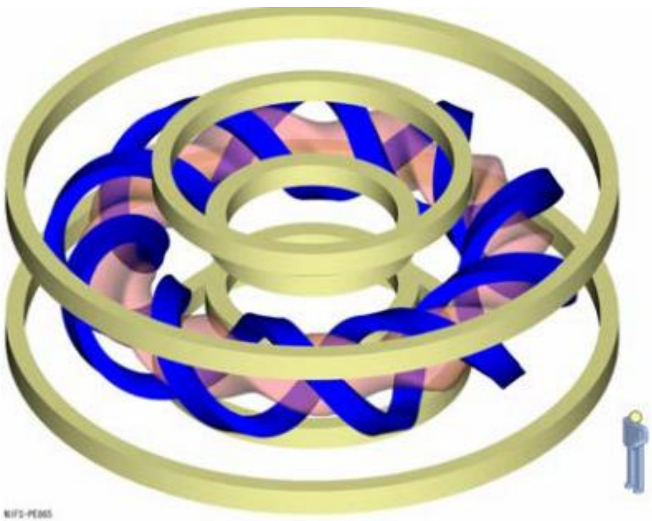

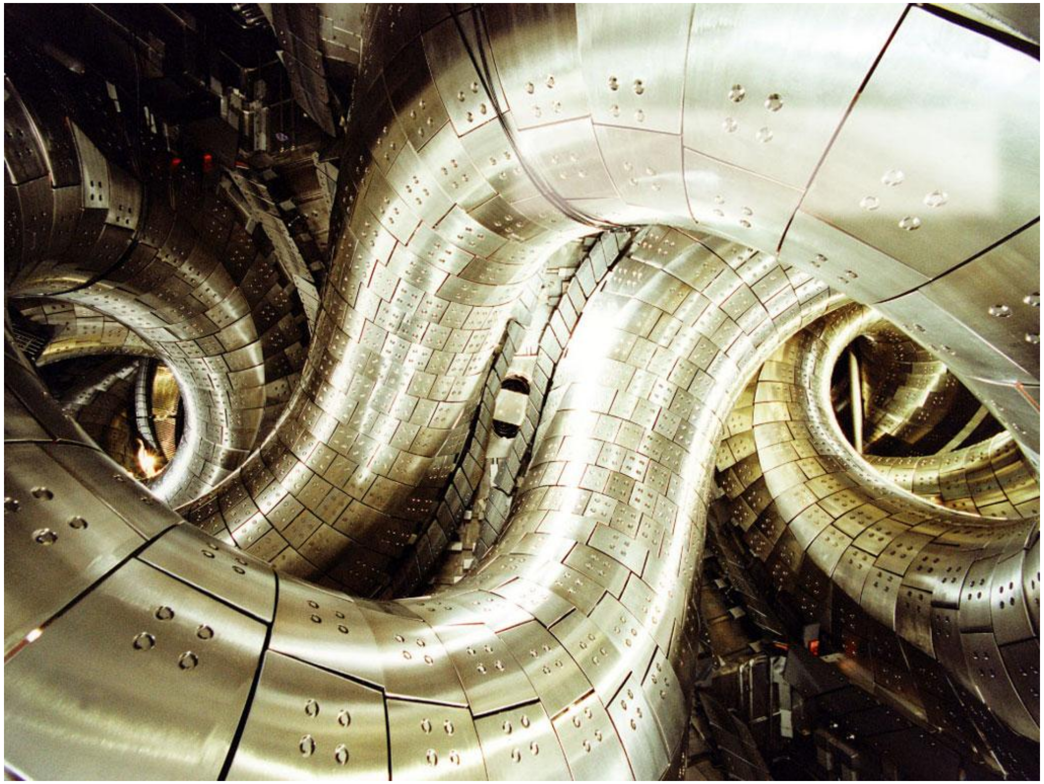

R [m]	a[m]	B [T]	M	A=R/a
3.9	< 0.6	< 4	10	6.5

Heliac

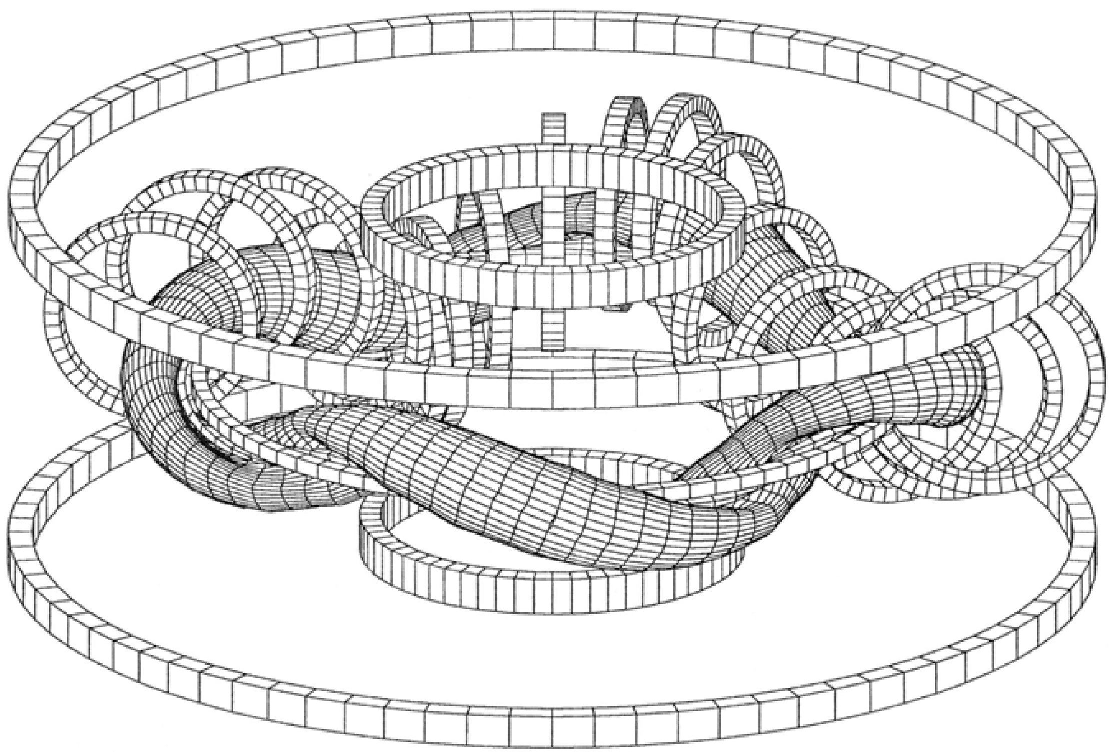

- 3D magnetic axis
- circular coils placed around a helical magnetic axis

Heliac TJ-II

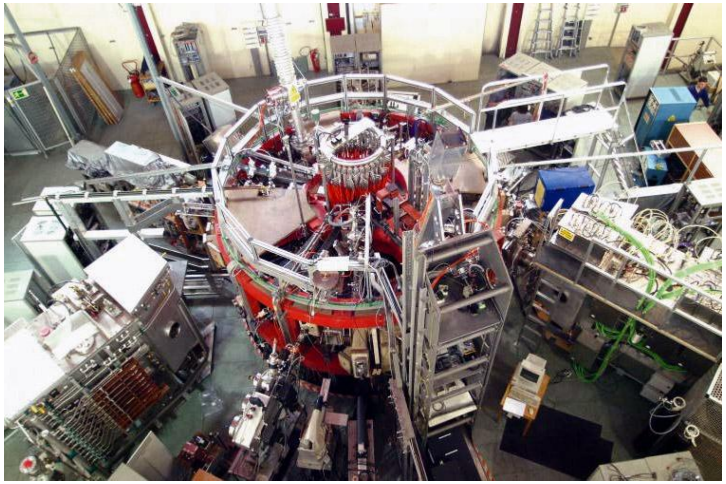

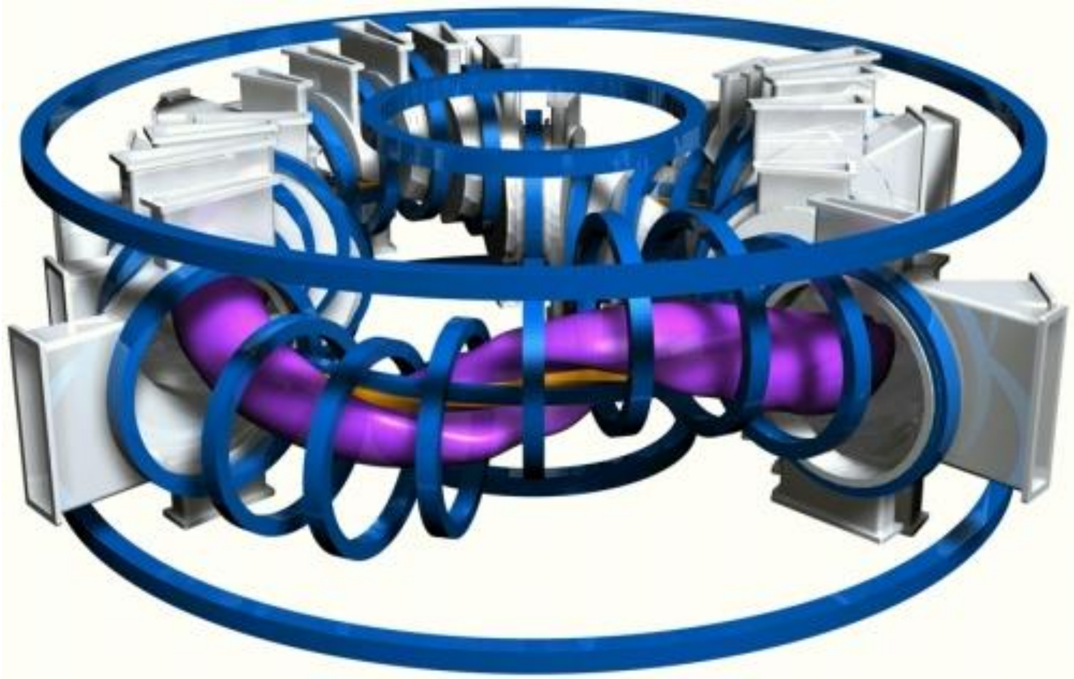

R [m]	a[m]	B [T]	M	A=R/a
1.5	0.22	< 1.2	4	6.8

Simple stellarators

Columbia Non-Neutral Torus (CNT)
Columbia University, New York, USA

Major radius:	R = 0.3 m
Minor radius:	a = 0.1 m
Magnetic field strength:	B = 0.2 T
Rotational transform	$\iota/2\pi$ = 0.2 - 0.6

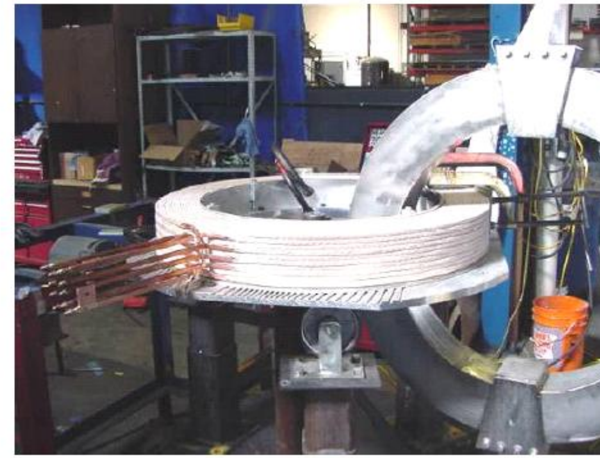

Fig. 2. The second internal coil at Alpha Magnetics after completion of winding, interlocked with the first internal coil.

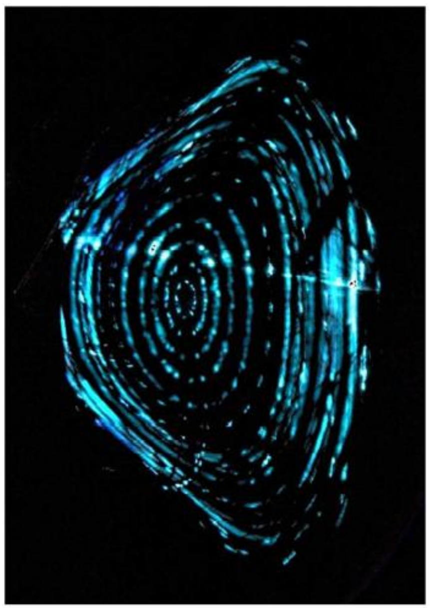

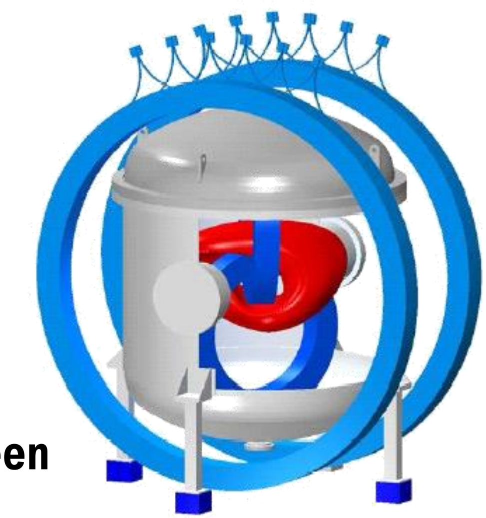

- adjustment of rotational transform by changing the angle between two inner coils
- plasma axis is twisted in space

The need for optimization

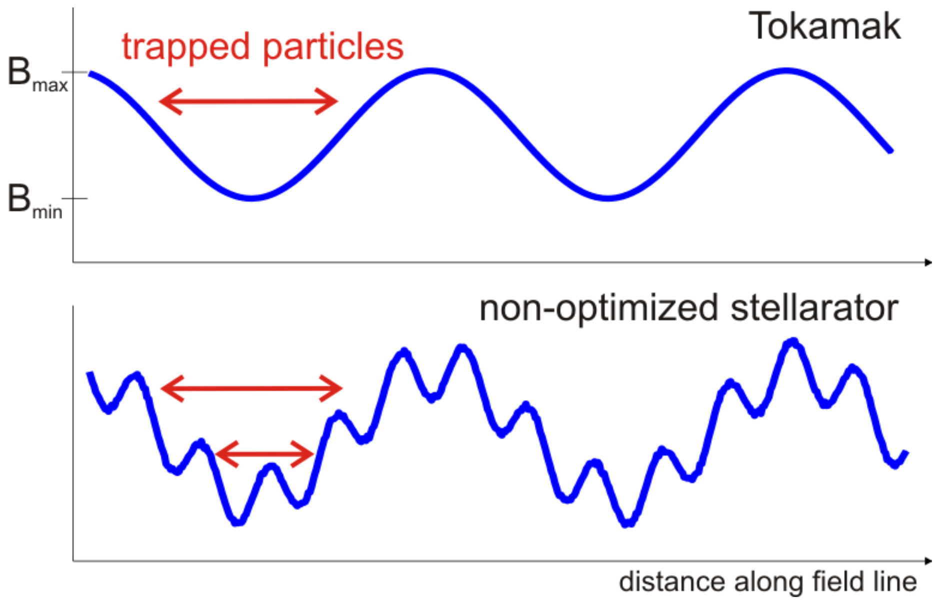

$$\frac{|v_{\|}|}{|v_{\perp}|} < \sqrt{\frac{B_{max}}{B_{min}} - 1}$$

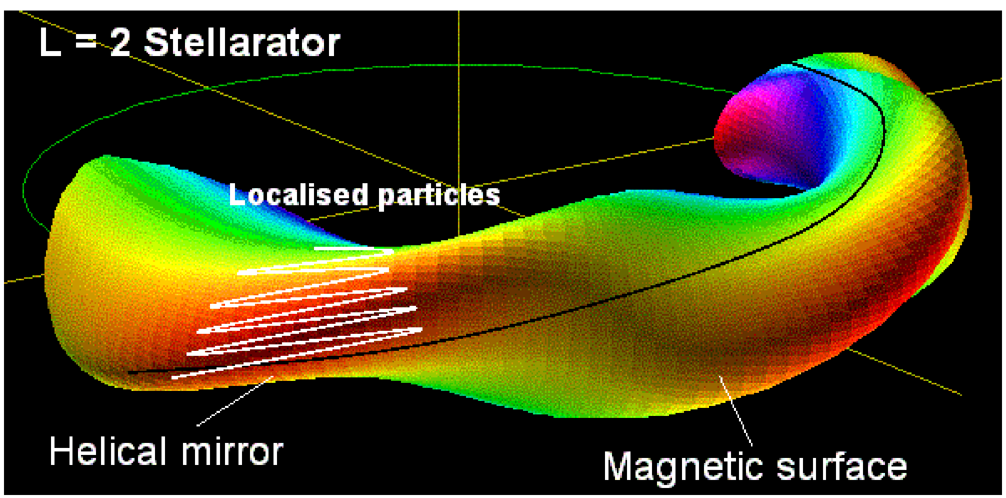

tokamak

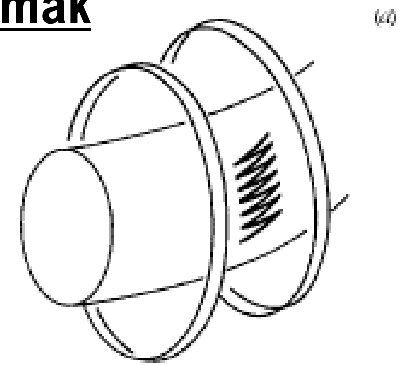

finite number of coils: small ripple

The need for optimization

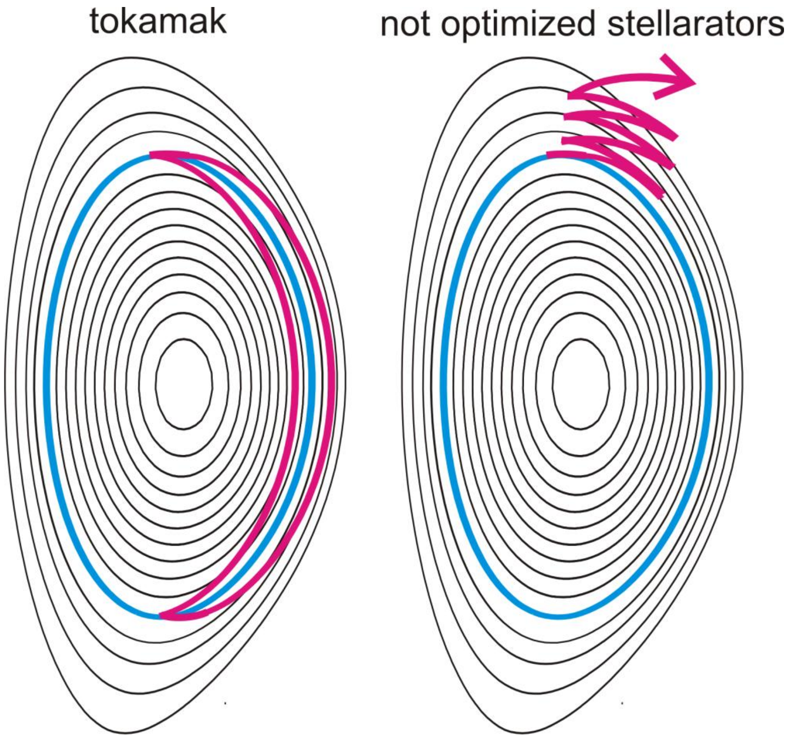

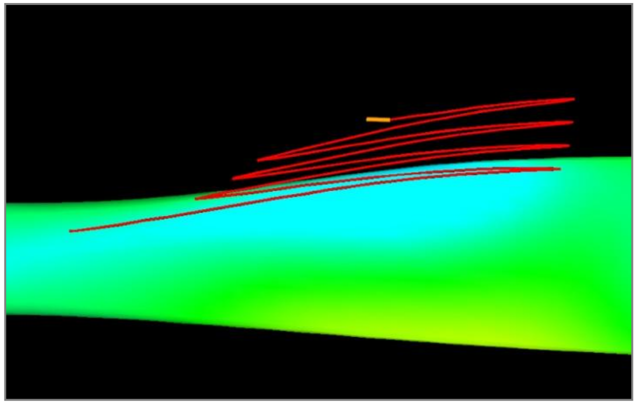

- fusion reactor: confinement of fast α – particles ?

- strategy: use freedom of 3D magnetic field to minimize drift

  - locate trapped particles in good curvature regions (have B_{max} at corners)

  - avoid isolated points of B_{max} and B_{min} on flux surface (closed curves)

Stellarator optimization philosophies

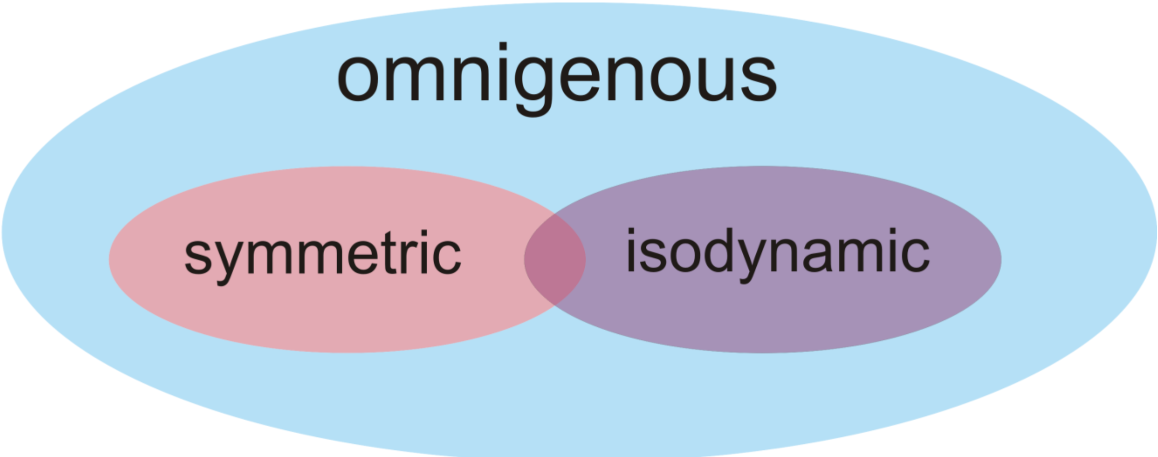

quasi-symmetric:

• accept pressure driven currents (bootstrap)

• add symmetry → conservation of can. momentum

• allows flows for turbulence reduction

quasi-isodynamic:

• stiff equilibria with increasing pressure

• reducing the poloidal variation of |B| → minimizes Pfirsch-Schlüter and bootstrap currents and $(B\times\nabla B)_r$-drift

Stellarator optimization

- **quasi-symmetric stellarators:**

$$B(\psi, \theta, \phi) = B(\psi, M\theta - N\phi)$$

quasi-helical symmetrix (HSX)

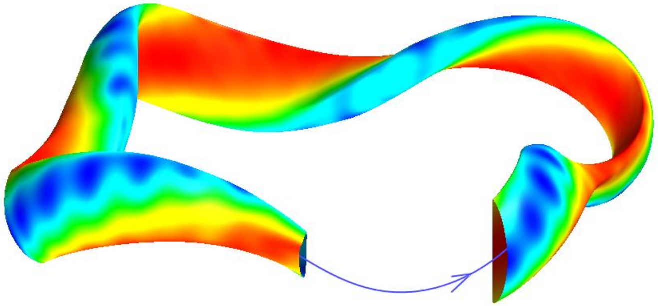

$N \neq 0, M \neq 0$

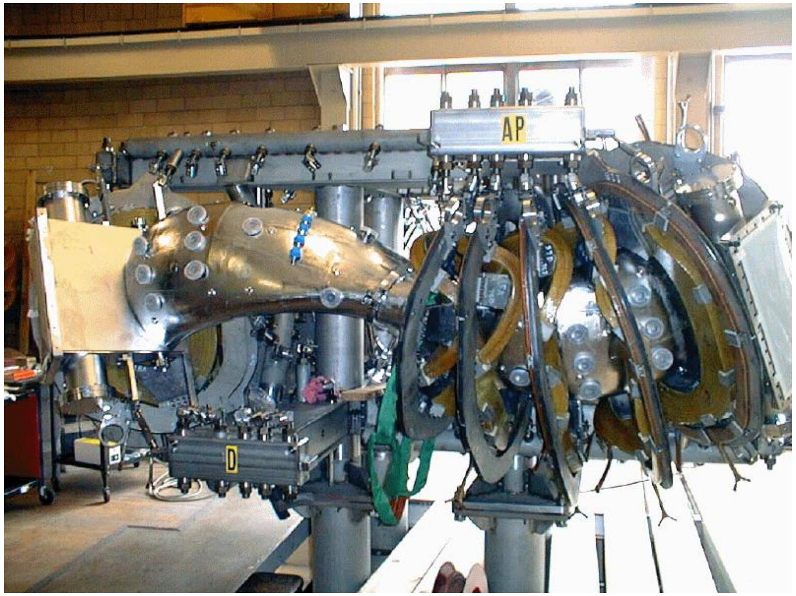

R [m]	a[m]	B [T]	M	A=R/a
1.2	< 0.15	0.5	4	8

Stellarator optimization

• **quasi-symmetric stellarators:**

$$B(\psi, \theta, \phi) = B(\psi, M\theta - N\phi)$$

quasi-axissymmetric (NSCX)

$N = 0$

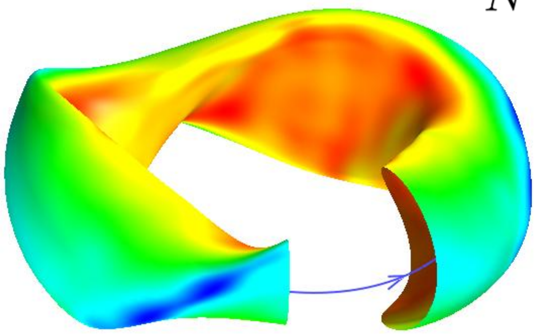

• 25% of transform from bootstrap current
• superconducting

R [m]	a[m]	B [T]	M	A=R/a
1.4	< 0.3	1.5	3	4.4

Stellarator optimization

•**quasi-isodynamic stellarators:**

W7-X

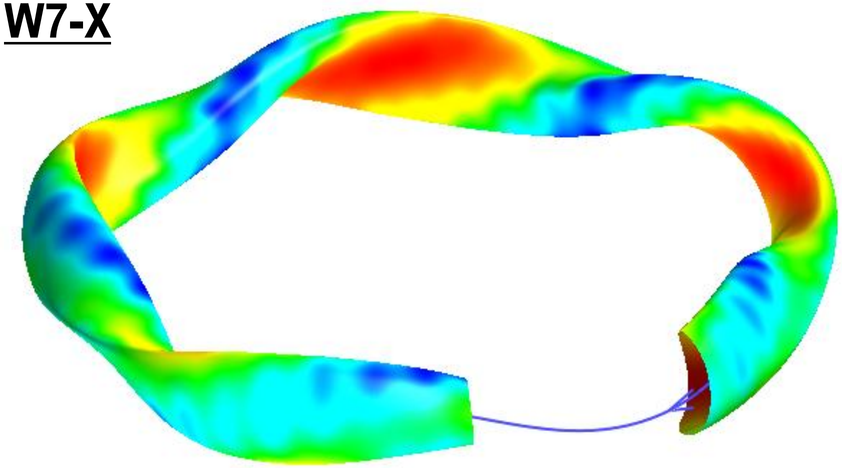

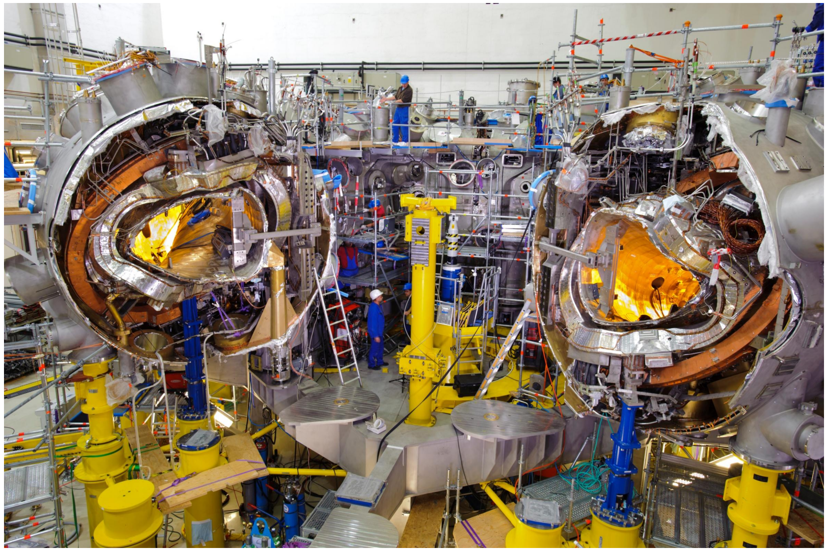

R [m]	a[m]	B [T]	M	A=R/a
5.5	0.5	< 3	5	11

B - contours in magnetic coordinates

tokamak | **stellarator w/o optimization** | **HSX** | **W7-X**

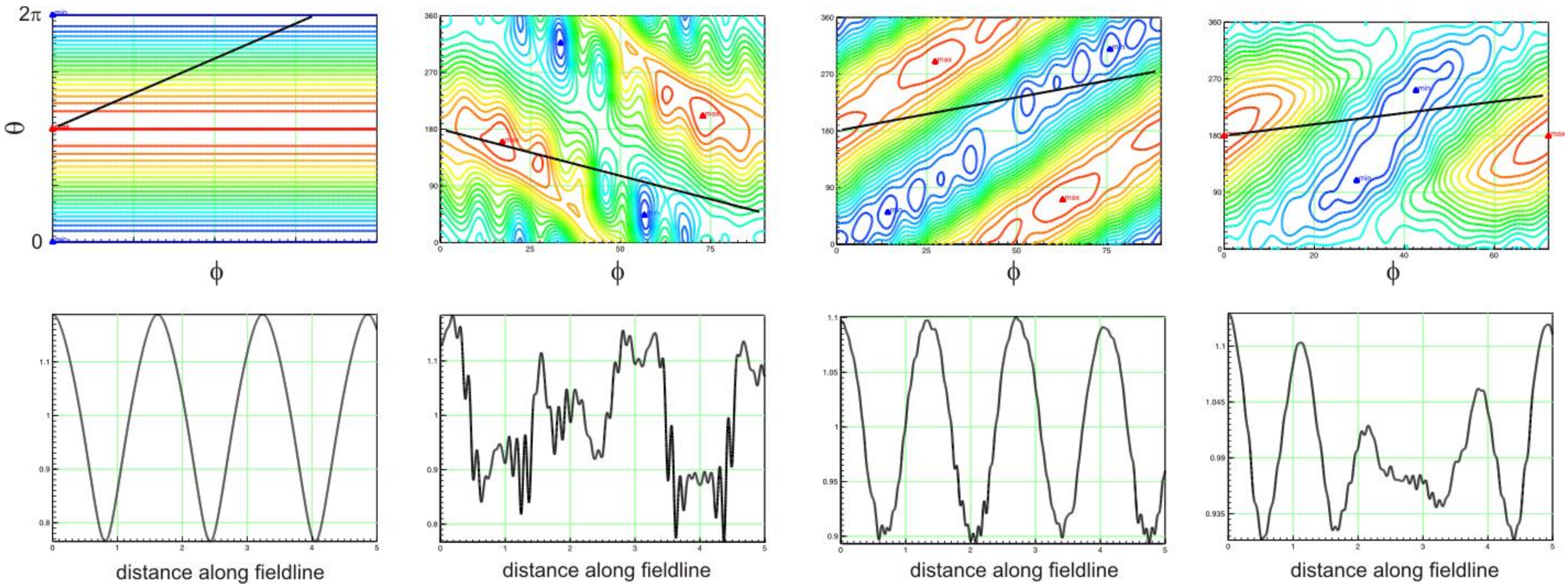

Concept of modular coils

Wobig, in: *Landolt-Börnstein*

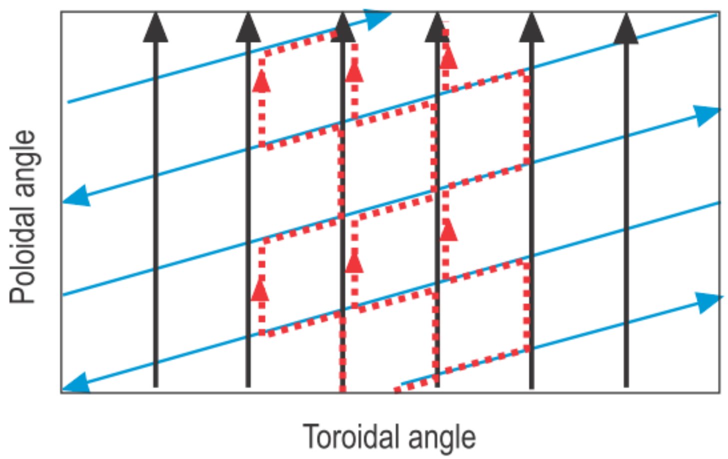

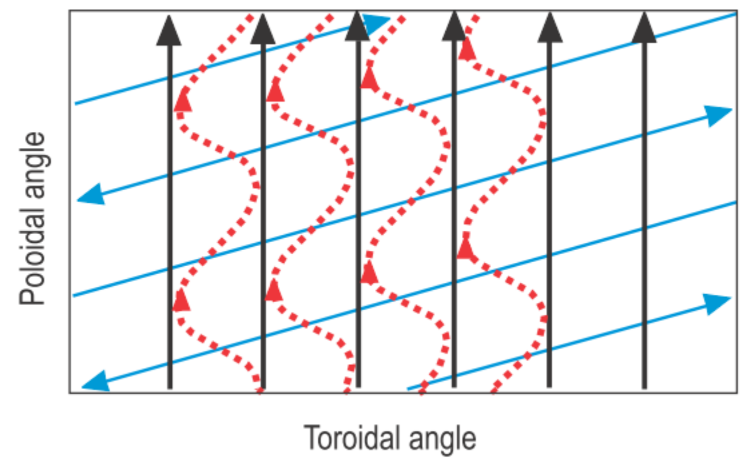

Helical windings
toroidal field coils

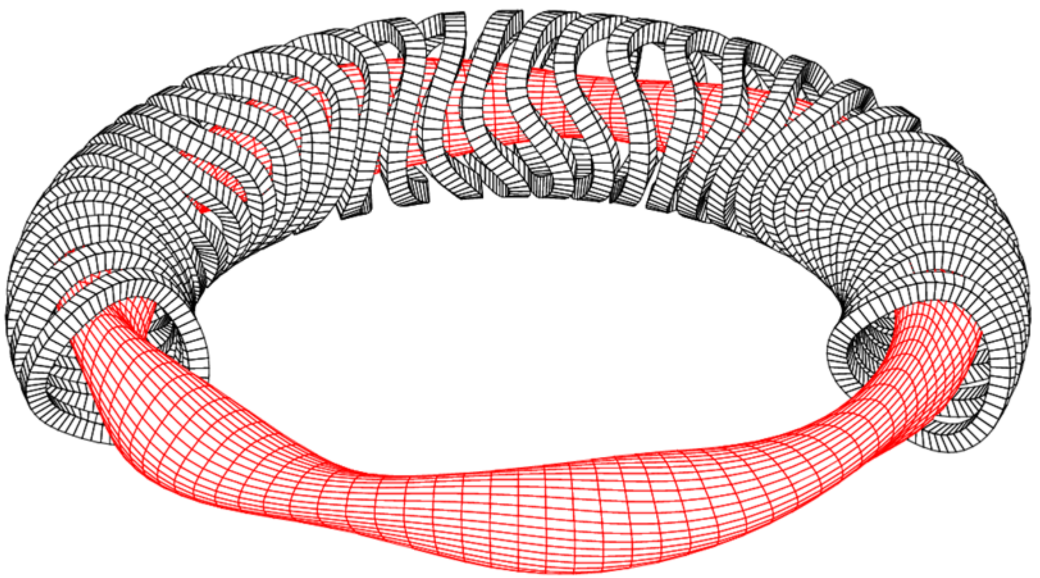

- **avoids large forces between helical coils**
- **forces remain in coil structure**
- **additional external coils allow flexible magnetic configuration**

W7-AS

• first modular stellarator

•first time in which desired magnetic configuration determined coil design

• additional planar coils allow flexible magnetic configuration

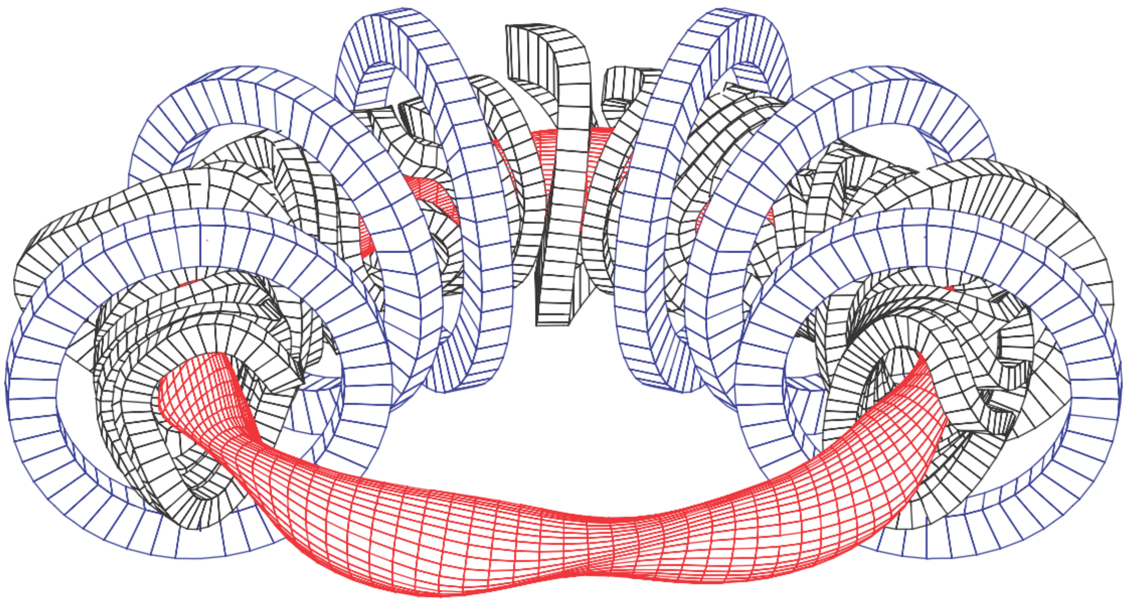

R [m]	a [m]	B [T]	M	A=R/a	V [m^3]
2	0.18	< 3	5	11	1

W7-X

• **demonstration of reactor capability of advanced stellarators**

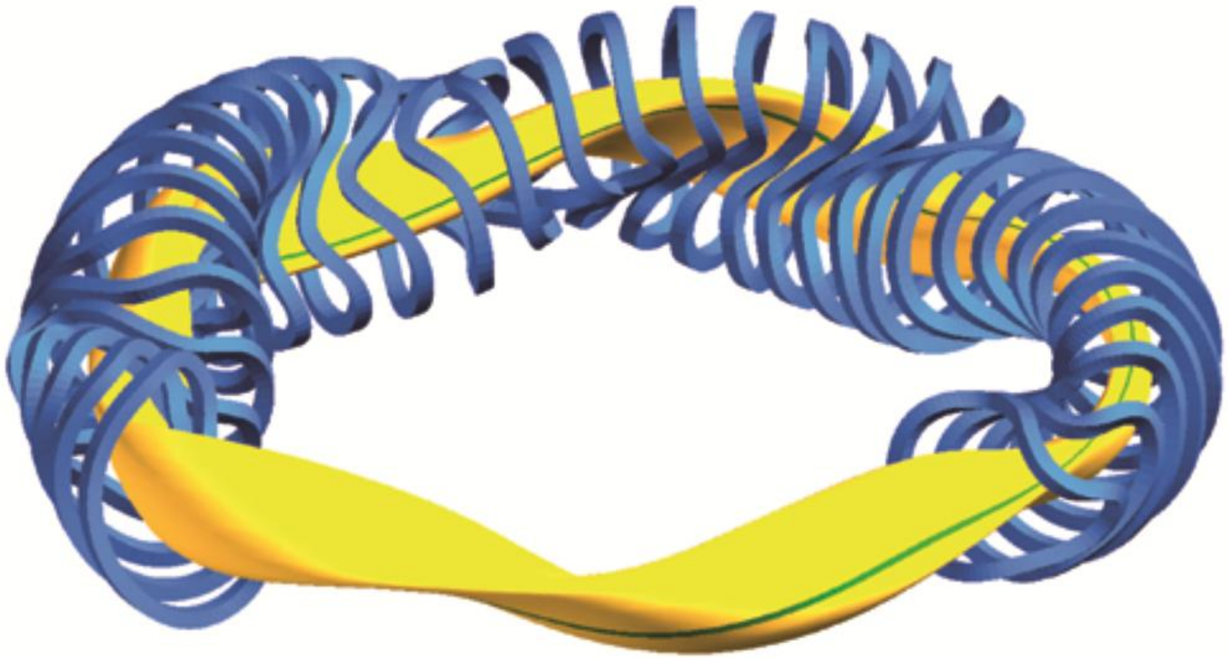

R [m]	a [m]	B [T]	M	A=R/a	V [m^3]
5.5	0.53	< 3	5	11	30

Vacuum magnetic field

field-line tracing (electron beam)

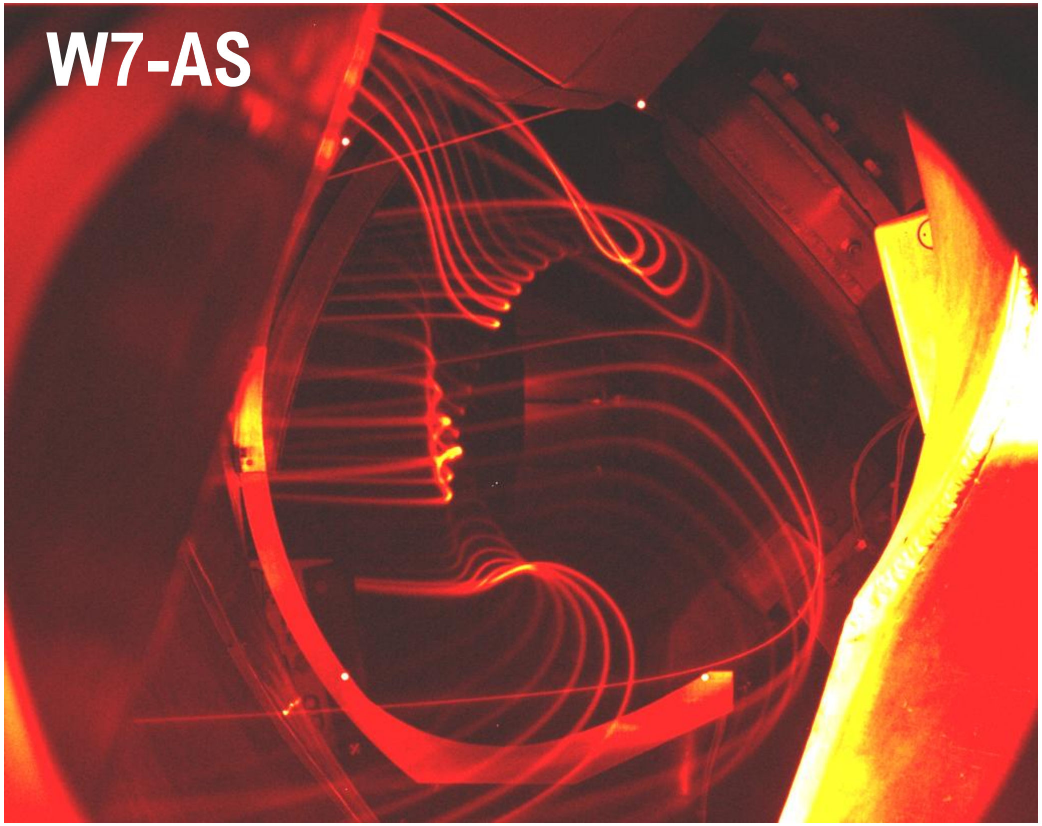

reconstructed flux-surfaces

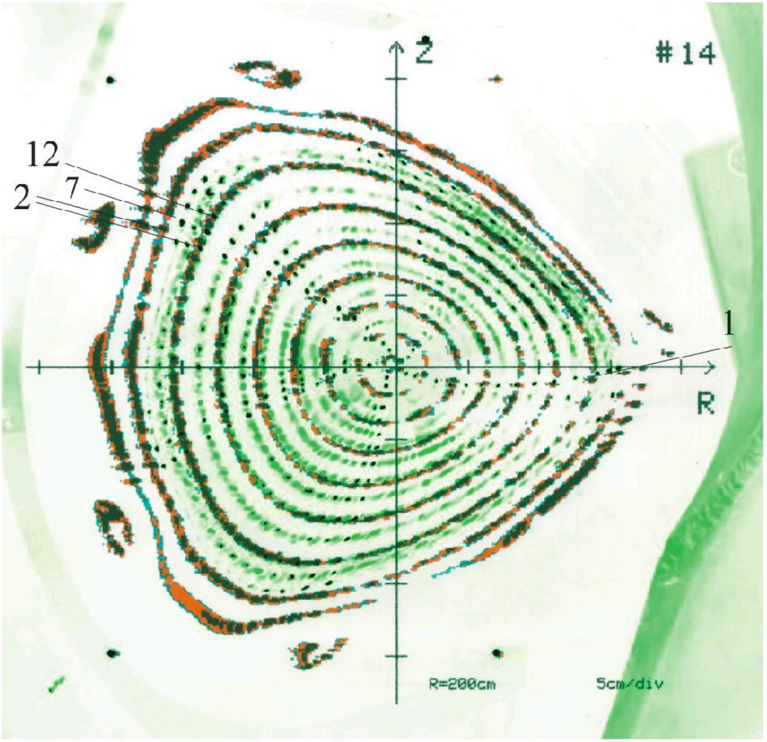

black: before operation

green: after 56000 discharges

Otte, Jaenicke, *Stell. News* (2006)

Magnetic islands

W7-AS

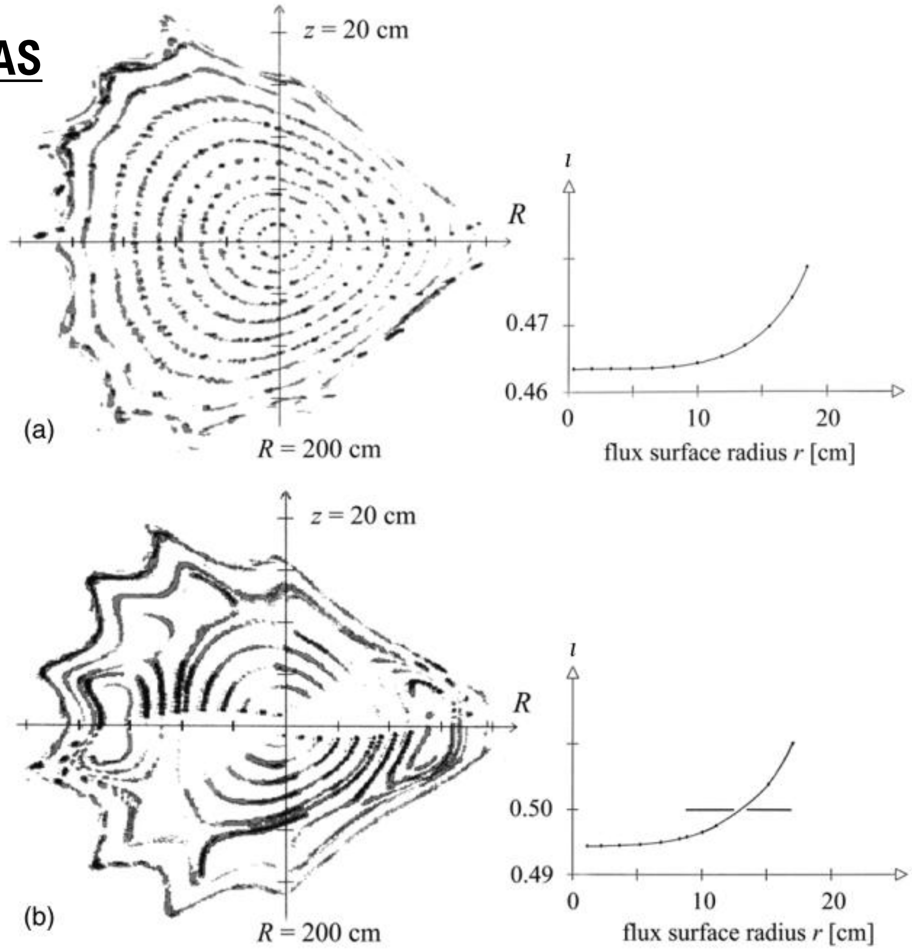

R. Jaenicke, *Nucl. Fusion* 33]

short-circuit of fluxes

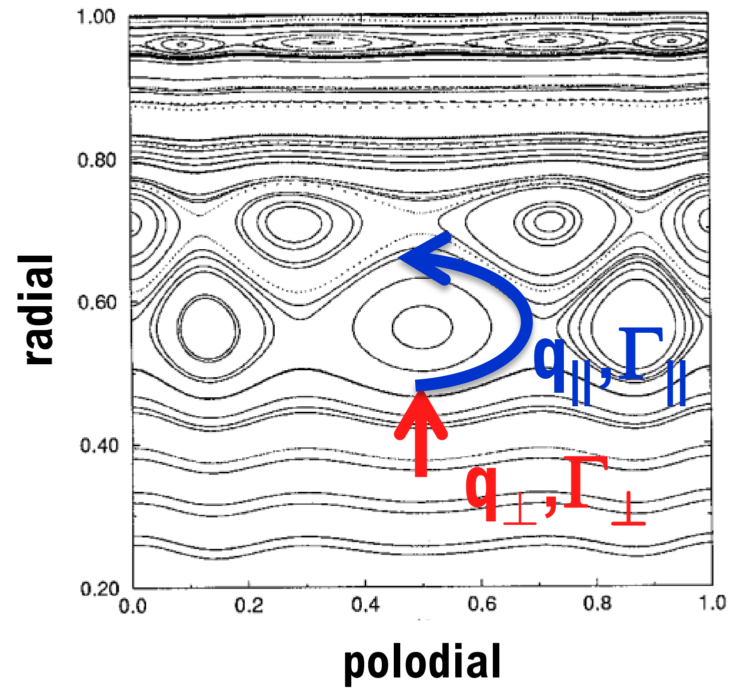

- if field perturbations are in resonance with rational field line
- possible perturbations: inherent field symmetry (5/m), error fields

Magnetic shear

- island width: $w = 4\sqrt{RB_{mn}/(m\iota')}$
- low order rationals (low m): larger islands

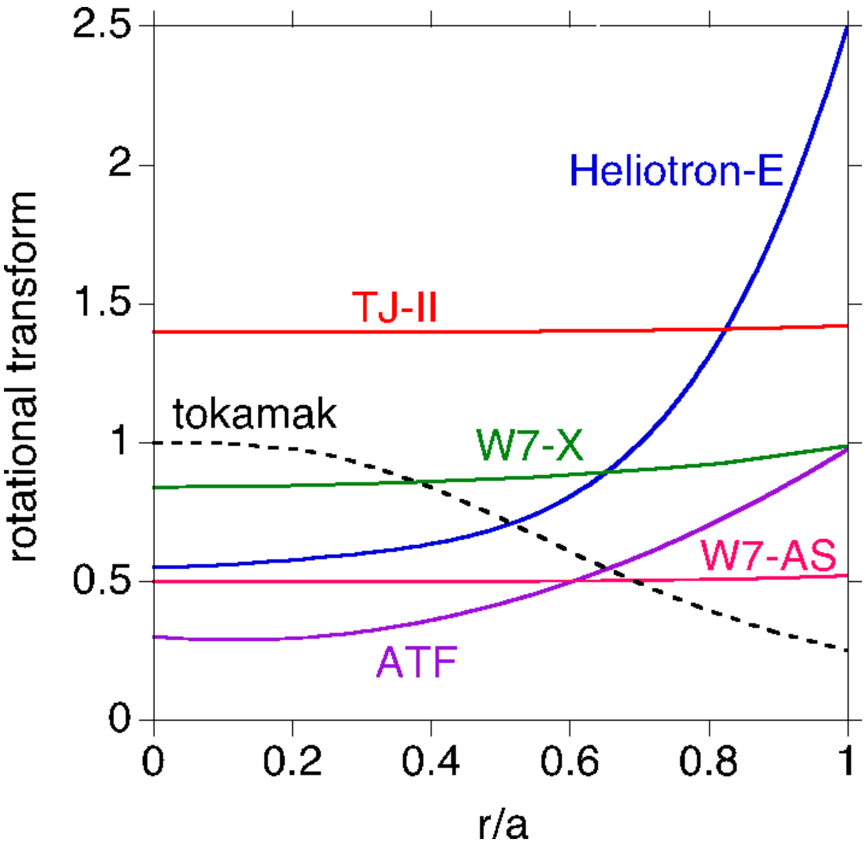

ergodic layer (LHD)

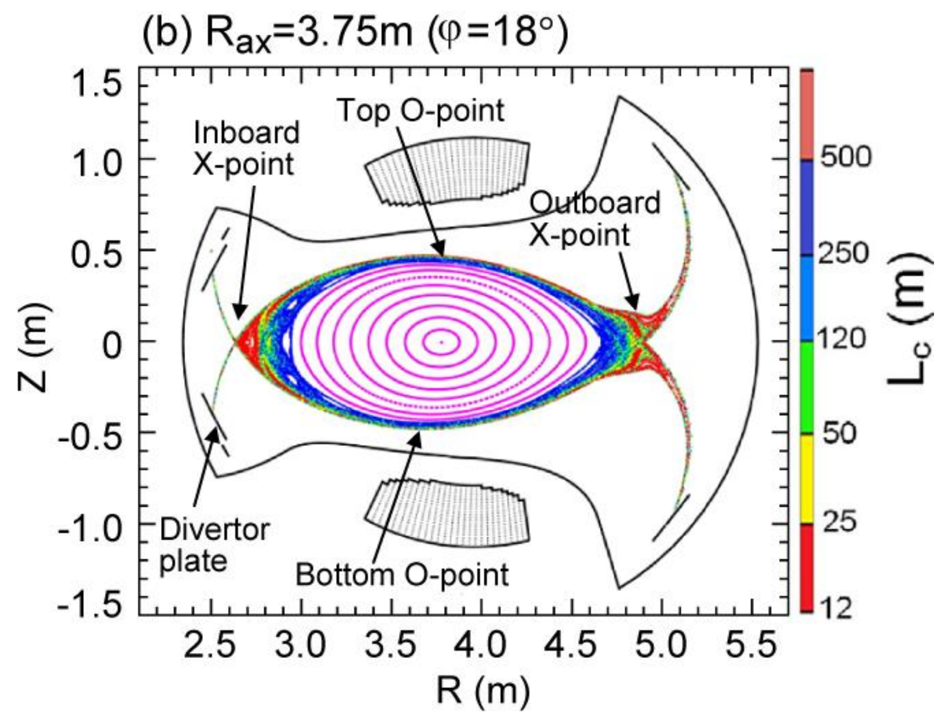

Morita, *Nucl. Fusion* 53

- shear is beneficial for MHD stability

Equilibrium: plasma currents

measured Pfirsch-Schlüter currents (HSX)

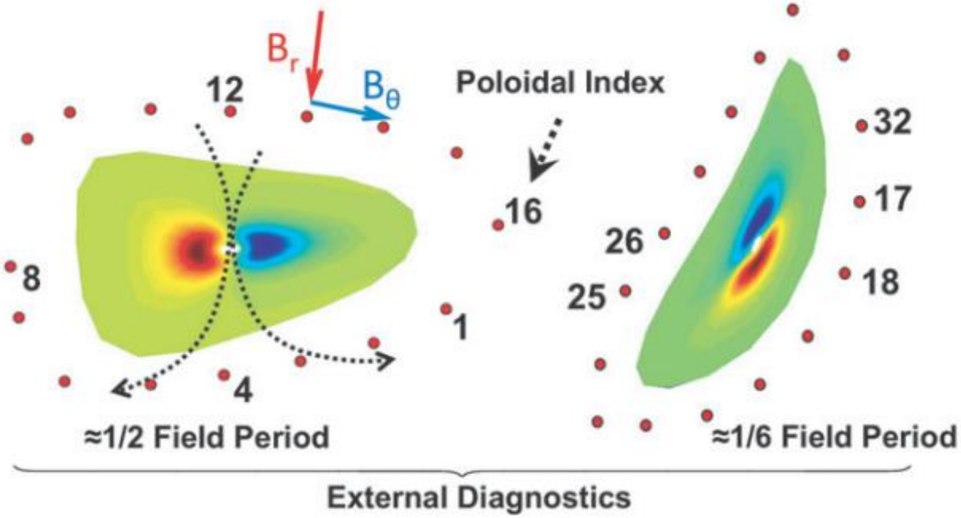

Schmitt ,*Nucl. Fusion* 53 (2013)

toroidal curvature

$$\triangle \sim R\left(\frac{\epsilon_{01}}{\epsilon_t}\right)^2 \frac{1}{\iota^2} < \beta >$$

- **operational limit:** $\triangle = \frac{a}{2}$

$$\boxed{\beta_{eq} \sim \frac{a}{2R}\iota^2}$$

resulting Shafranov shift (W7-AS)

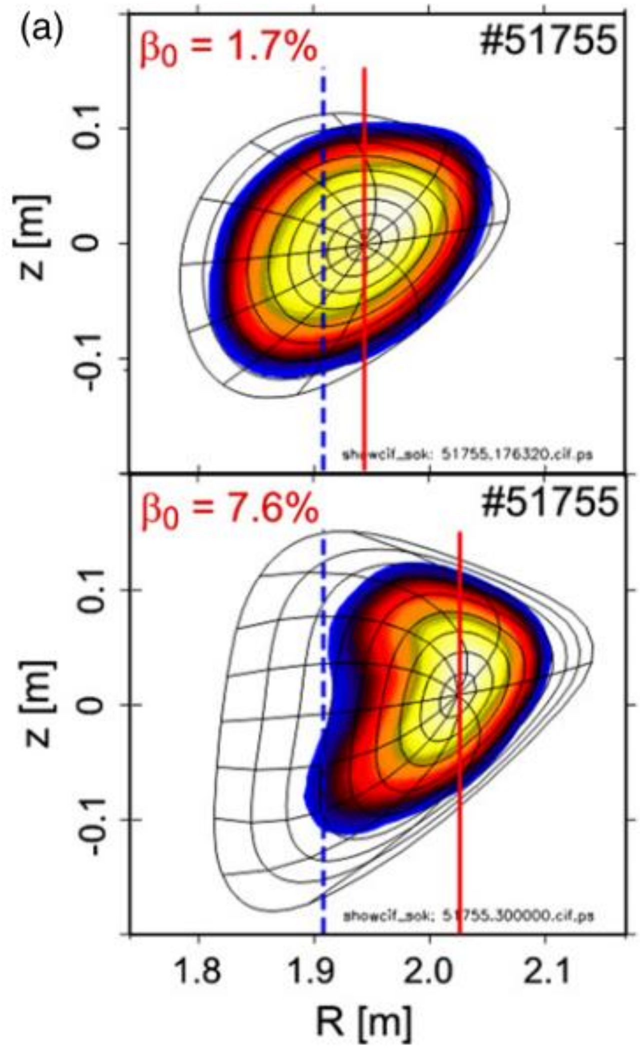

Hirsch, *PPCF 50 (2008)*

Equilibrium: plasma currents

measured Pfirsch-Schlüter currents (HSX)

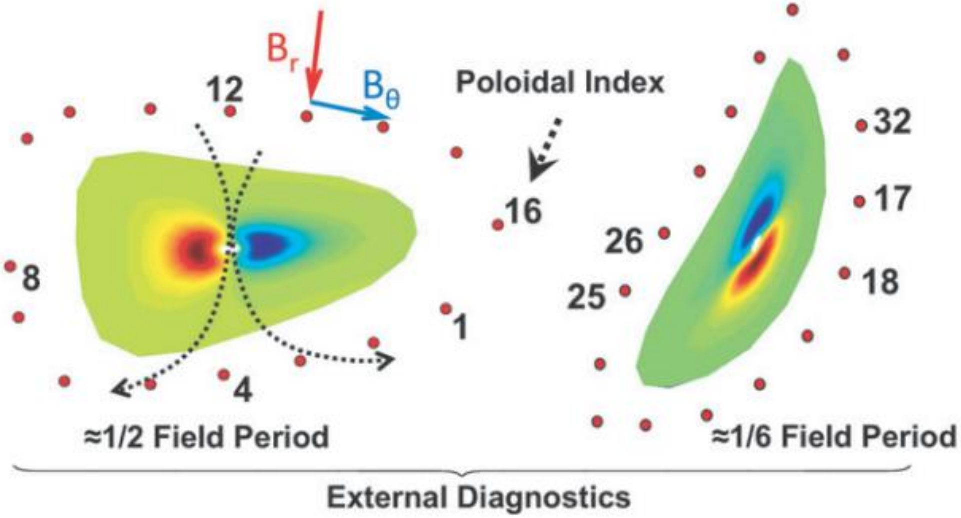

Schmitt , *Nucl. Fusion* 53 (2013)

toroidal curvature

$$\Delta \sim R\left(\frac{\epsilon_{01}}{\epsilon_t}\right)^2 \frac{1}{\iota^2} < \beta >$$

- **operational limit:** $\Delta = \dfrac{a}{2}$

$$\boxed{\beta_{eq} \sim \frac{a}{2R}\iota^2}$$

LHD

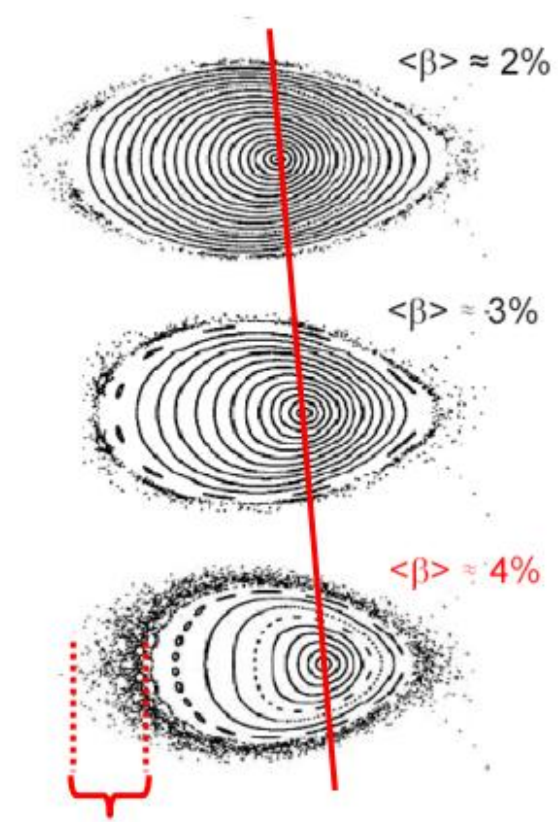

Increasing ergodization of the plasma boundary
Reduction of the confining volume

from Suzuki et al.

Shaping minimizes Shafranov shift

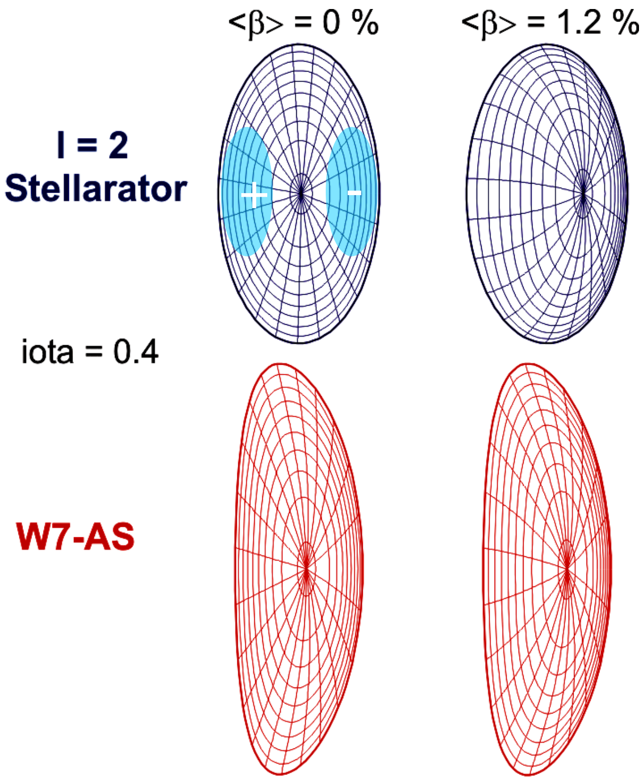

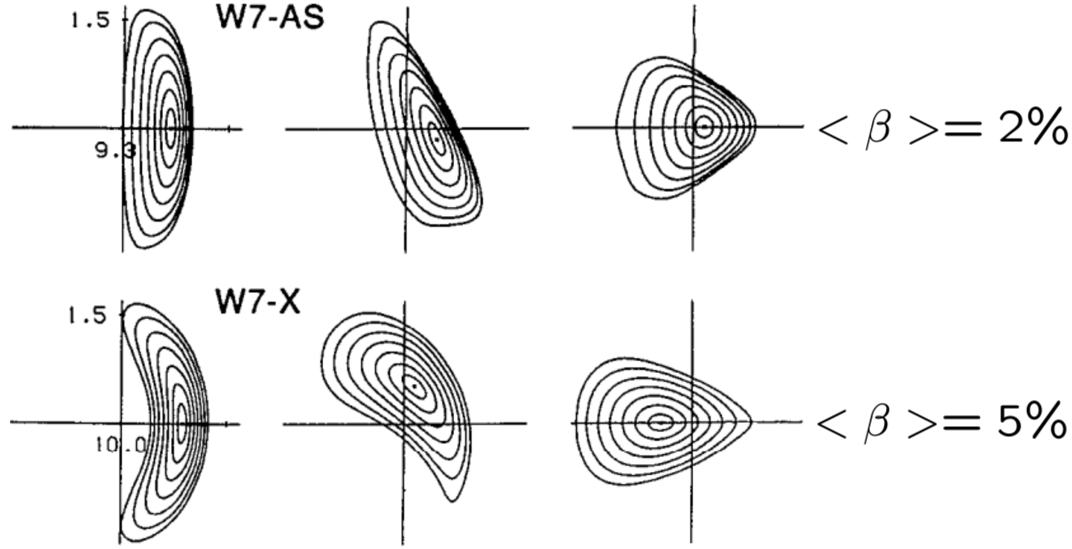

Grieger, *Phys. Fluids* B 4 (1992)

- **inrease of average elongation reduces toroidal curvature**
- **elongation reduces also poloidal variation of B (reduces ripple losses)**
- **W7-X: β=5% limit caused by economic reasons $P_{\text{fus}} \sim \beta^2$**

Equilibrium: Bootstrap current

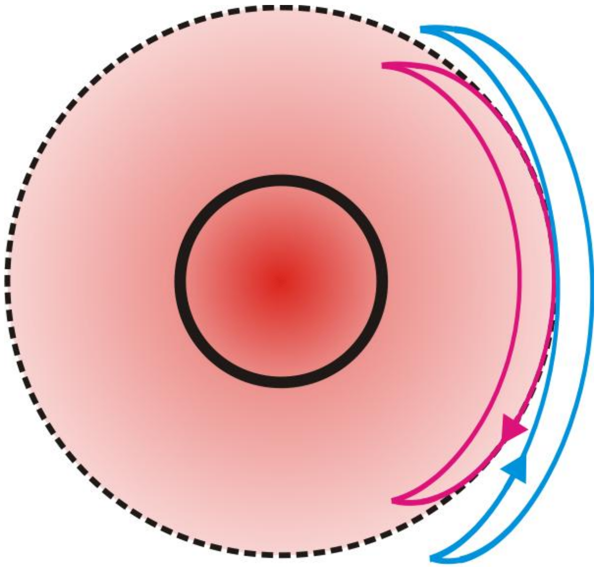

- trapped particle diamagnetic current
- momentum transfer from trapped to passing particles

$$j_B \sim \frac{f_t}{f_p} \nabla p$$

- tokamaks: increases ι
- stellarators: reduces ι

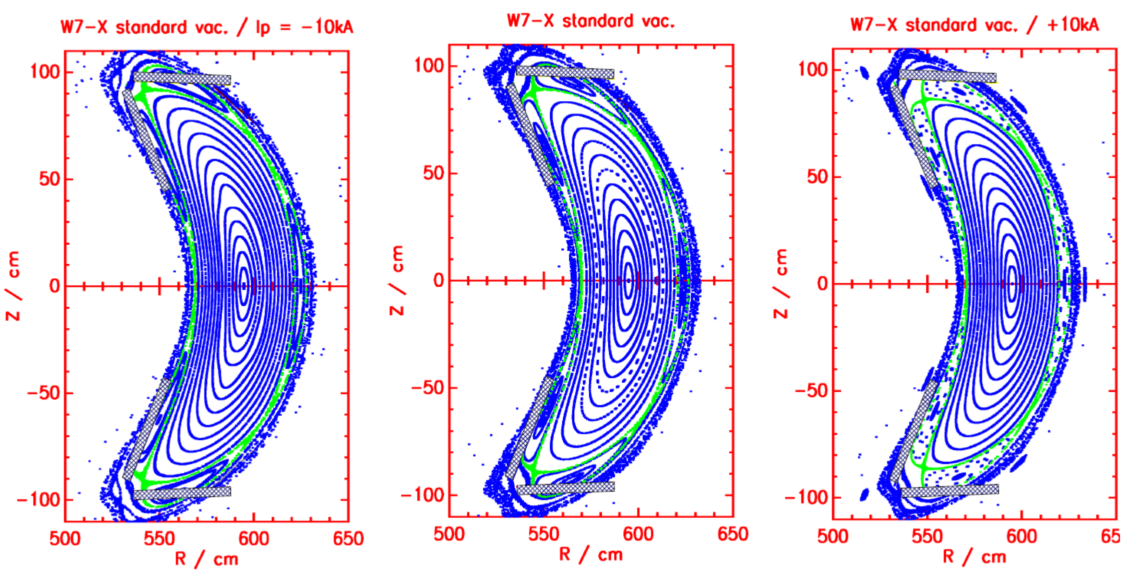

net-current free plasmas (ATF)

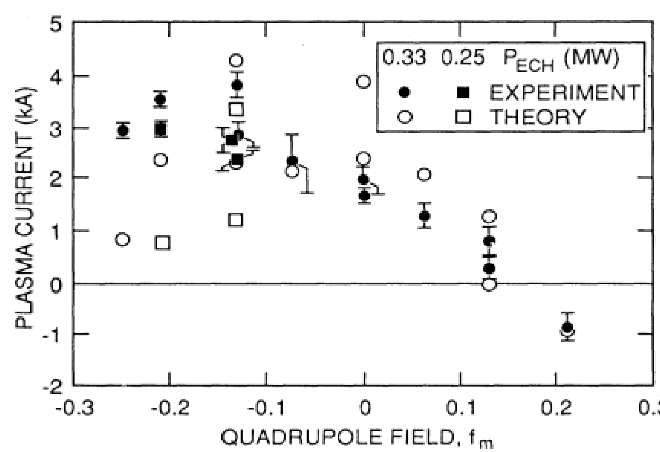

Murakami, PRL 66 (1991)

MHD stability

- destabilizing sources of free energy:

  pressure gradient

  parallel current

- stabilizing:

  magnetic well (increases with β)

  magnetic shear

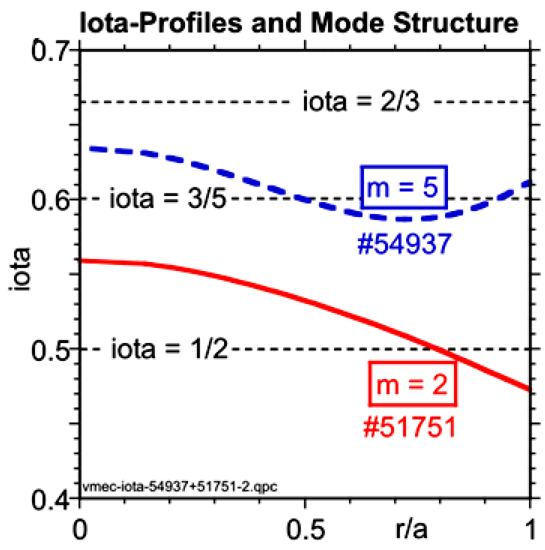

- no current driven instabilities:

  disruptions, resistive wall modes,

  tearing modes

- stellarator MHD stability determined

  by interchange and ballooning modes

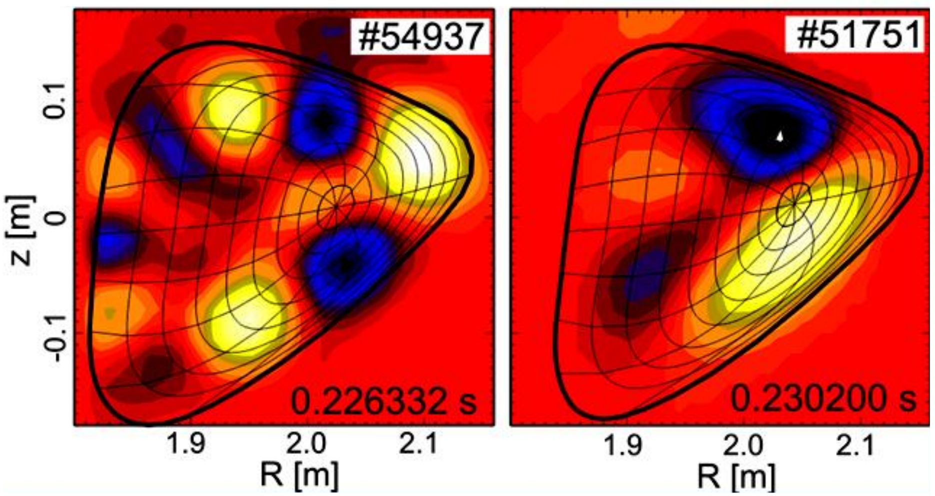

MHD stability

- **destabilizing sources of free energy:**
  pressure gradient
  parallel current
- **stabilizing:**
  magnetic well (increases with β)
  magnetic shear
- **no current driven instabilities:**
  disruptions, resistive wall modes,
  tearing modes
- **stellarator MHD stability determined**
  by interchange and ballooning modes

soft disruption during ohmic current ramp (W7-AS)

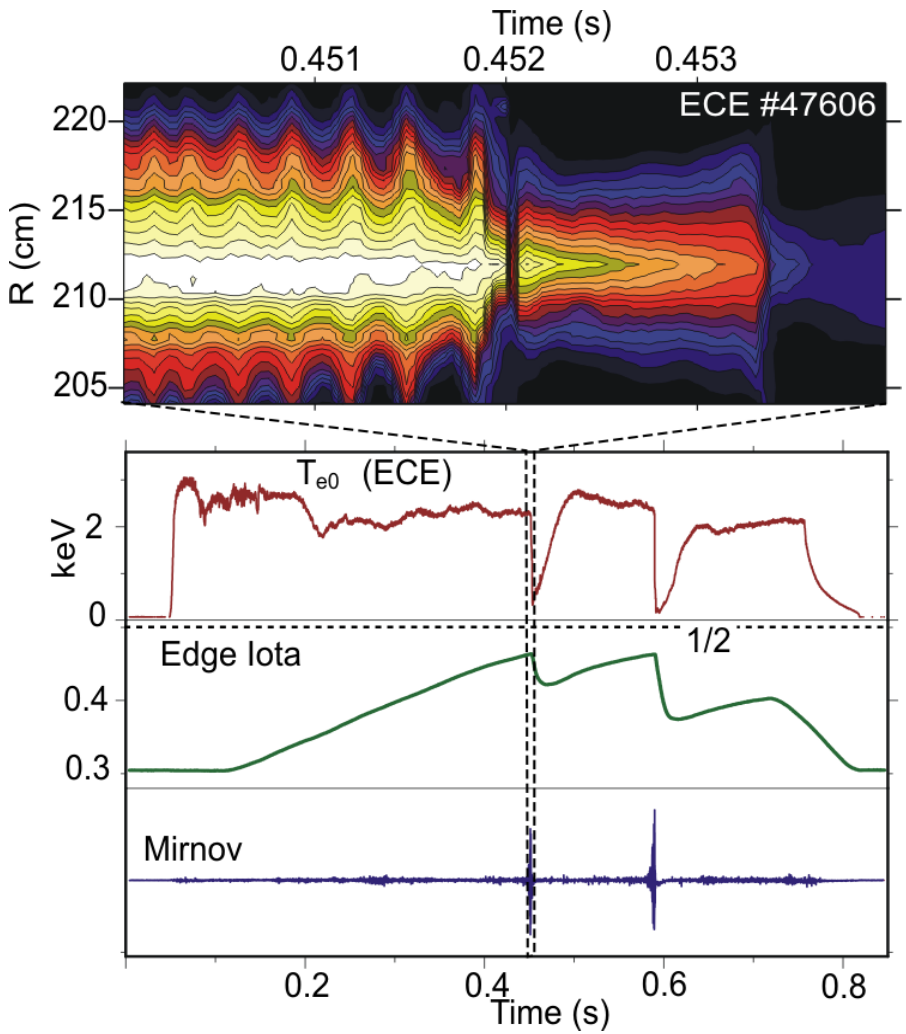

MHD stability

- **destabilizing sources of free energy:**

  pressure gradient

  parallel current

- **stabilizing:**

  magnetic well (increases with β)

  magnetic shear

- **no current driven instabilities:**

  disruptions, resistive wall modes,

  tearing modes

- **stellarator MHD stability determined by interchange and ballooning modes**

soft disruption during ohmic current ramp (W7-AS)

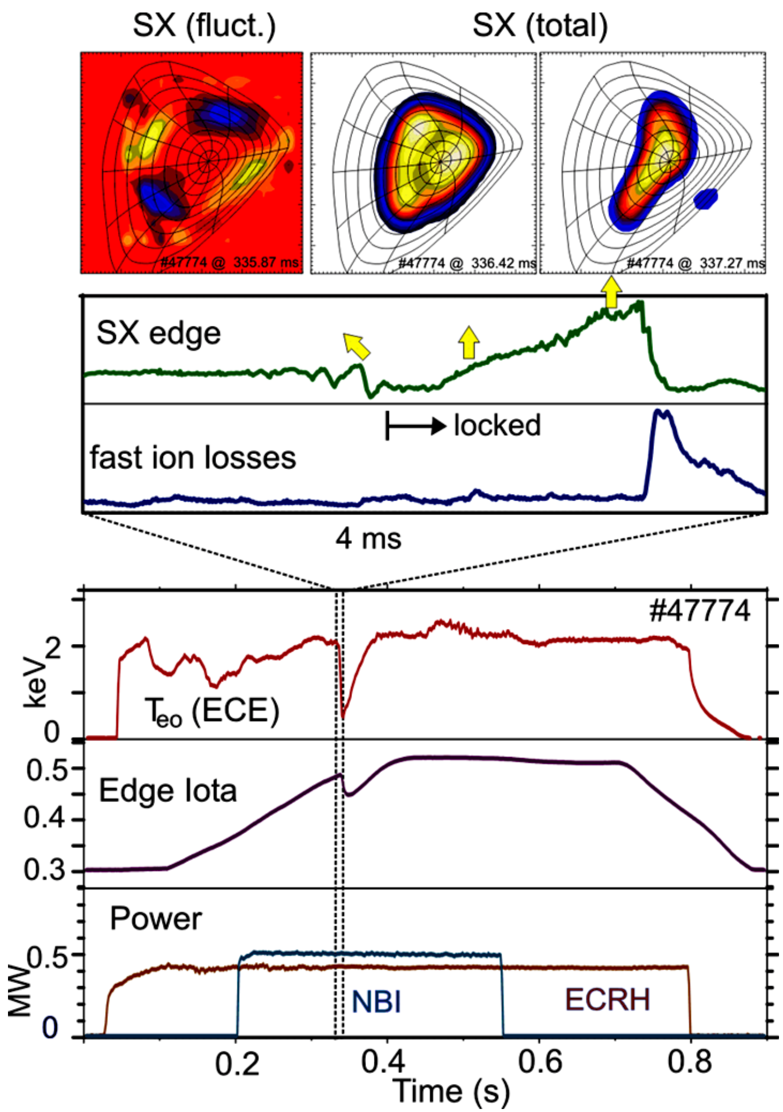

MHD waves and fast ion losses

- Alfvèn wave excitation due to Landau damping of fast ions
- frequently observed in NBI heated plasmas
- very complex eigenmode structure in stellarators
- energy sink of fusion born α- particles

x-ray tomography $B/B_0 \sim 10^{-4}$

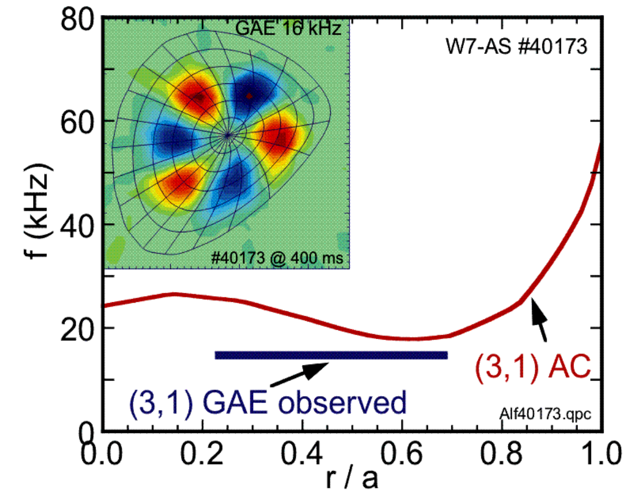

magnetic fluctuations

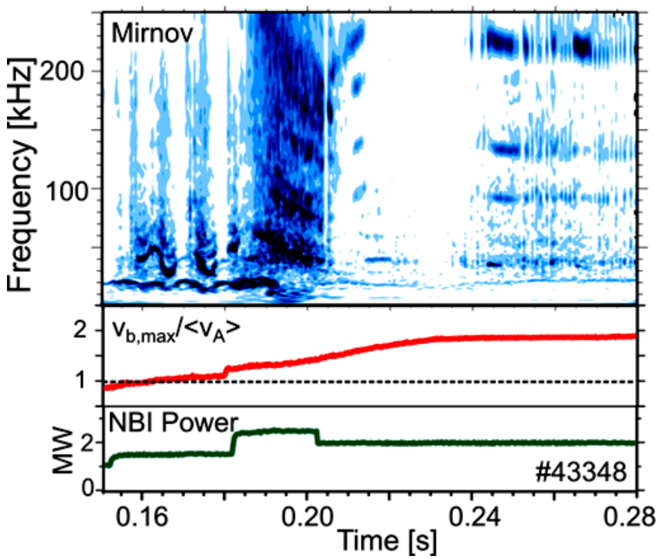

eigenmodes

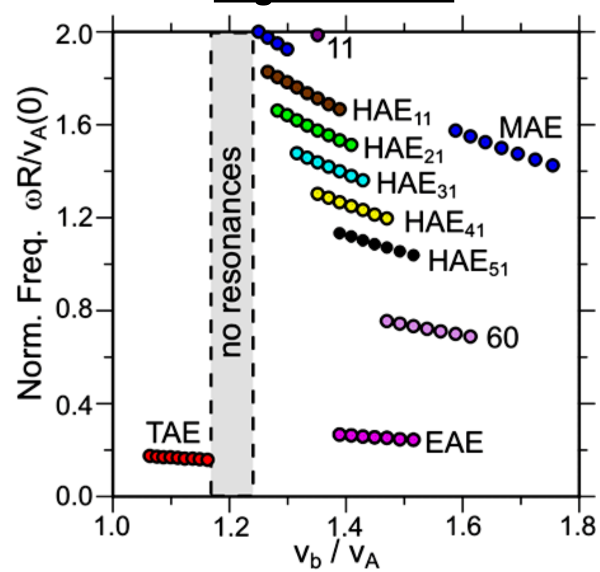

MHD waves and fast ion losses

- Alfvèn wave excitation due to Landau damping of fast ions
- frequently observed in NBI heated plasmas
- very complex eigenmode structure in stellarators
- energy sink of fusion born α- particles
- nonlinear interaction

Alfvèn induced ion losses in W7-AS

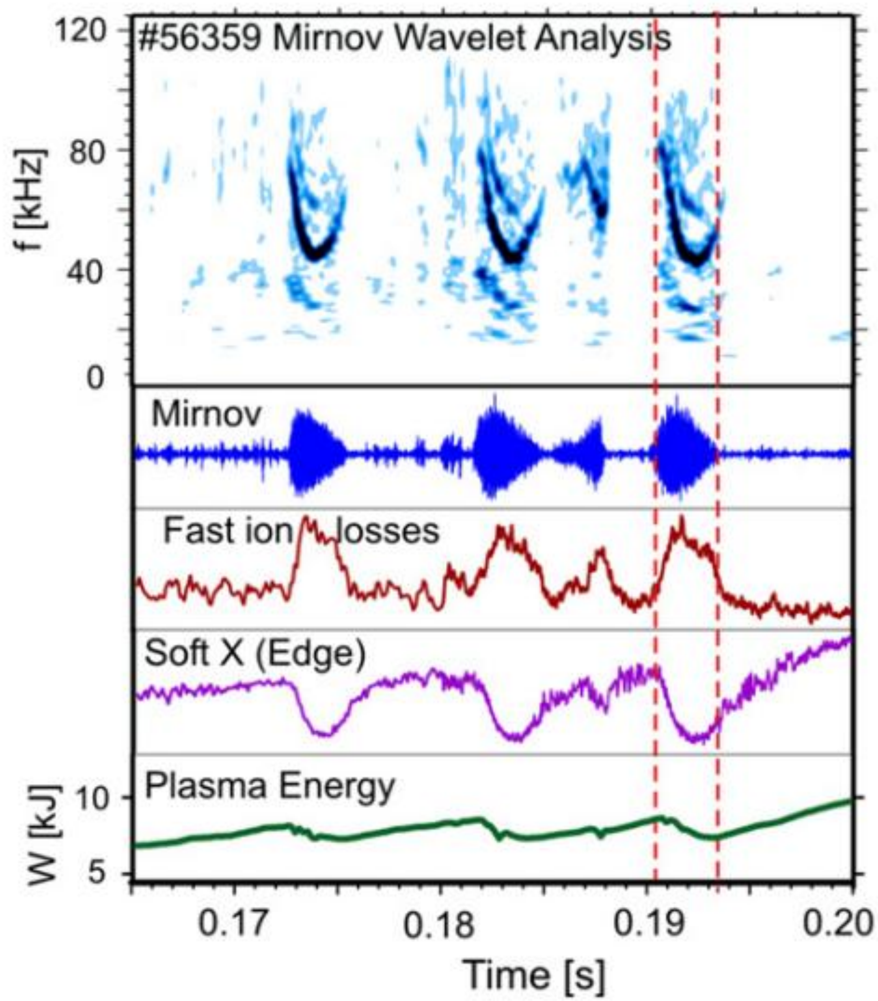

Neoclassical transport

particle flux

$$\Gamma = -D\nabla n + Vn$$

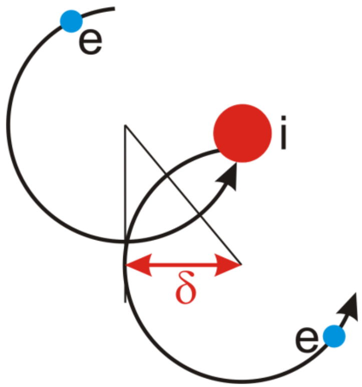

- **particle picture:**

random-walk diffusion coefficient $D = \dfrac{\Delta x^2}{2\tau}$

- **homogeneous magnetic field:**

collisional diffusion $D_{class} = \dfrac{\rho_e^2}{2\tau_{ei}}$

random walk

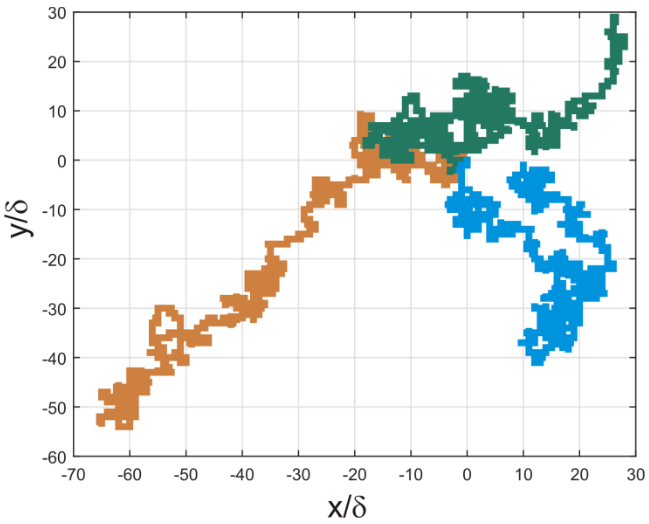

Neoclassical transport

particle flux

$$\Gamma = -D\nabla n + Vn$$

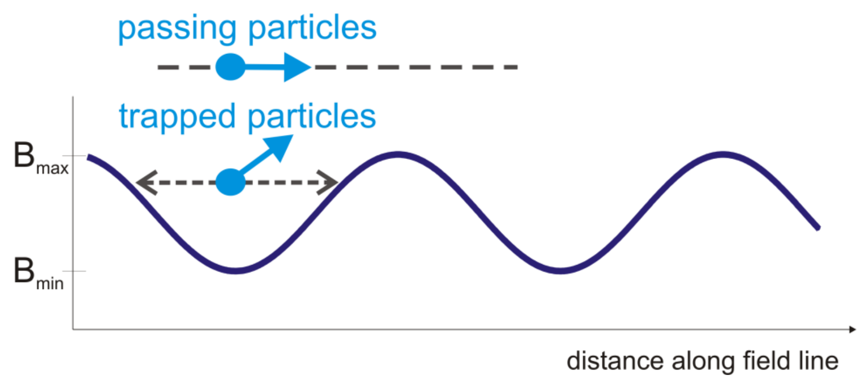

toroidal geometry

- **passing particles: δ given by deviation of drift surface from flux surface**

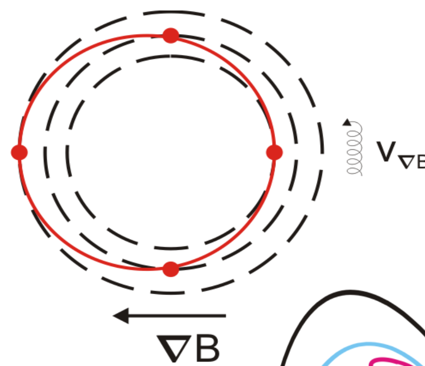

Pfirsch-Schlüter diffusion: $D_{PS} = \frac{\delta^2}{2\tau_{ei}} = D_{class}\frac{1}{\iota^2}$

- **trapped particles: can become passing particles again by small change of pitch angle due collision ->δ given by banana width δ_{Ba}**

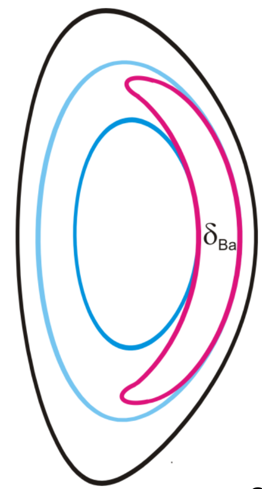

Banana diffusion: $D_{Ba} = \frac{\delta_{Ba}^2}{2\tau_{eff}} = D_{PS}\frac{1}{\epsilon^{3/2}}$

Neoclassical transport

particle flux

$$\Gamma = -D\nabla n + Vn$$

in stellarators: **additional $D_{1/\nu}$-regime due to helically trapped particles ($1/\nu=\tau_{ei}$)**

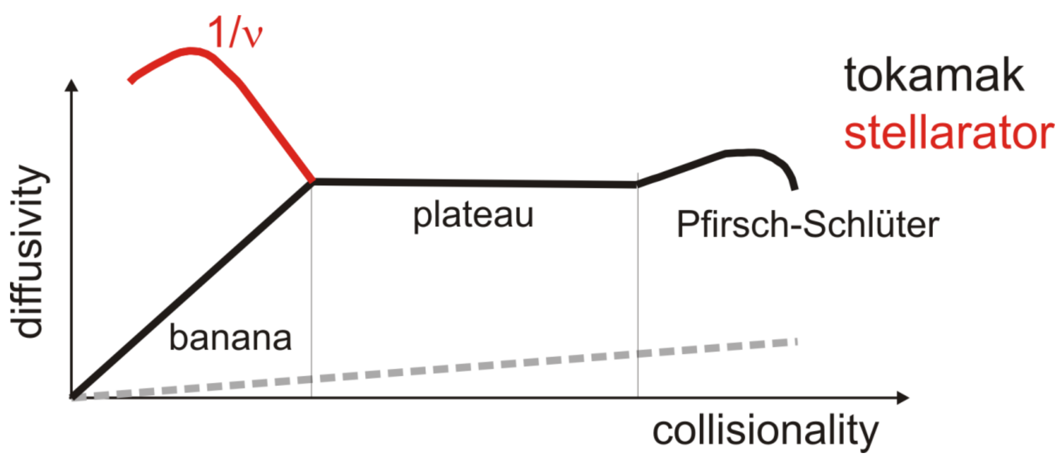

- **long mean-free-path (low collisionality regime) most relevant for fusion reactor**
- **scaling in lmfp-regime:**

tokamak: $D \sim T^{1/2}$ **stellarator:** $D \sim T^{7/2}$

Radial electric field

- **<u>stellarator ν-regime</u>**

  poloidal drift due to radial electric E_r field partly averages out ∇B – drift

- **E_r arises from non-ambipolar radial flux (e.g. electrons in the ν-regime, ions in the 1/ν-regime)**

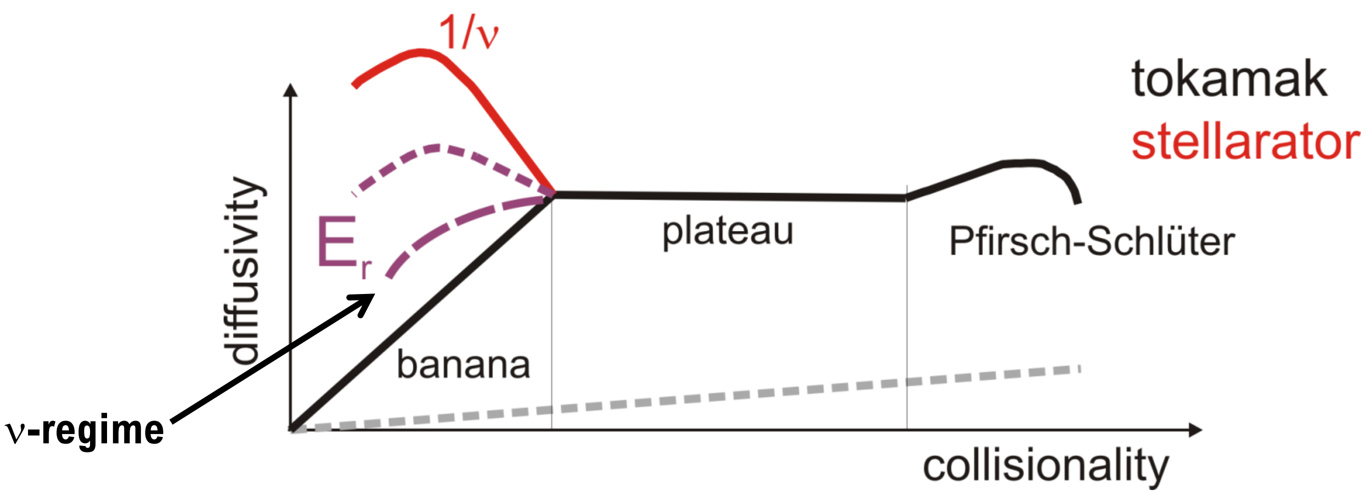

Ambipolar electric field

- ambipolarity constraint: balance of thermal electron and ion fluxes

$$\Gamma_e = Z_i \Gamma_i$$

$$\Gamma_\alpha = -n_\alpha \left[D_{11}^\alpha \left(\frac{\nabla n_\alpha}{n_\alpha} - \frac{q_\alpha E_r}{T_\alpha} \right) + D_{12}^\alpha \frac{\nabla T_\alpha}{T_\alpha} \right] \quad \alpha = e, i$$

- DKES solutions for W7-AS:

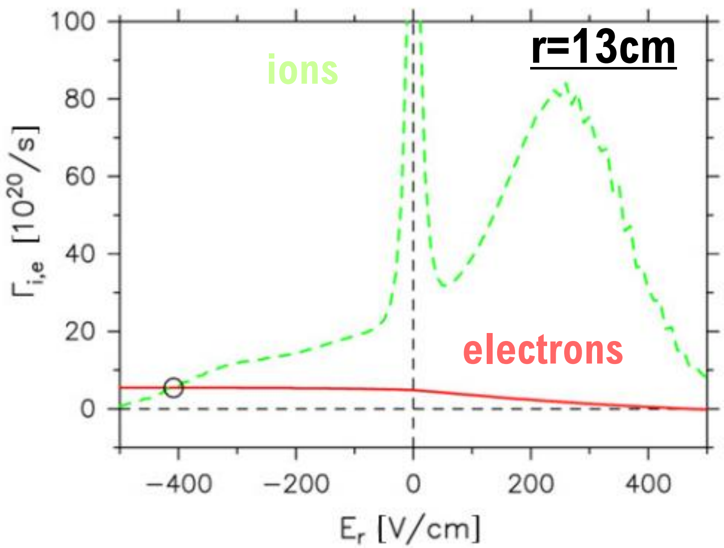

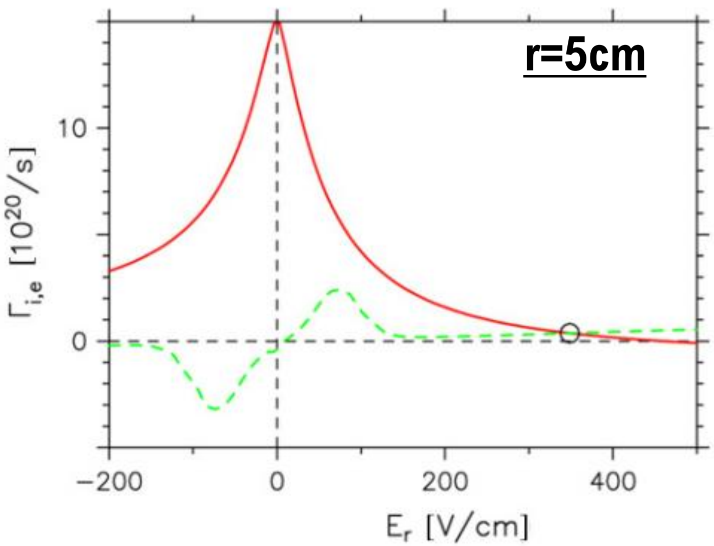

W7-AS electron root

- low-density ECRH discharges with $T_e \gg T_i$: positive electric field

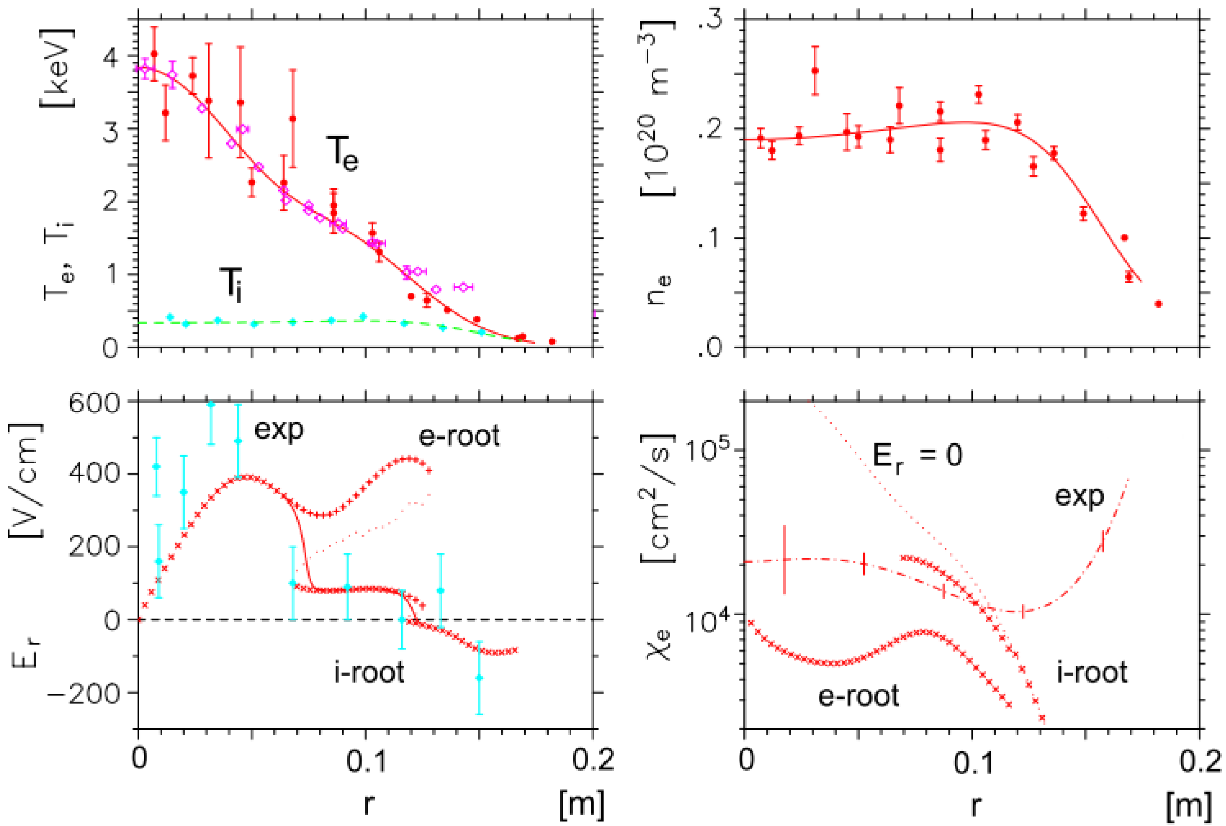

Brakel, *PPCF* 39 (1997)

- negative edge electric fields caused by ion fluxes due to ∇T_i
- 'anomalous' heat diffusivity in edge

W7-AS ion root

- high density with $T_e \approx T_i$: ion flux causes negative electric field

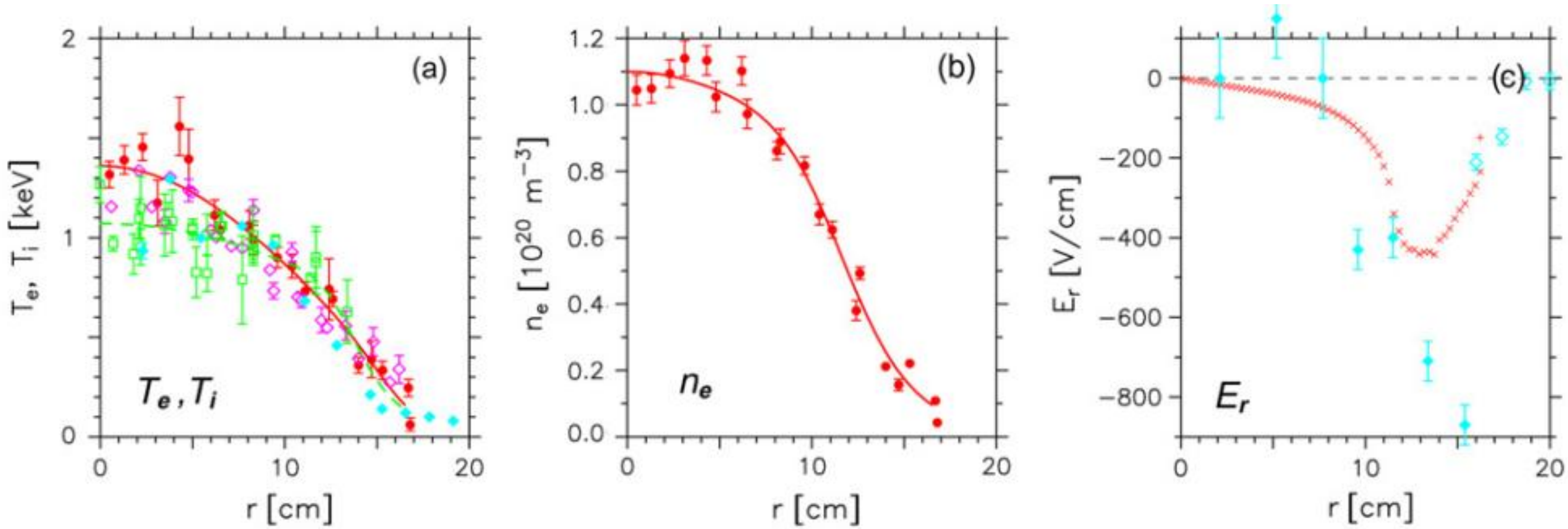

- ion root is fusion reactor relevant $\rightarrow$ moderate radial el. fields

- but: E_r needed to overcome poor $1/\nu$ - scaling

  $\rightarrow$ use proper magnetic field geometry

Effective helical ripple

• **radial transport coefficient:** $D_{11} \sim \epsilon_{eff}^{3/2}$

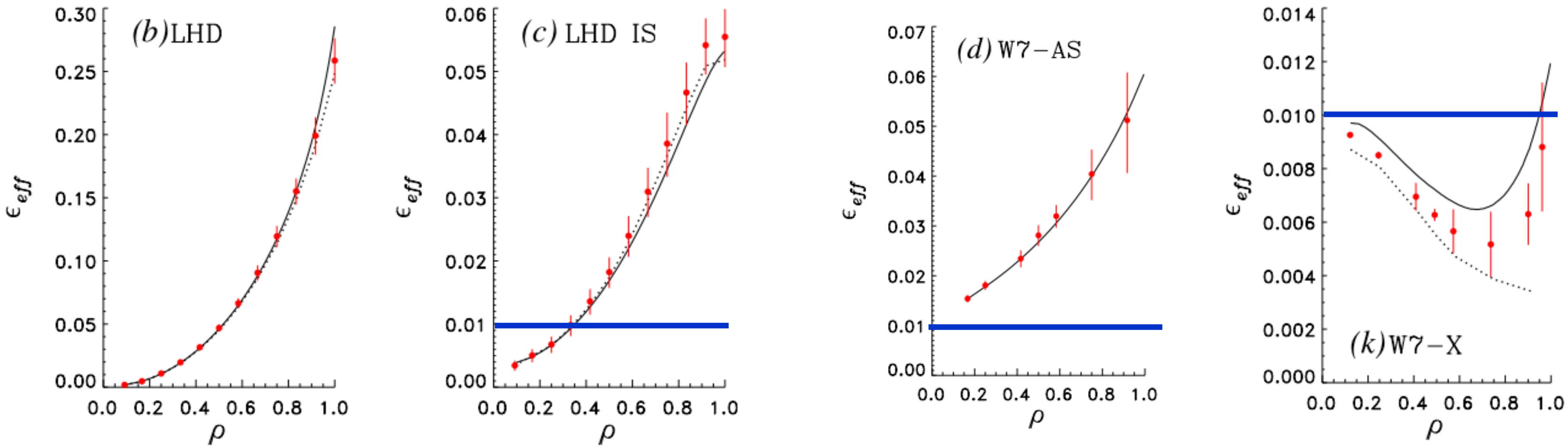

Beidler, *Nucl. Fusion* 51 (2011)

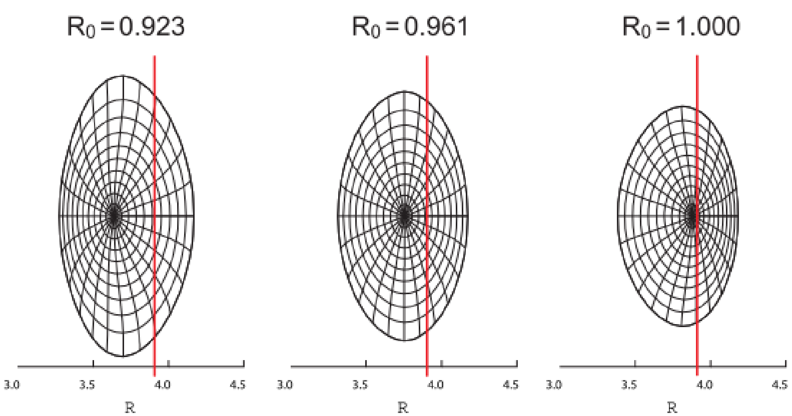

LHD vacuum magnetic axis shift:

• **inward shifted: small toroidal field ripple reduces neocl. transport losses**

• **outward shifted: large field ripple, large losses**

Okamura, *Contr. Plasma Physics* 50 (2010)

Predictive neoclassical transport modelling

cross-sections

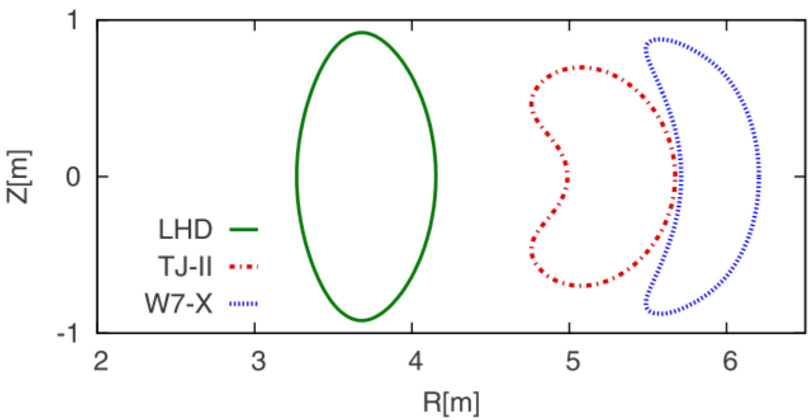

- **scale different devices to same volume at fixed aspect ratio**
- **same magnetic field, density and ECRH power**

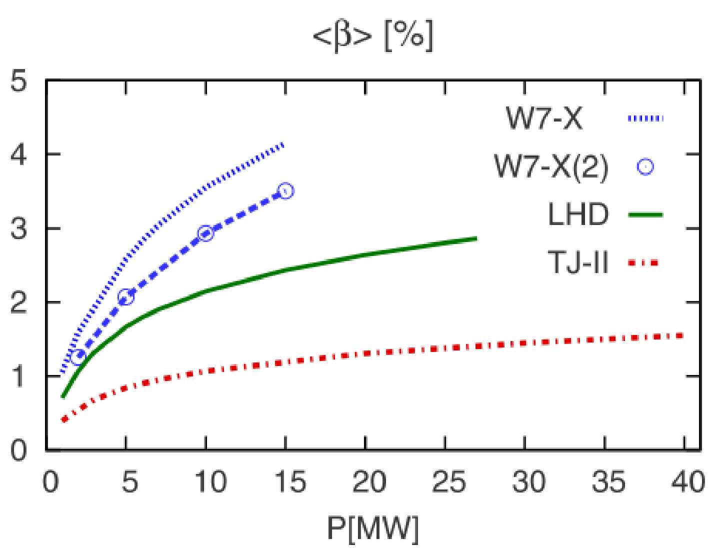

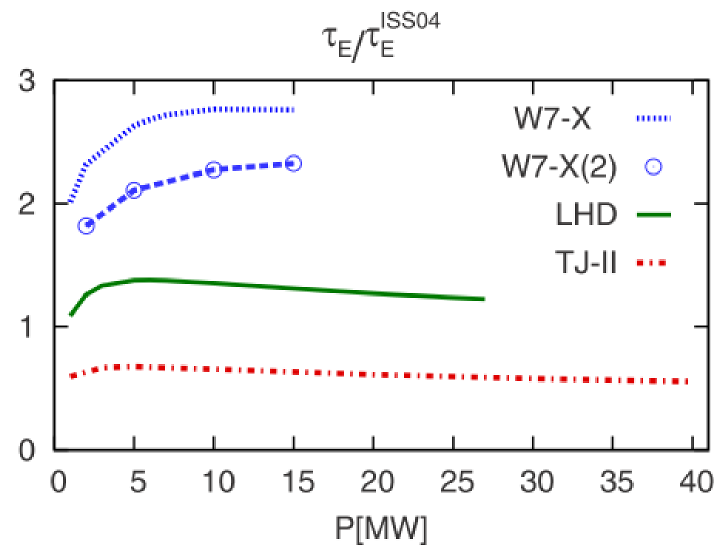

Turkin, ***Phys. Plasmas 18 (2011)***

Neoclassical optimization demonstrated in HSX

- **two different magnetic configurations:**
  - **quasi-helical symmetric (standard)**
  - **mirror (broken helical symmetry)**

- **different heating power to fit electron temperature profile**

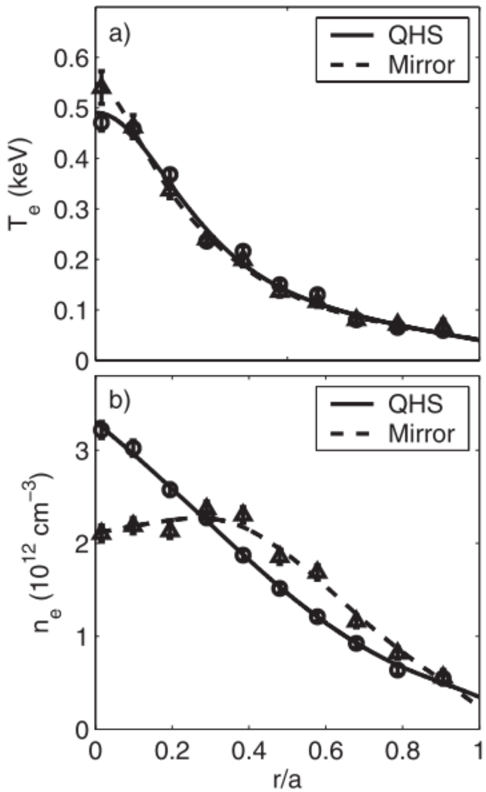

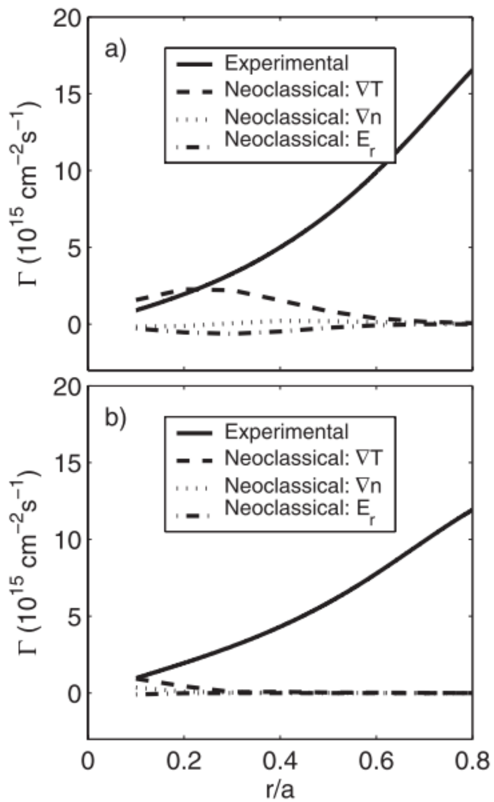

mirror

QHS

Canik, Phys. Rev. Lett 98 (2007)

Particle transport peculiarities

$$\Gamma = -D\nabla n + Vn$$

- **tokamak: particles drift towards magnetic axis (ware pinch)** $V = -\frac{E_\phi}{B_\theta}$
- **stellarator: no ware pinch, outward thermodiffusion** $\sim -\nabla T_e$

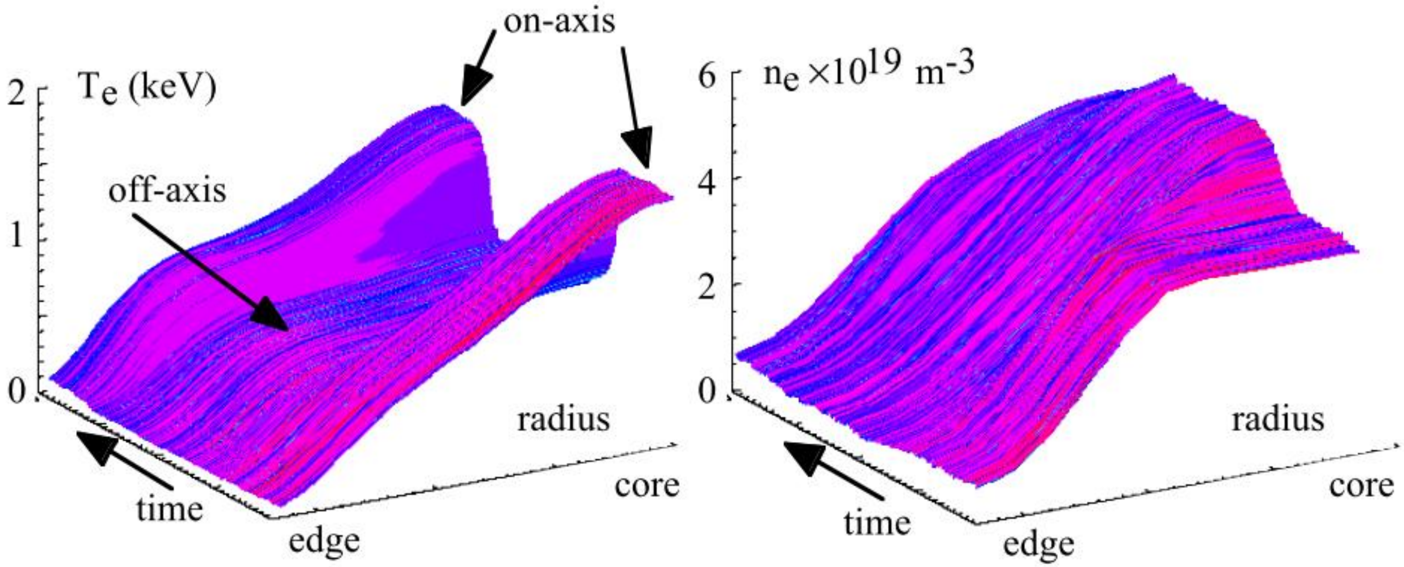

Brakel

- **on-axis ECRH: strong central heating causes flat / hollow density profiles**
- **off-axis ECRH: density peaking due to** E_r/T_e

Anomalous heat flux: microinstabilities

e.g. Ion temperature gradient turbulence (ITG):

• **driven by magnetic curvature (curvature drift v_d)**

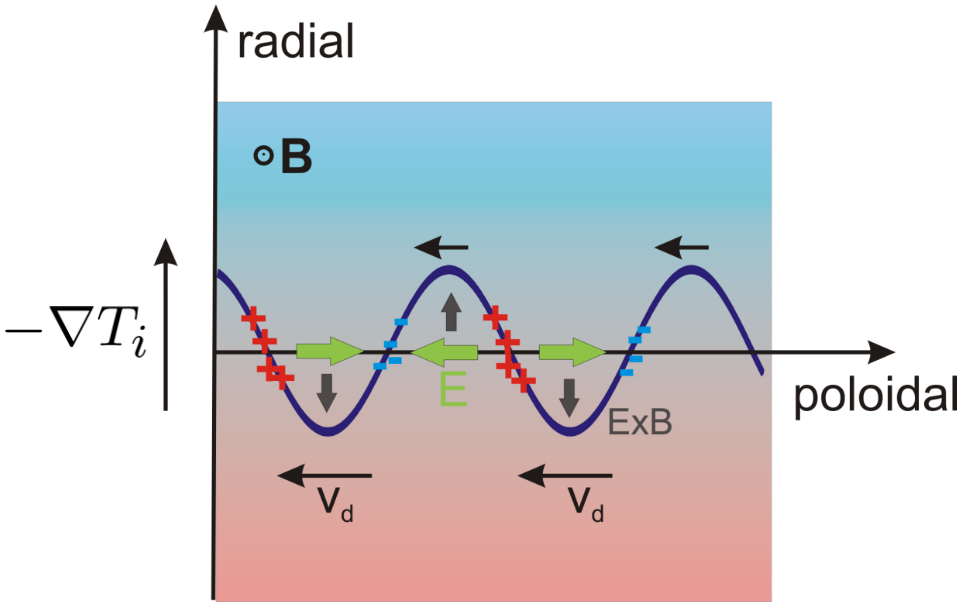

|B| tokamak

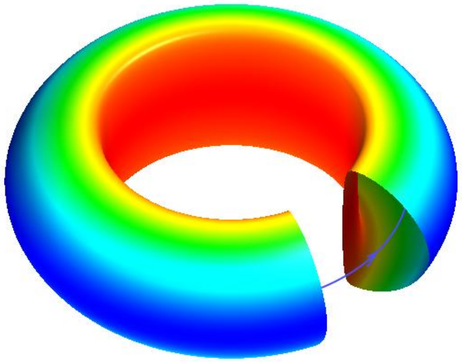

ITG turbulence (DIII-D)

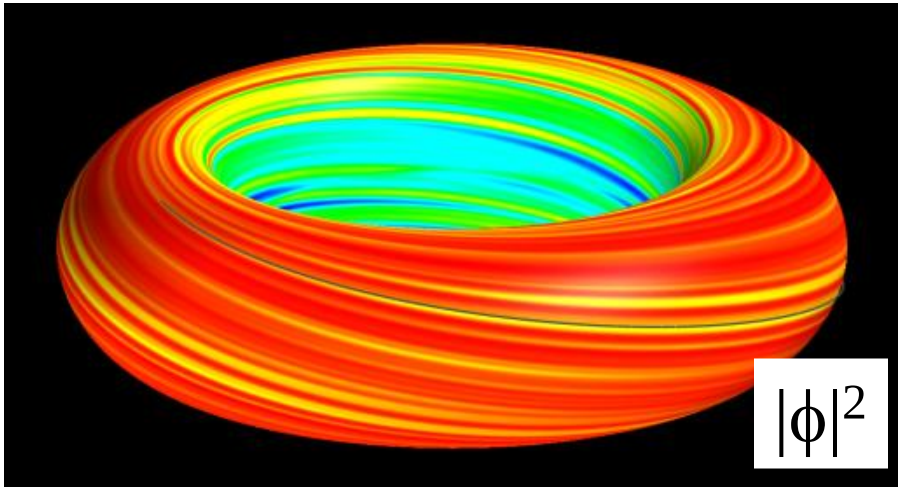

P. Xanthopoulos (www.ipp.mpg.de/~pax)

Anomalous heat flux: microinstabilities

|B| W7-X

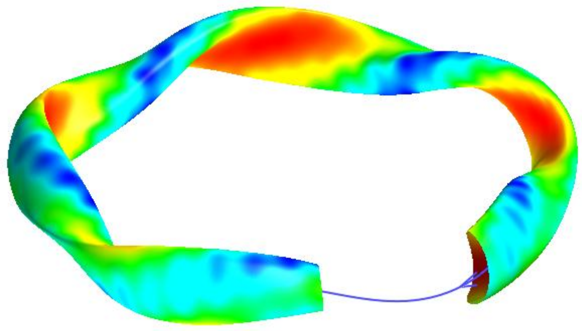

P. Xanthopoulos

ITG growth rate

bean plane

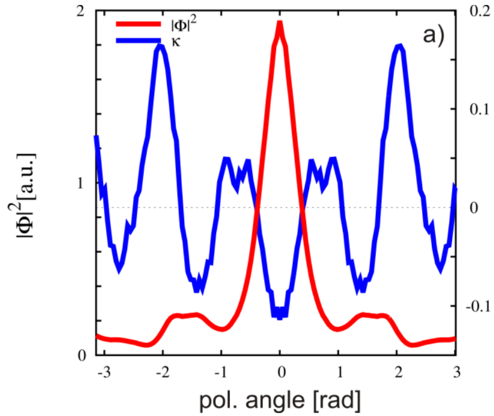

triangular plane

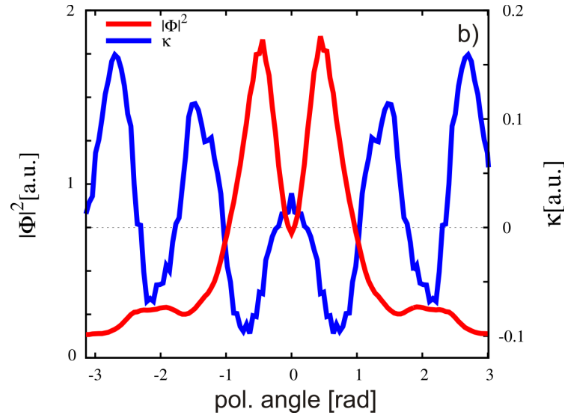

ITG turbulence (W7-X)

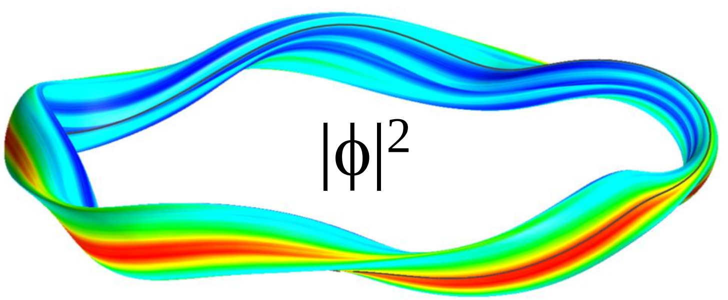

J. Proll, P. Xanthopoulos (www.ipp.mpg.de/~pax)

Anomalous heat flux: microinstabilities

|B| W7-X

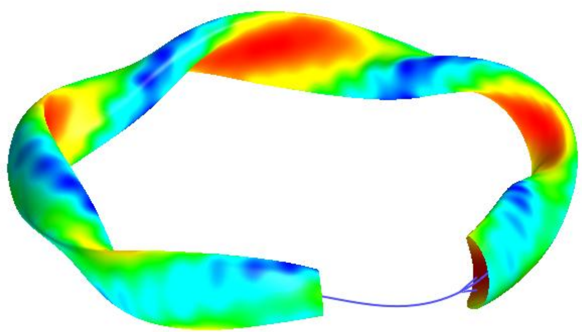

P. Xanthopoulos

ITG growth rate

bean plane

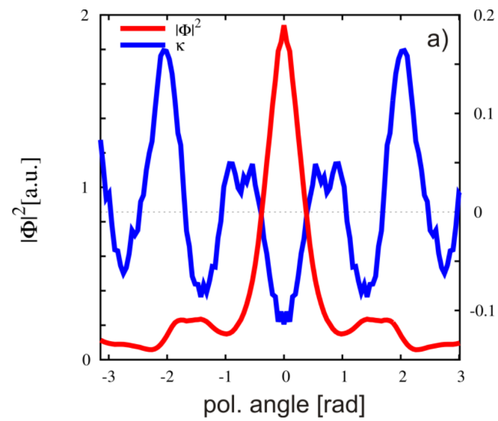

triangular plane

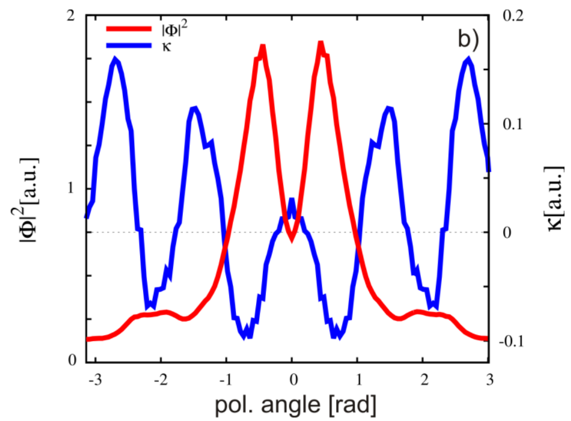

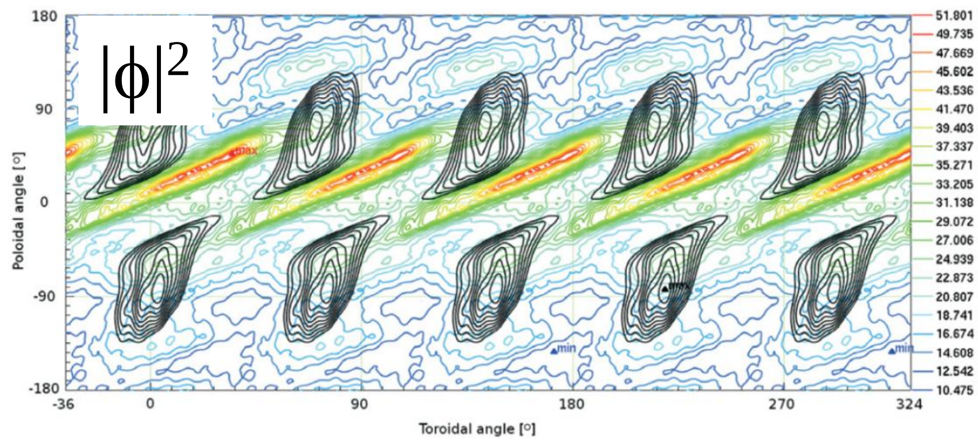

P. Helander, PPCF 54 (2012)

Energy confinement times

- **energy confinement time** $\tau_e = \frac{W}{P - dW/dt}$

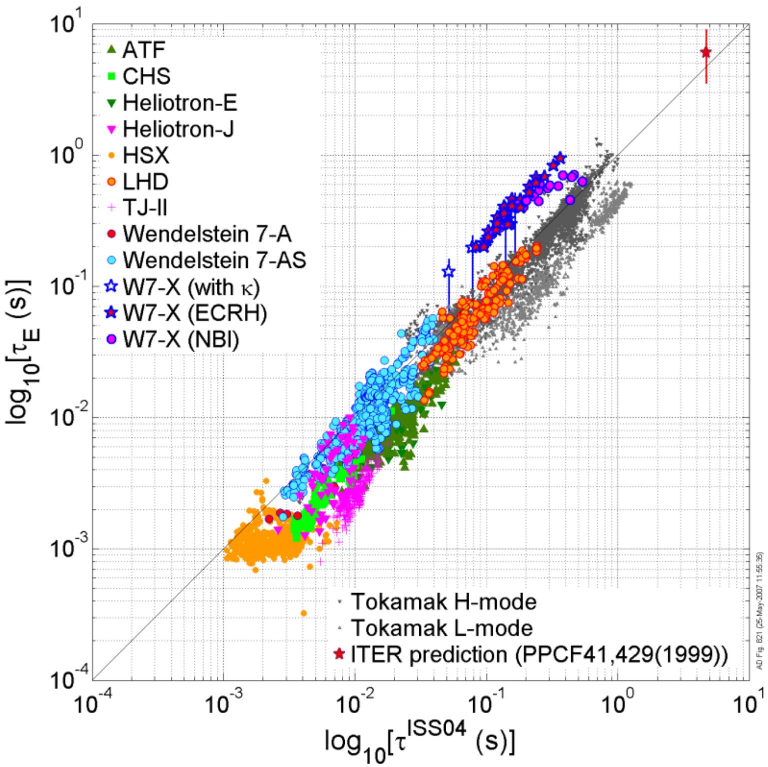

Dinklage, *Nucl. Fusion* 47 (2007)

$$\tau_e^{ISS04} = f \cdot 0.134 a^{2.28} R^{0.64} \bar{n}_e^{0.54} B^{0.84} (\iota_{2/3}/(2\pi))^{0.41},$$

- **stellarator confinement times comparable to tokamak devices**

Energy confinement: ι -dependence

W7-AS

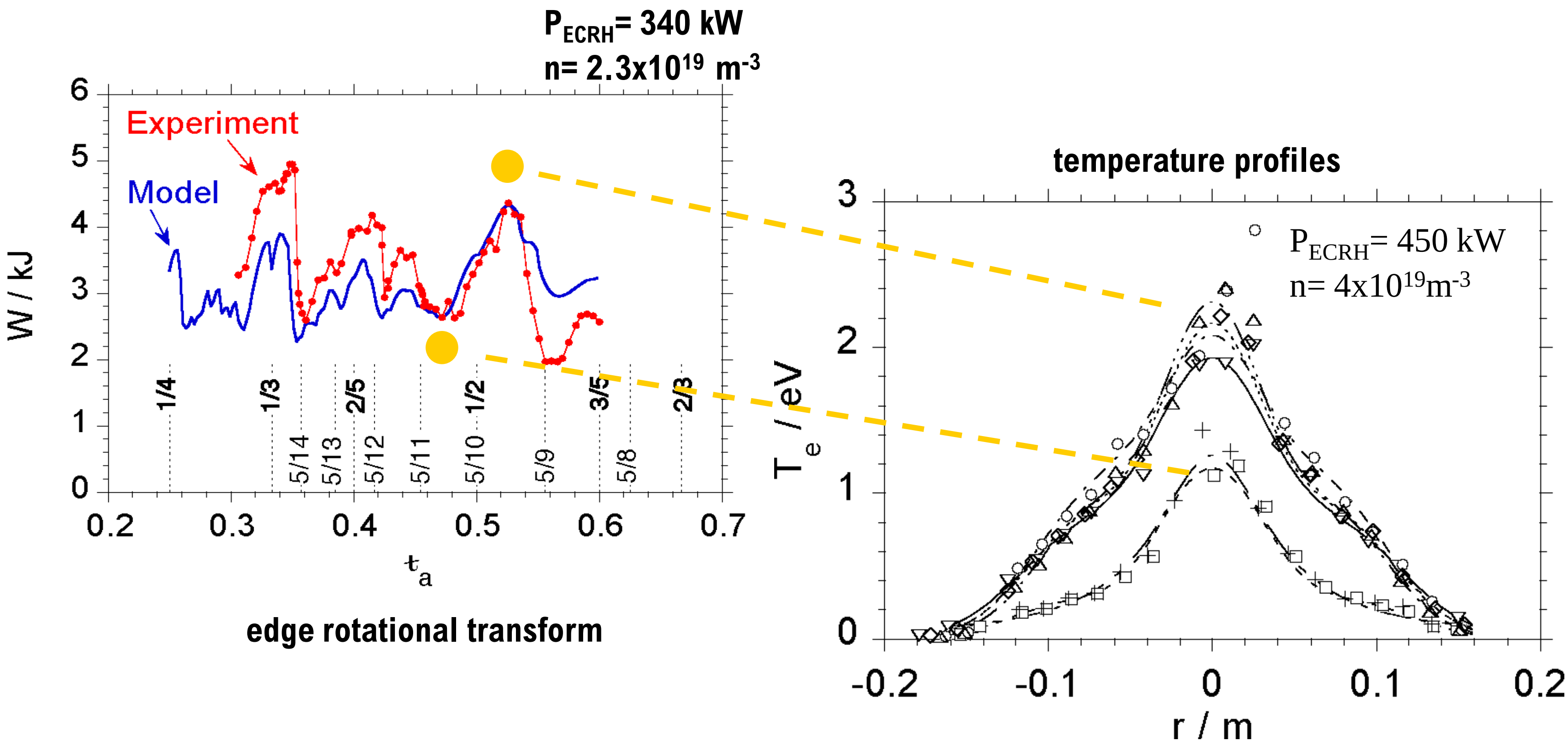

R. Brakel, *Nucl. Fusion* (2002)

- ι-dependence: enhanced heat diffusivity across magnetic islands

High confinement regimes (H-mode)

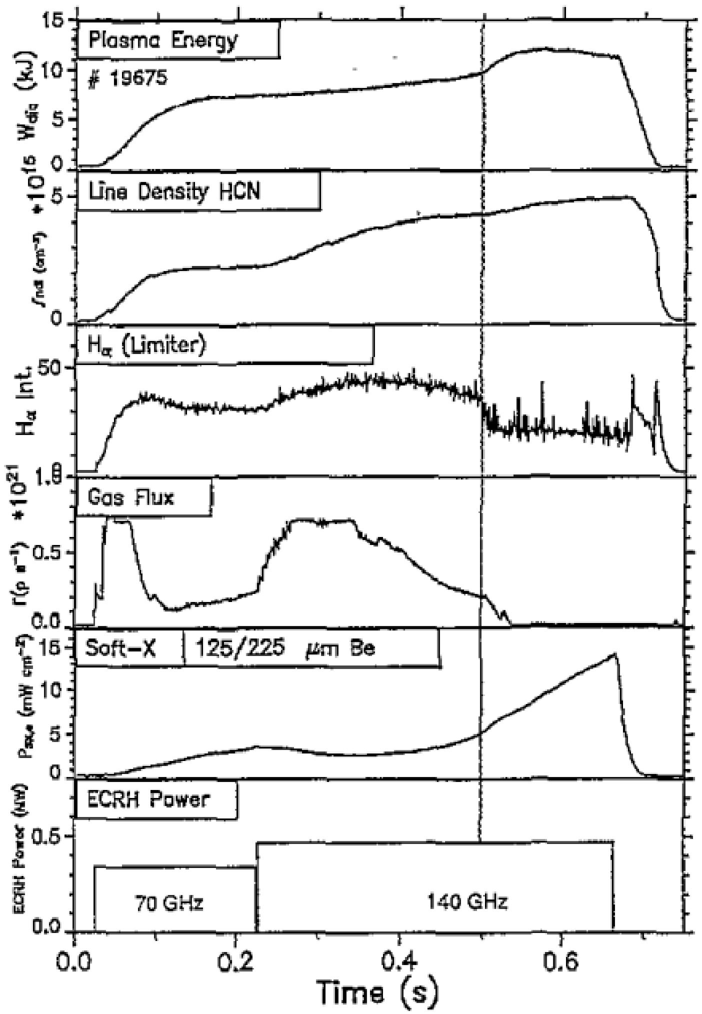

Wagner, *PPCF* 36 (1994)

- first stellarator H-mode: W7-AS (1992)
- shares characteristics with tokamak H-mode

power/density threshold in W7-AS

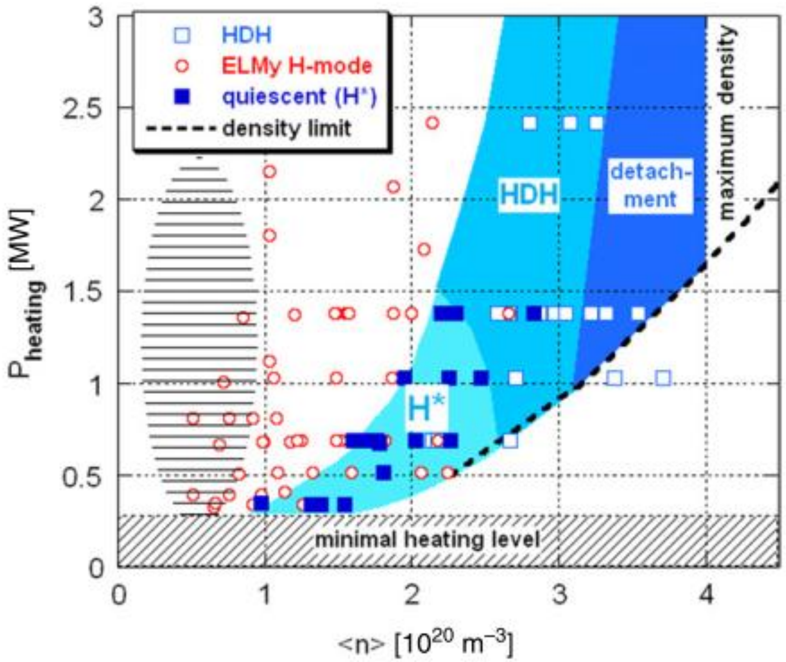

- ELMy H-mode: ELM related particle and energy fluxes can damage first wall

High confinement regimes (H-mode)

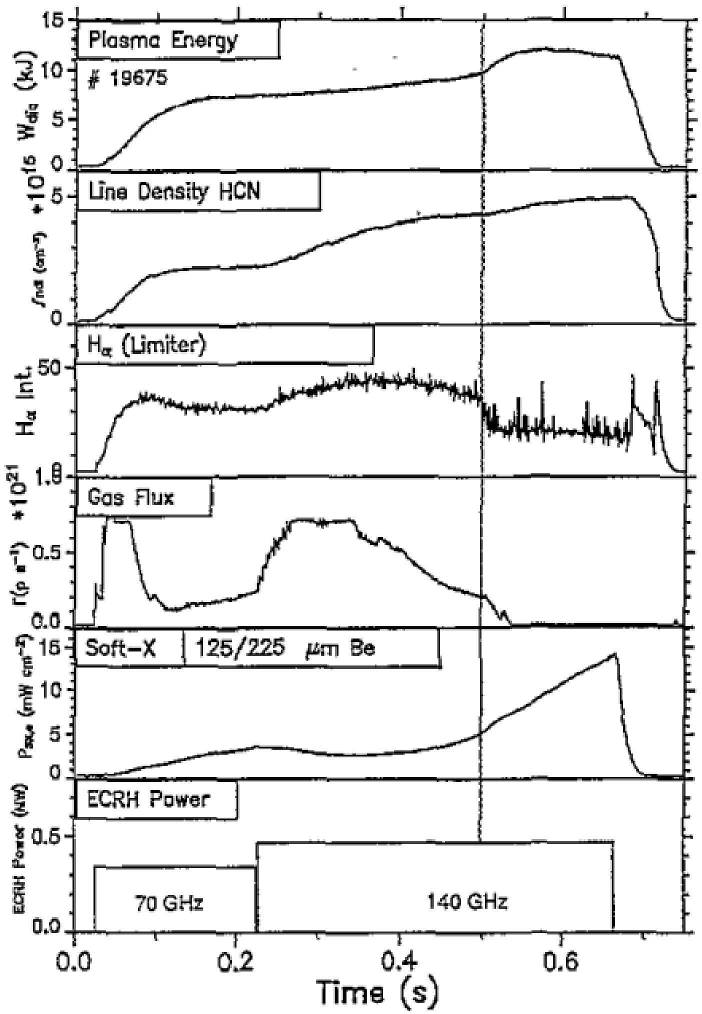

Wagner, *PPCF* 36 (1994)

- first stellarator H-mode: W7-AS (1992)
- shares characteristics with tokamak H-mode
- high density regimes (no Greenwald limit)

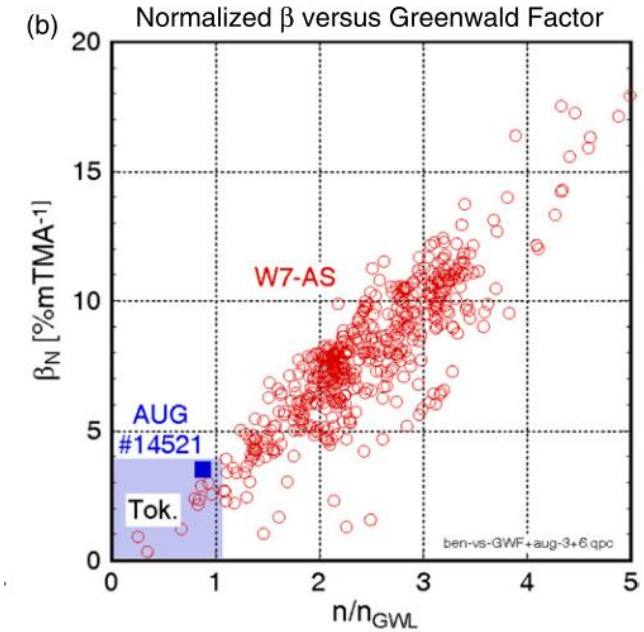

- ELMy H-mode: ELM related particle and energy fluxes can damage first wall

High confinement regimes (H*-mode)

•quiescent H-mode: no ELMs - radiative collapse due to impurity accumulation in core

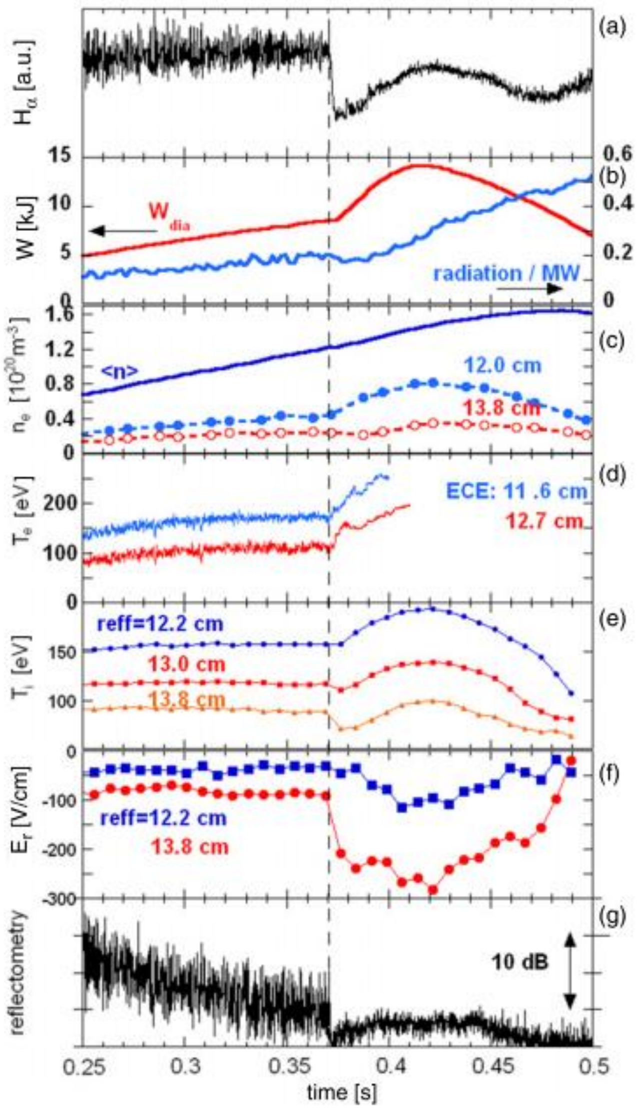

impurity radiation limit

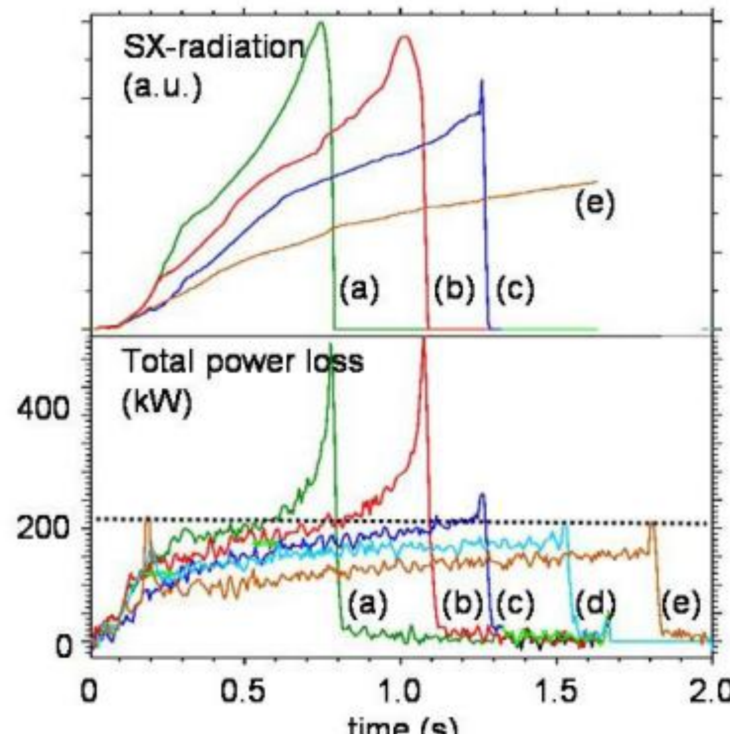

$0.4P$

a) $1.25 \cdot 10^{19}\,\mathrm{m}^{-3}$

e) $0.87 \cdot 10^{19}\,\mathrm{m}^{-3}$

Impurity accumulation

- **impurity transport:**

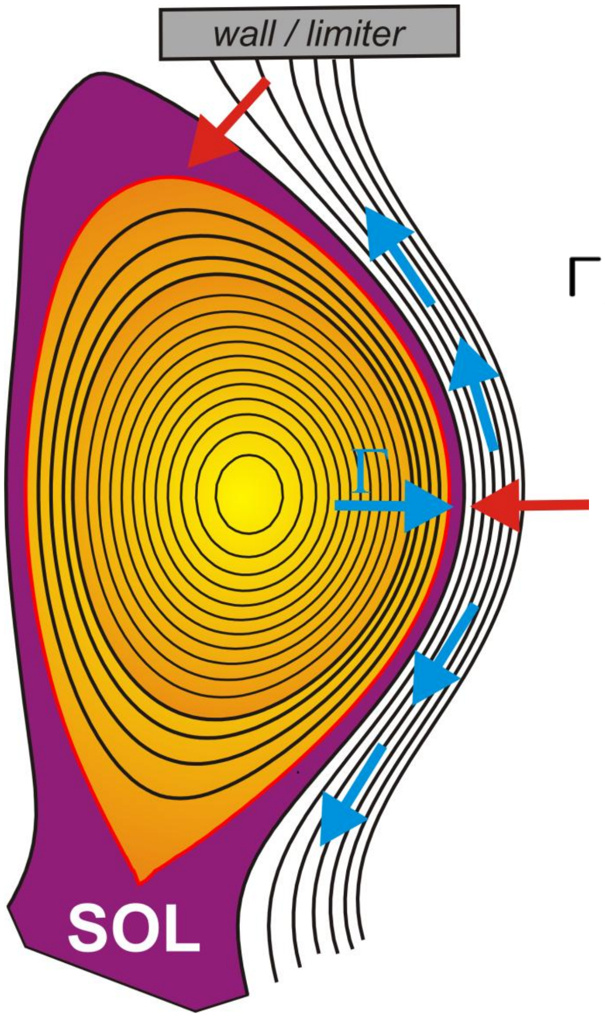

- **neoclassic impurity transport for ion root:**

$$\Gamma_z = -n_z D_{11}^{z} \left[\frac{\nabla n_z}{n_z} - Z \left(\frac{\nabla n_i}{n_i} + \underbrace{\frac{D_{12}^{i}}{D_{11}^{i}}}_{\alpha} \frac{\nabla T_i}{T_i} \right) \right]$$

tokamak: $\alpha < 0$ **(temperature screening)**

stellarator: $\alpha > 0$ **(accumulation)**

High confinement regimes (HDH-mode)

• W7-AS: quasi-steady state High Density H-mode operation with no measurable impurity accumulation

• LHD: superdense core plasmas with internal diffusion barrier (pellet injection)

impurity confinement

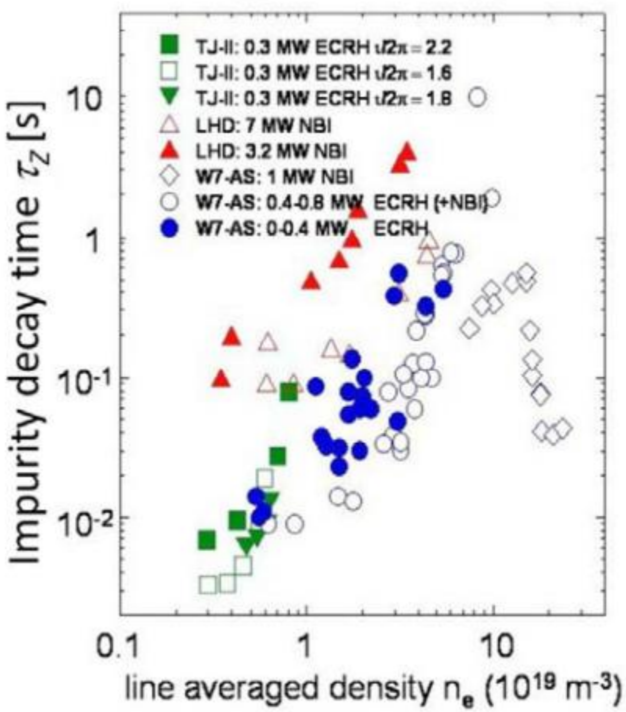

W7-AS

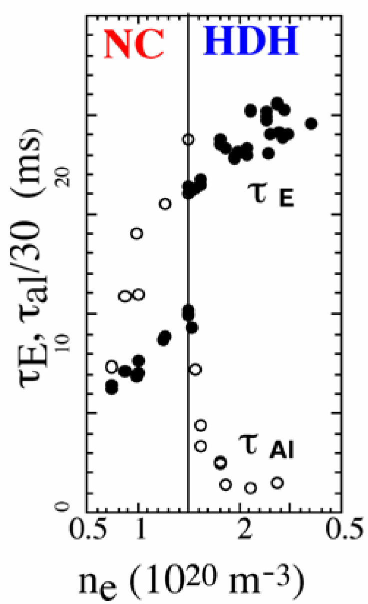

LHD (n_0=4.2·10^{20} m^{-3})

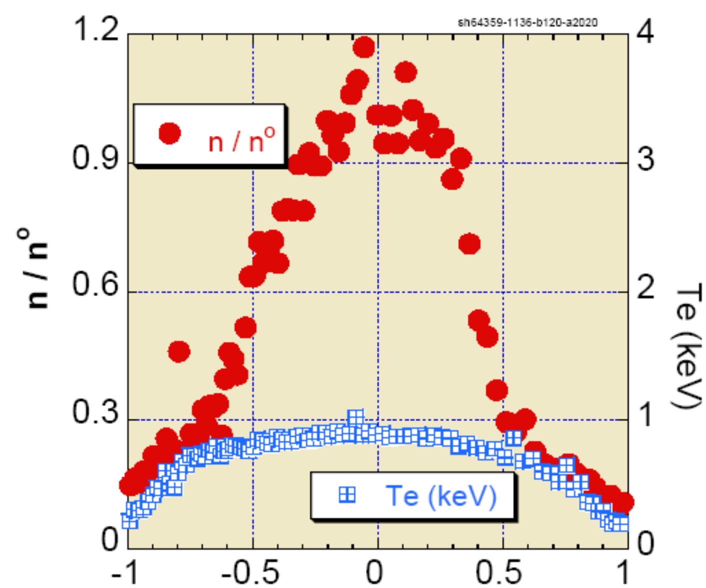

Ohyabu et al. EPS 2006

• tokamak: such high densities not accessible (Greenwald limit)

Divertor configurations

- Spitzer (1951): keep plasma surface interactions away from confined region

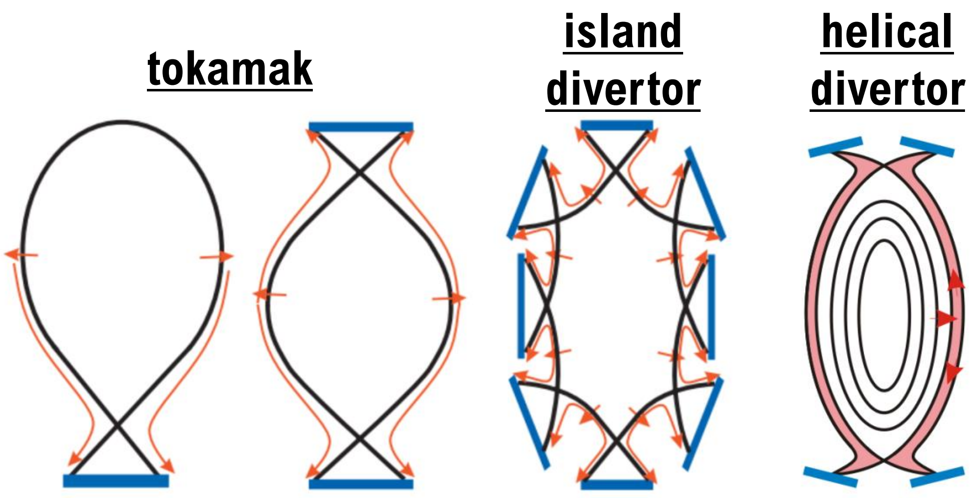

W7-AS island divertor

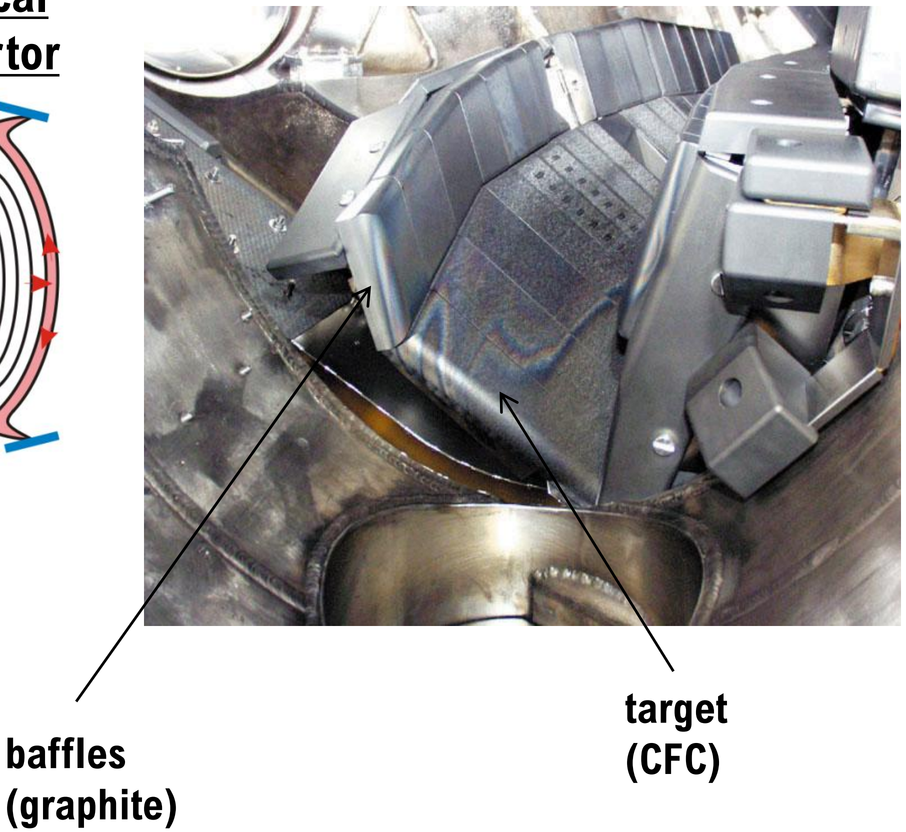

W7-X island divertor

W7-X standard configuration ι=1 (5/5 island)

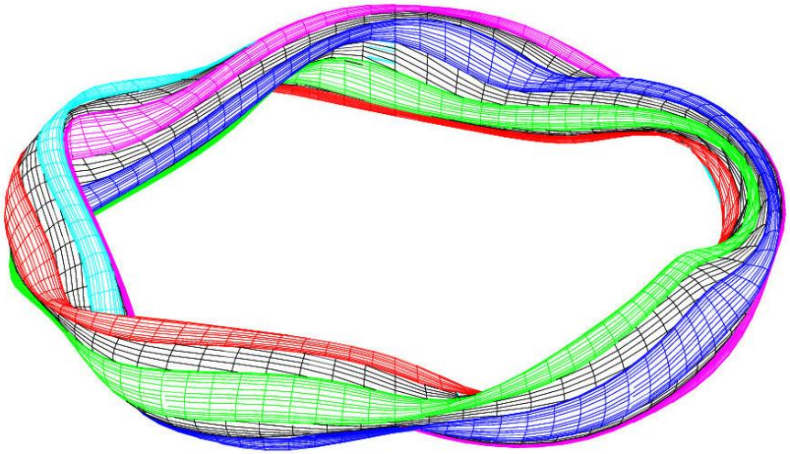

10 discrete divertor modules

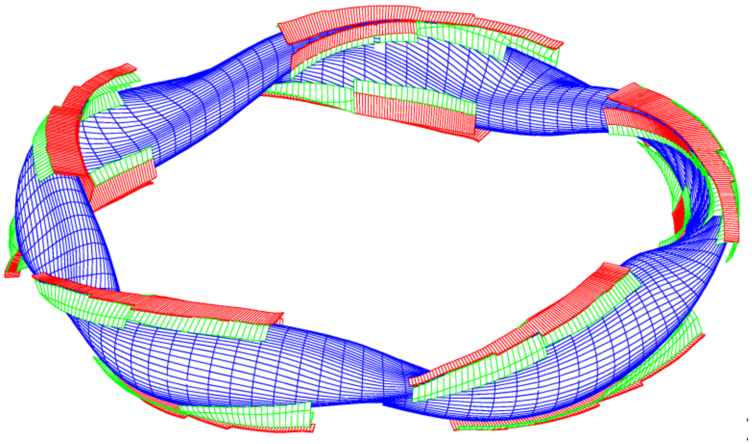

- **island divertor has much larger connection lengths**

$\rightarrow$ **perpendicular transport becomes important**

$\tau_{||} = L/c_s \qquad \tau_{\perp} = 2r_i^2/D$

	L [m]	Θ
AUG	30	0.1
W7-X	300	0.001

field line pitch inside island: $\Theta = \Delta x/L$

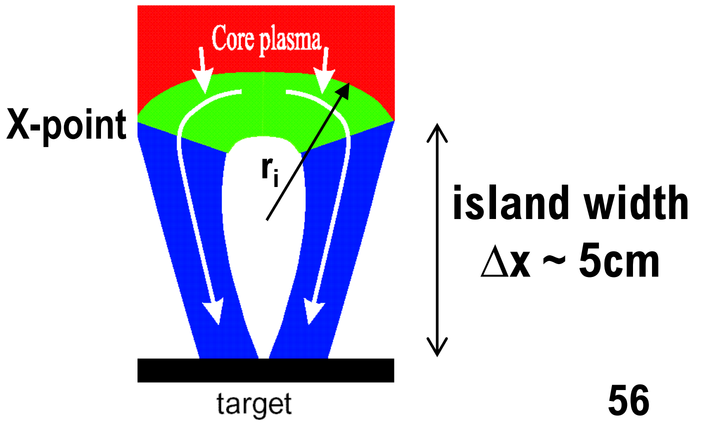

W7-X island divertor

W7-X standard configuration ι=1 (5/5 island)

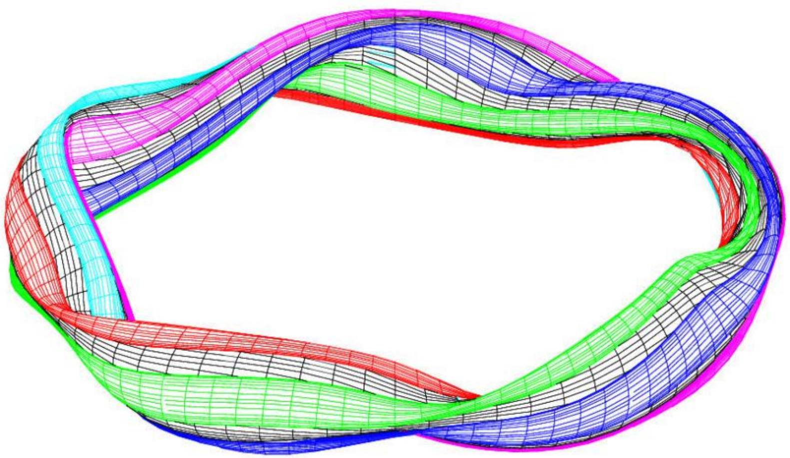

10 discrete divertor modules

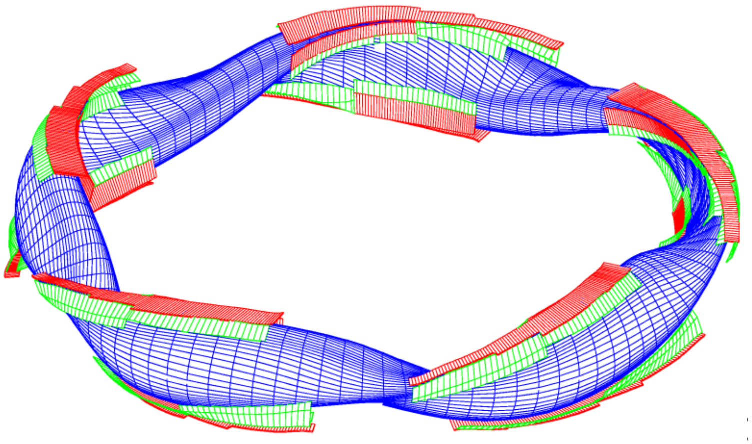

- **island divertor has much larger connection lengths**

$\rightarrow$ **perpendicular transport becomes important**

- **islands effect on impurity reduction:**
  - **screening the neutrals (ionization due to high density in islands)**
  - **transport across islands smoothes $\nabla_{||} T_i$ that drives impurities into SOL: ion-neutral friction becomes dominant in momentum balance**

W7-X island divertor (ι=5/6 - 5/4)

possible field configurations

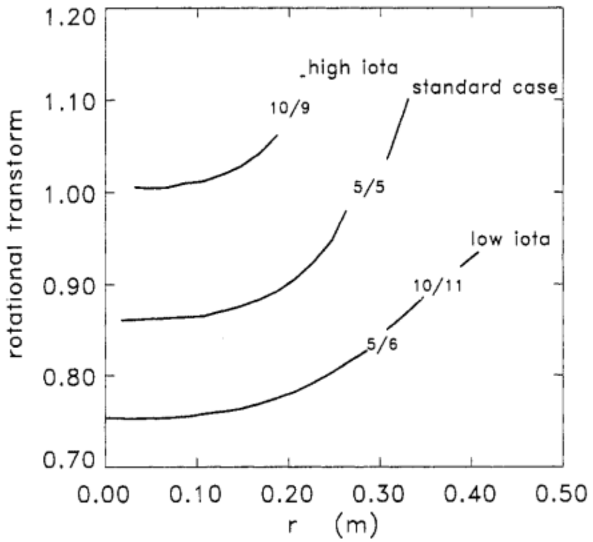

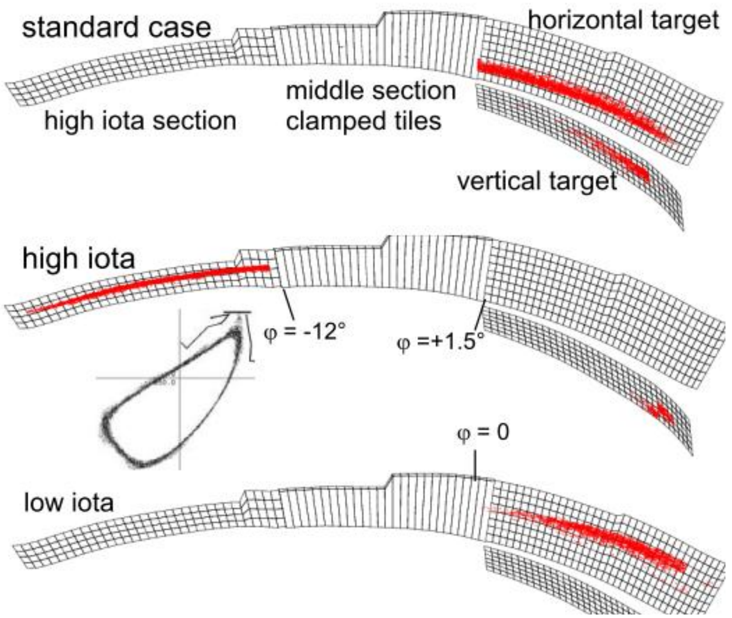

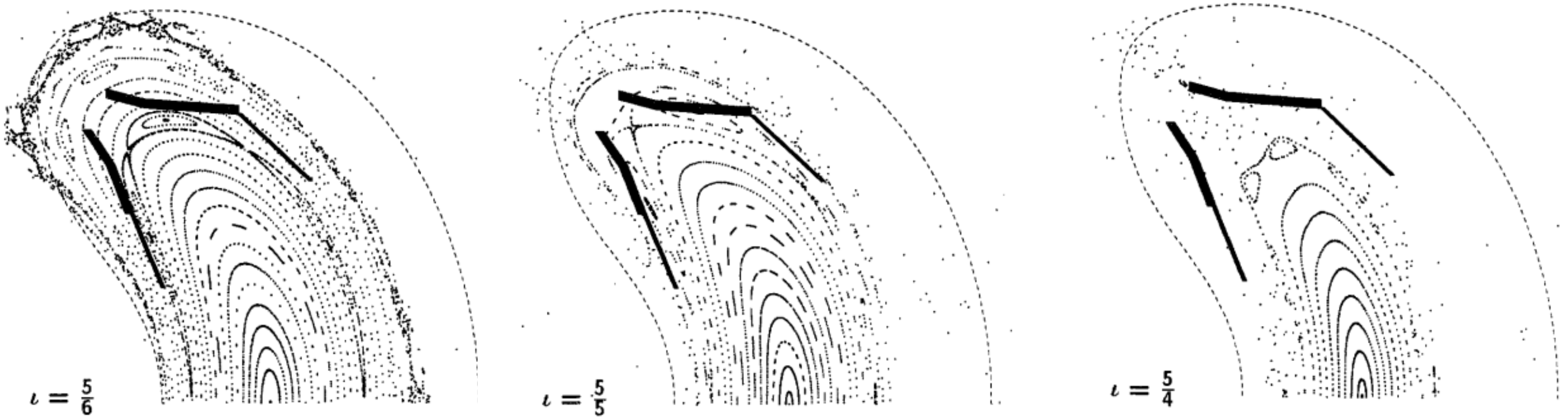

Strumberger, Nucl. Fusion 36 (1996)

At even higher densities: Detachment

• 80-90 % of power in the SOL radiated: reduced fluxes to divertor

• favourable regime for fusion reactor

W7-AS radiation layer

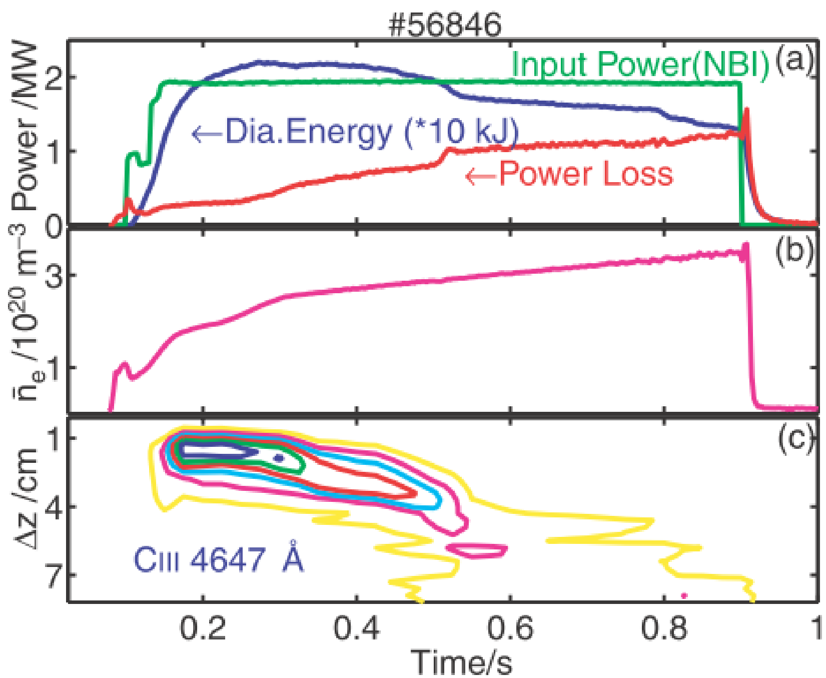

Ramasubramanian, Nucl. Fusion 44 (2004)

W7-AS divertor heat load

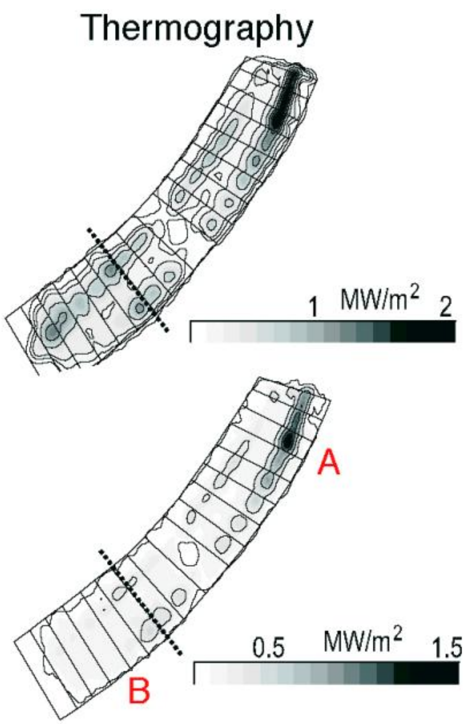

Brakel, 19th IAEA conference (2002)

• no stable detachment regime achieved in W7-AS

summary of optimization criteria

- good magnetic surfaces of vacuum magnetic field
- stiff equilibrium (low Shafranov shift) and MHD stability up to $<\beta>=5\%$
- small neoclassical losses
- small bootstrap current
- good confinement of fast ions
- good technical feasability

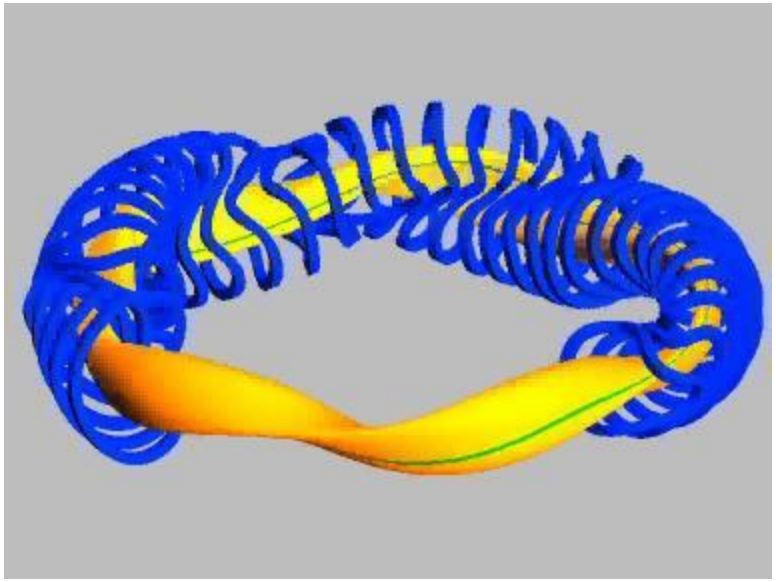

goals

- verify the stellarator optimization
- develop an integrated high-density scenario as baseline for high-power steady-state operation in the 2nd operation phase

  (configuration control, heating, acceptable low impurity confinement, divertor compatible edge conditions)

W7-X (Status 2013)

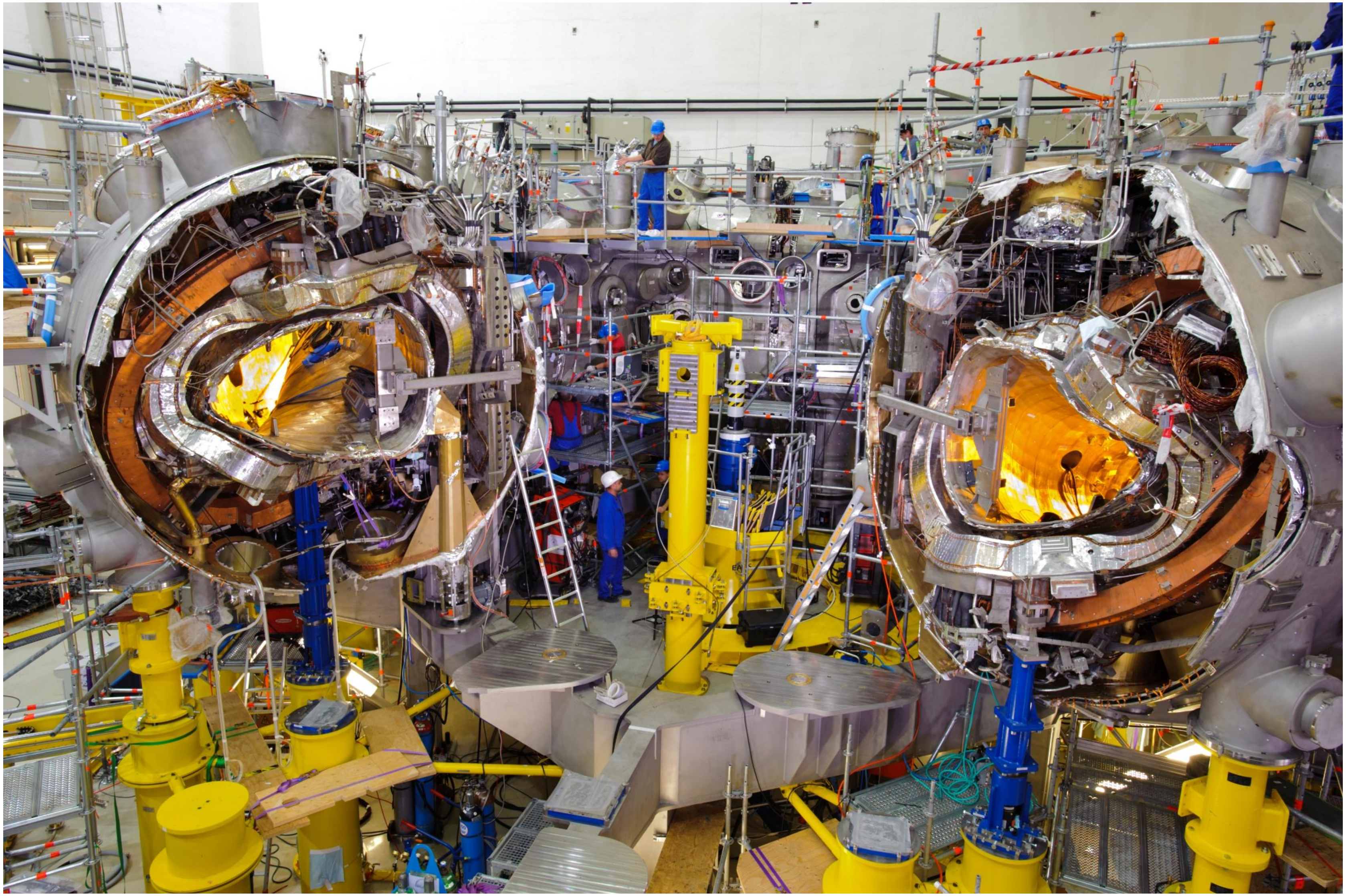

W7-X (Status June 2014)

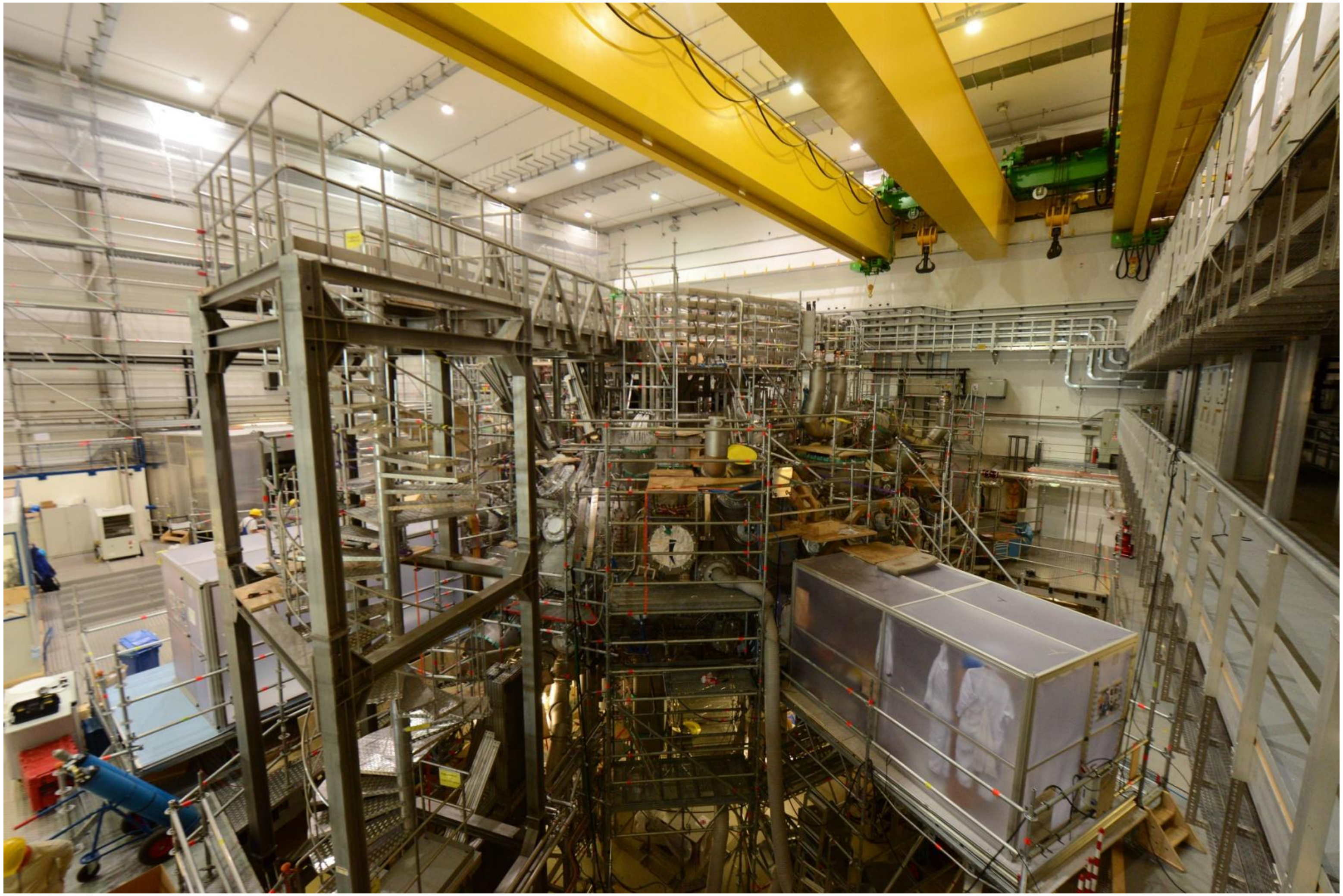

W7-X operation: schedule

A. Lorenz

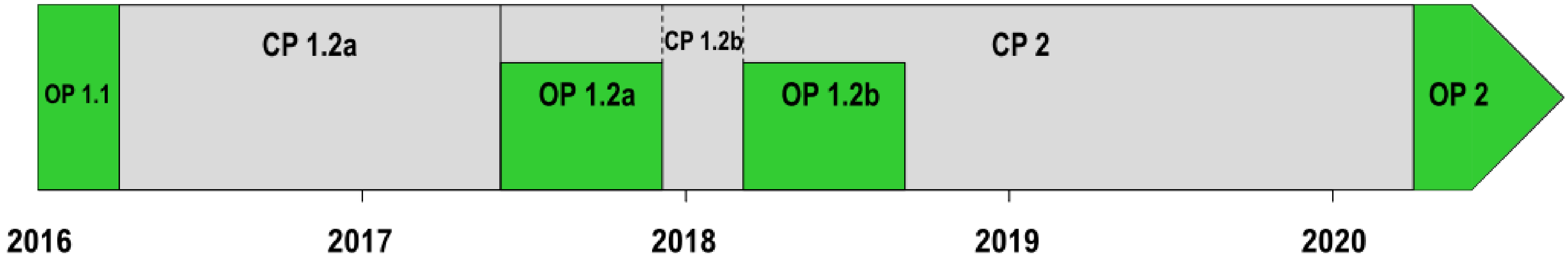

- **comissioning phase OP1.1:** **vacuum, cool-down, magnetic field, flux surface measurements**
- **operation phases**

OP1.1	**limiter plasmas (2 (4) MJ (0.4 s @ 5 MW), uncooled first wall)**
OP1.2	**inertially cooled test divertor, water cooled first wall, 10s @ 8MW**
OP2	**water cooled divertor (1800s @ 10MW)**

W7-X operation: flux surface measurements

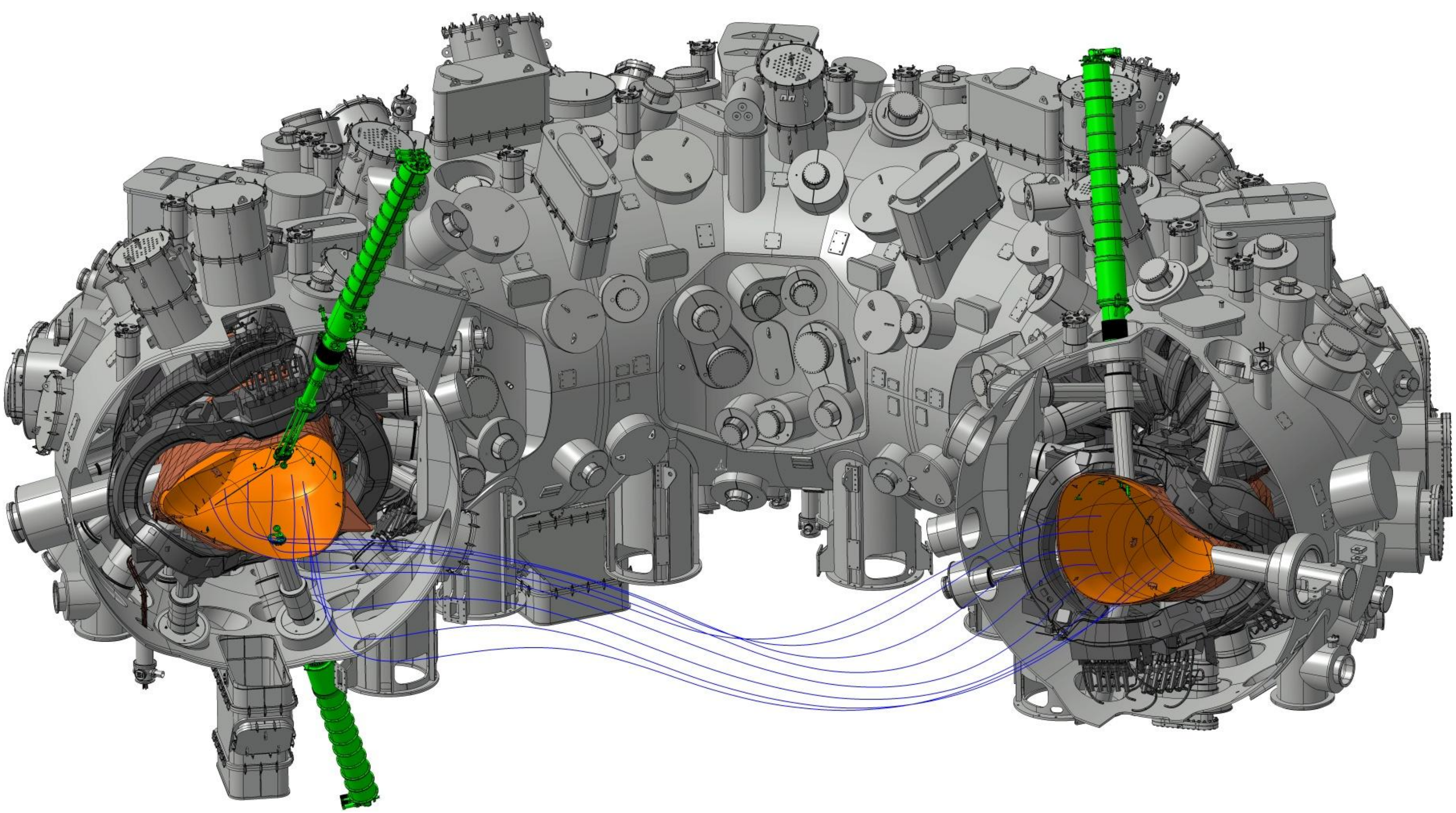

W7-X operation: first results

flux surface measurements

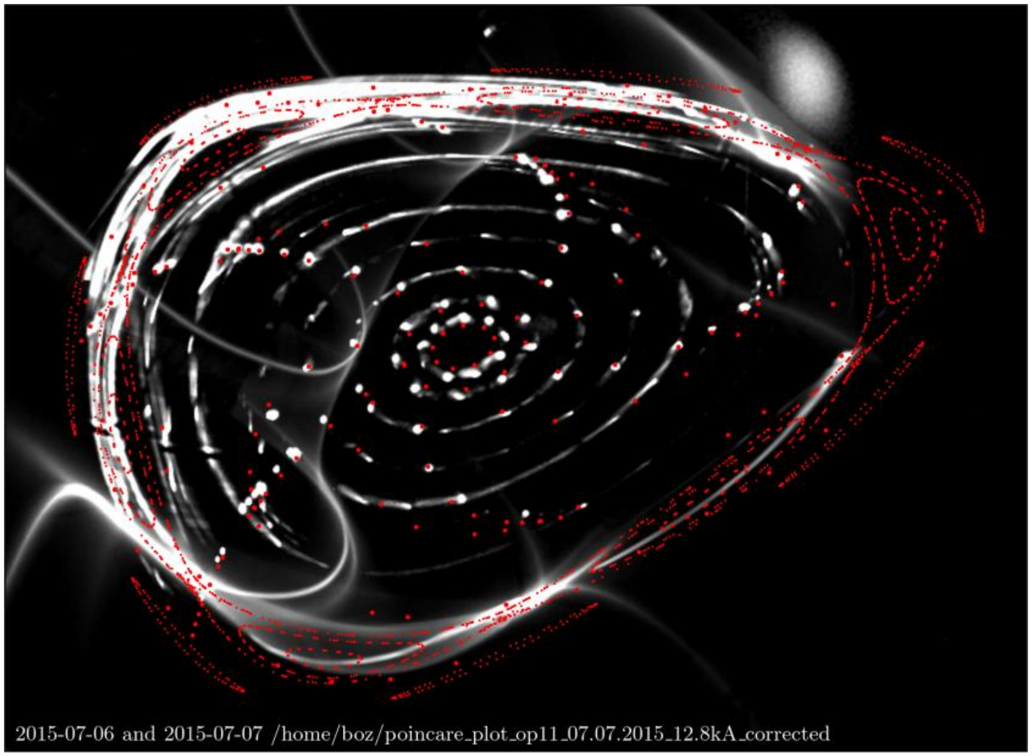

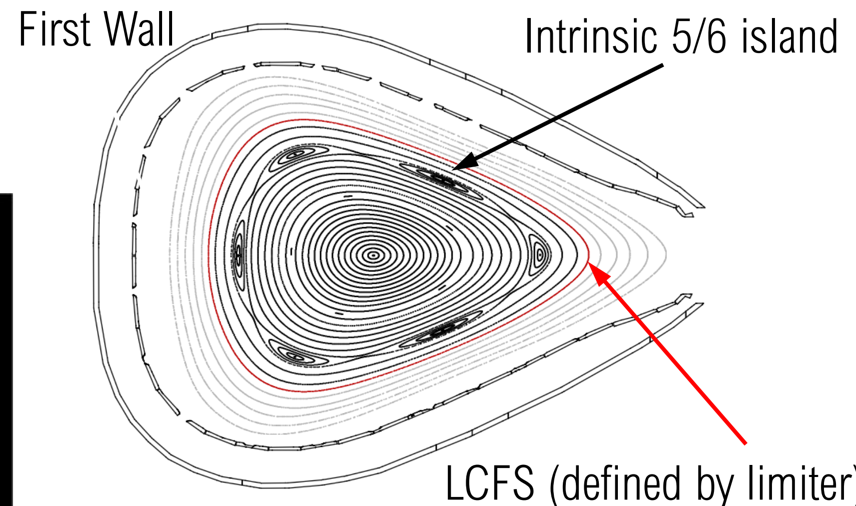

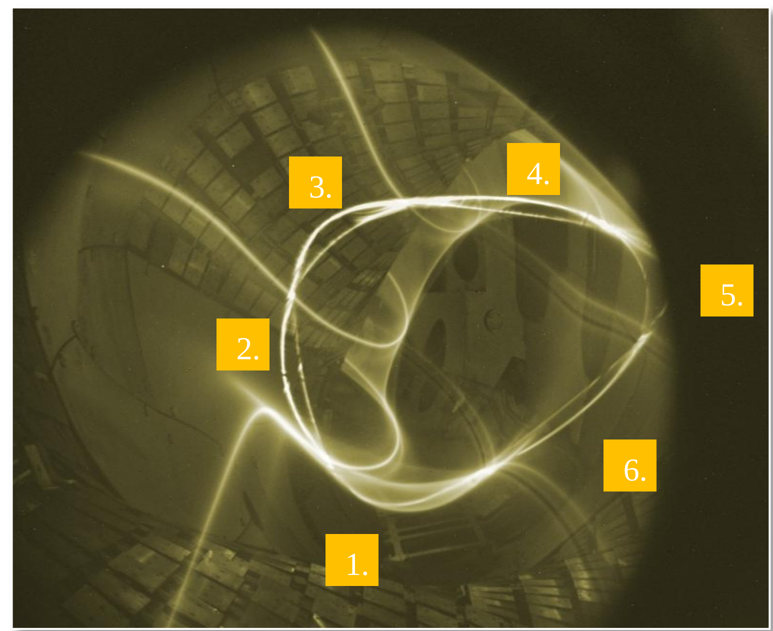

W7-X operation: error field compensation

- W7-X edge ι=1 in resonance with B_{11}, B_{22}, B_{33} , … components

with manufacturing and positioning errors (av. 2.5 mm, $B_{11}/B_0 = 2.7 \cdot 10^{-4}$)

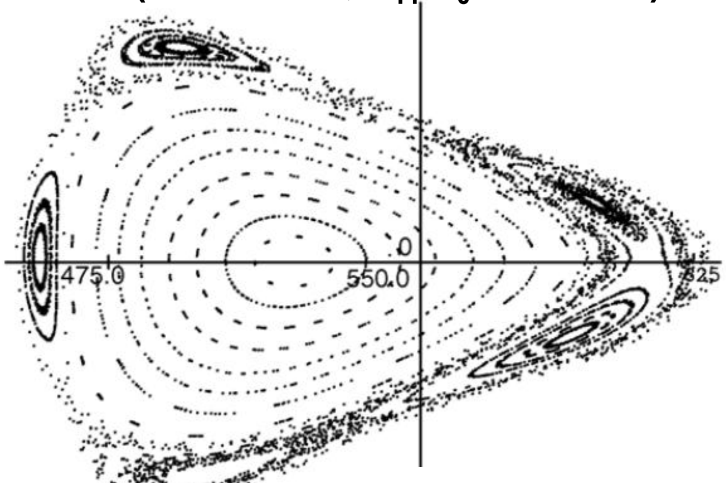

FEM calculation of displacement due to loading of support structure

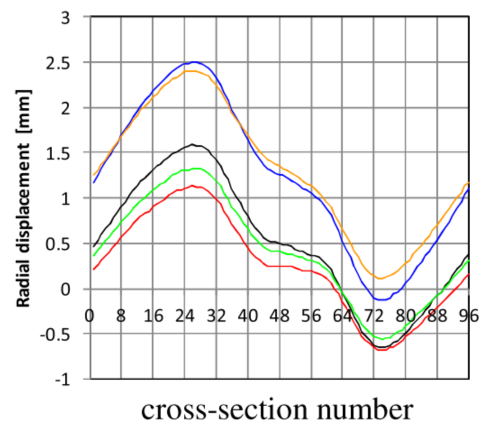

Reference case	$B_{11}/B_0/10^{-4}$
Standard case	1.20
Low shear case	1.19
Inward shifted case	1.19
Outward shifted case	1.21
Low mirror case	1.22
High mirror case	1.18
Limiter case	1.21
Low iota case	1.24
High iota case	1.16

corrected positioning

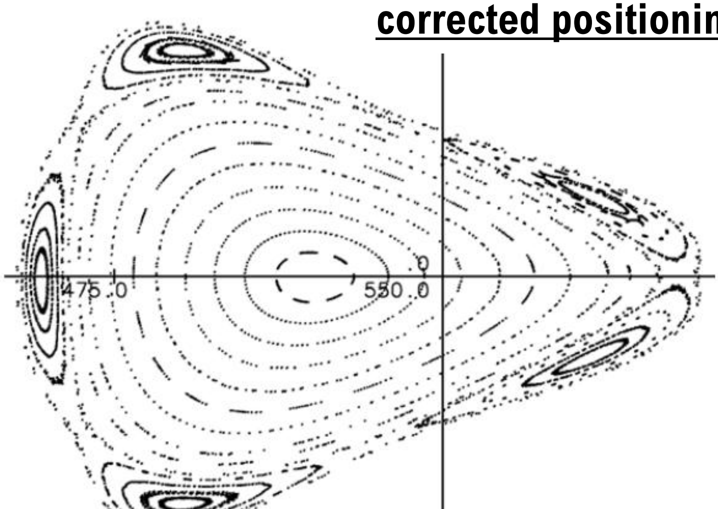

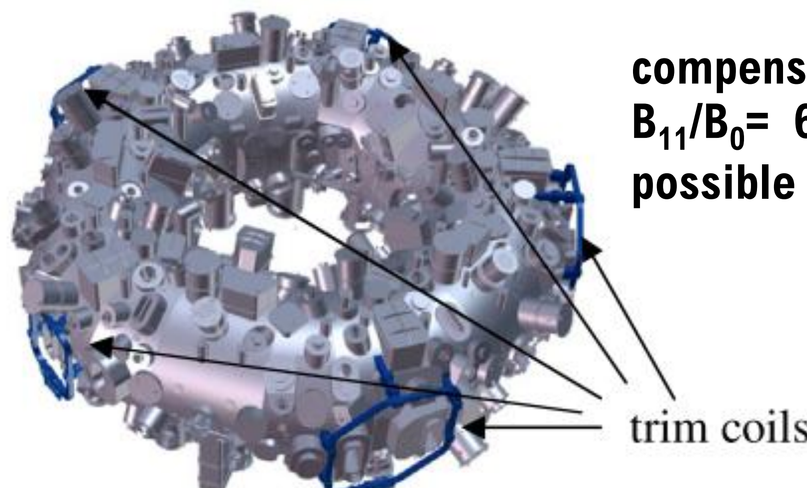

compensation up to $B_{11}/B_0 = 6 \cdot 10^{-4}$ possible

J. Kißlinger, T. Andreeva FED 74 (2005)

W7-X error fields: divertor operation

- small error fields strongly affect the divertor operation
- no common LCFS for all five islands -> asymmetric divertor load (e.g. only 2 out of 5 loaded)

<u>w/ error fields</u>

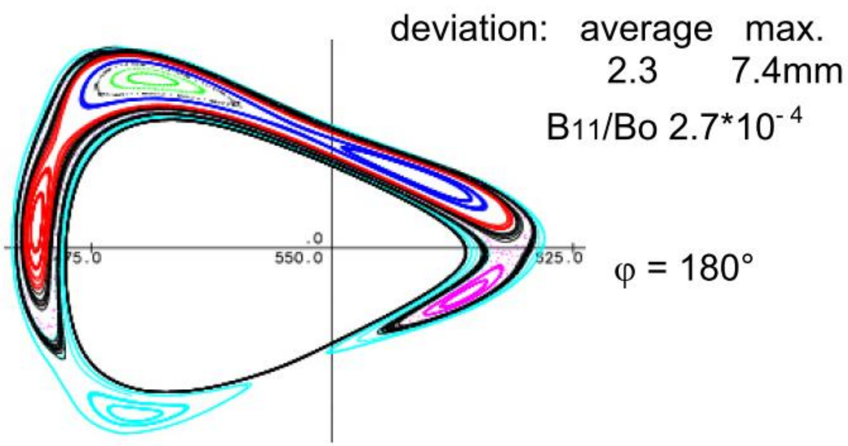

<u>w/o error fields</u>

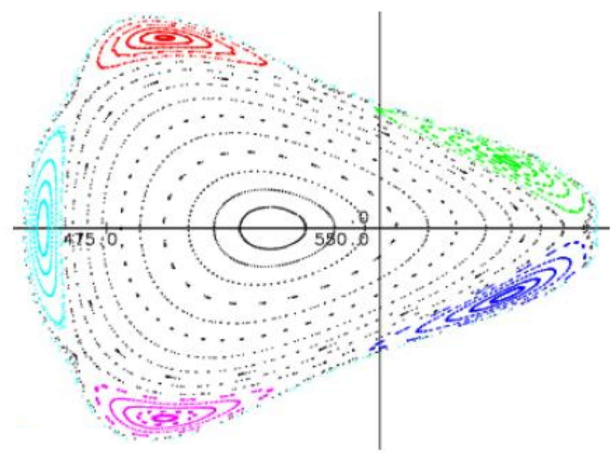

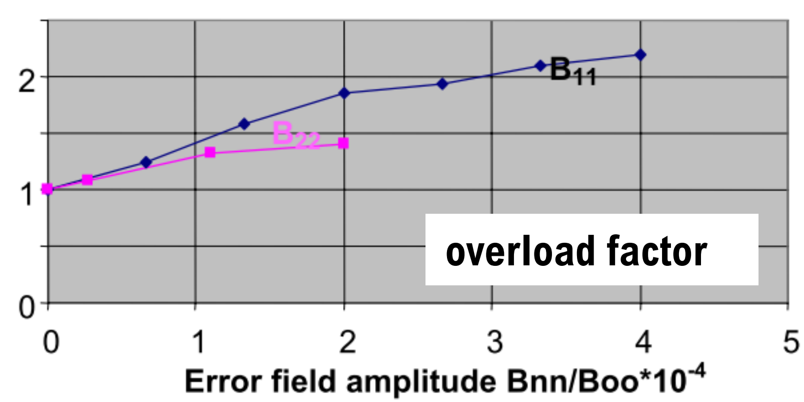

Helical reactor: open and solved issues

- vacuum magnetic field: good nested flux surfaces, small islands in the core (W7-X)
- good divertor edge structure (acceptable heatload, radiating edge) (which divertor ?)
- good plasma equilibrium even at high pressure (W7-X)
- good MHD stability properties even at high pressure (W7-X)
- reduced drift losses of fast alpha / heating paticles (W7-X)
- reduced drifts of thermal particles "neoclassical transport" mandatory !! (W7-X)
- low level of turbulent transport -> turbulence and flows at plasma edge !
- impurity accumulation (radiation prop. Z^2)

- sufficient space between plasma and coil for breeding blanket and bio-shield-> same as tokamak (1-1.3 m)
- tolerable mechanical forces and feasible coil system -> engineering

Helical reactor: studies

HELIAS-5B

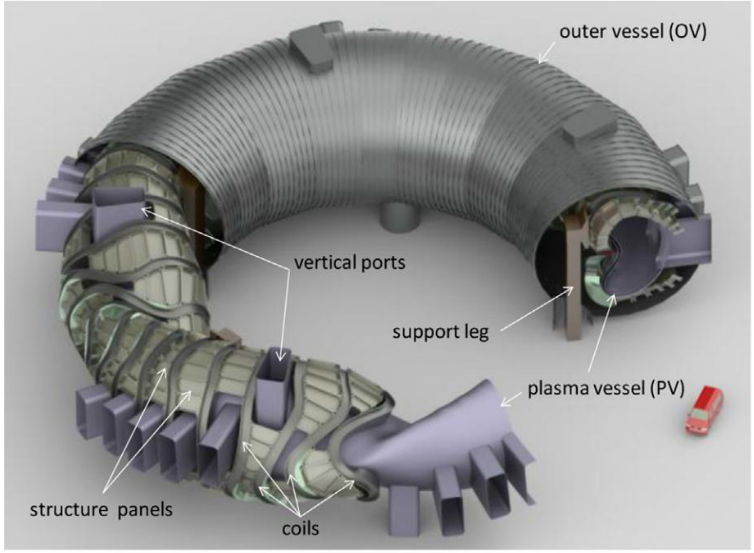

Schauer, Fusion Engineering Design 88 (2013)

FFHR-1

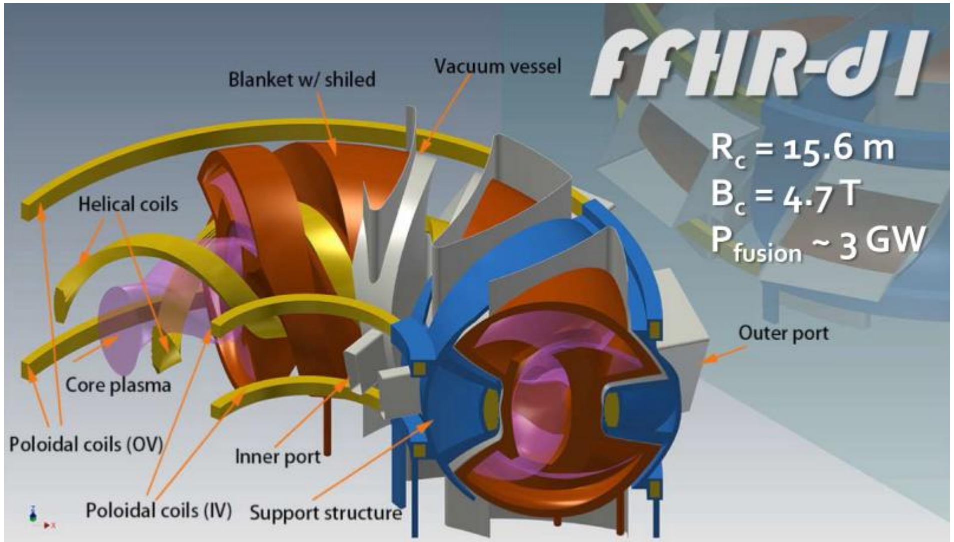

Sagara, Fusion Engineering Design 89 (2014)

	W7-X	HELIAS-5B	FFHR-d1	ITER
major radius [m]	5.5	22	15.6	6.2
av. minor radius [m]	0.53	1.8	2.54	2
plasma volume [m^3]	30	1407	1878	837
B0 [T]	2.5	5.0	4.7	5.3
density [10^{20} m^{-3}]	3	2.1	2	1
β [%]	5	4.2	5	3
Fusion power [GW]	0	3	3	0.5

Helical reactor: Helias operation scenarios

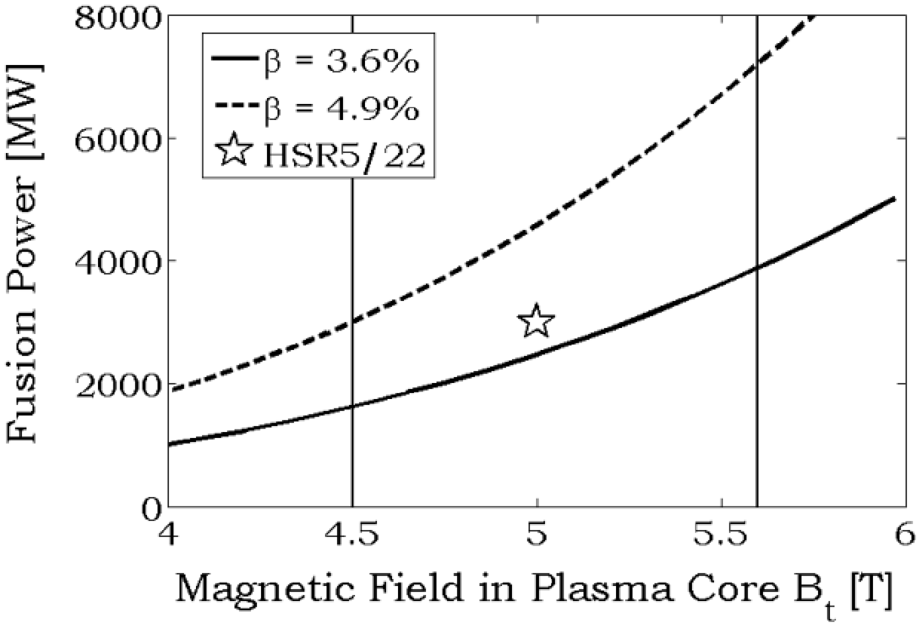

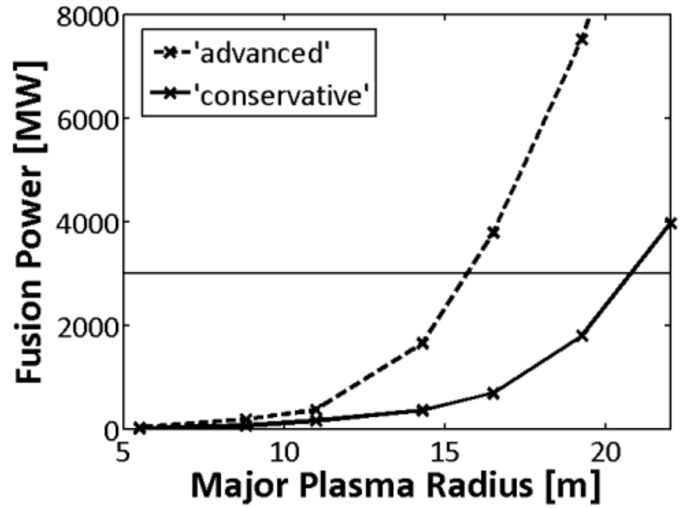

scenario	SC	B_0 [T]	n [10^{20} m^{-3}]
conservative	NbTi	4.5	1.8
advanced	Nb_3Sn	5.5	2.4

Helical reactor: support structure

approaching the Virial limit

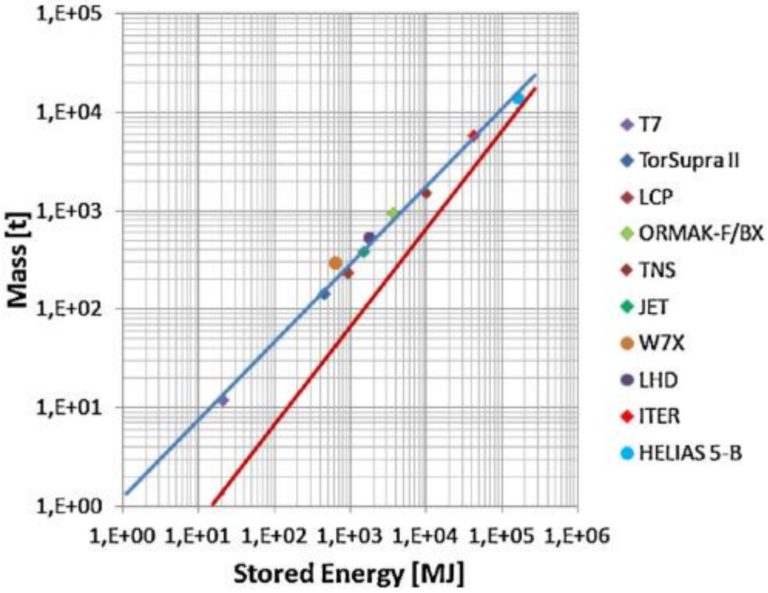

stress distribution [MPa]

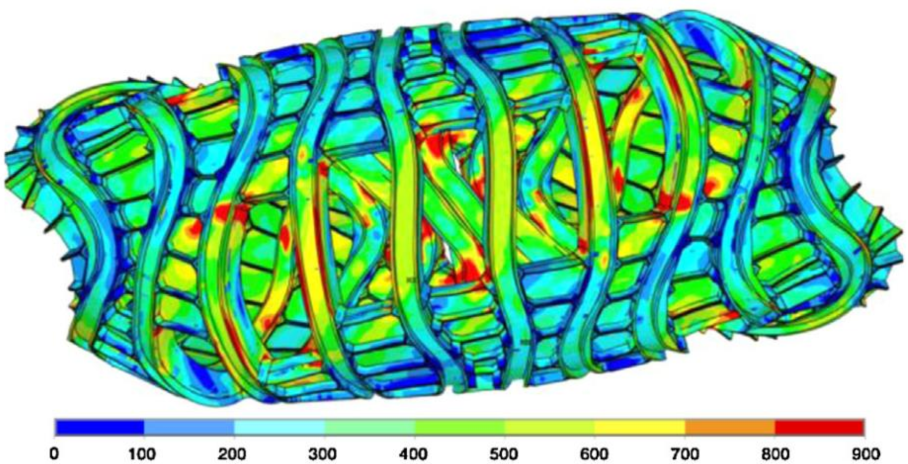

F. Warmer, F. Schauer, FED (2014)

Helical reactor: fast ion confinement

- **normalized fast ion gyro-radius:** $\frac{\rho}{a} \sim \frac{(mE)^{1/2}}{ZBa}$
- **W7-X NBI protons at 60 keV @ 2.5 T same ρ/a as 3.5 MeV α-particles in larger device**
- **NBI: broad radial deposition profile with non-uniform pitch angle distribution**

standard configuration

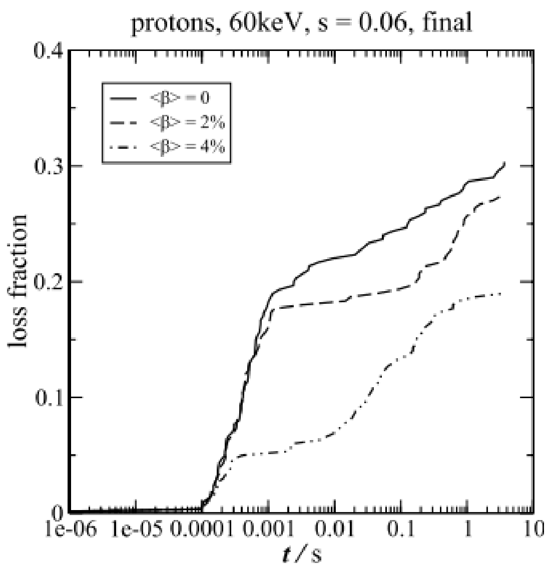

opt. configuration a

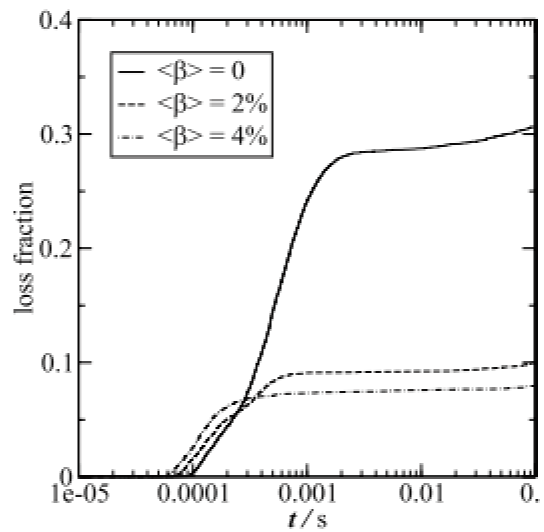

opt. configuration b

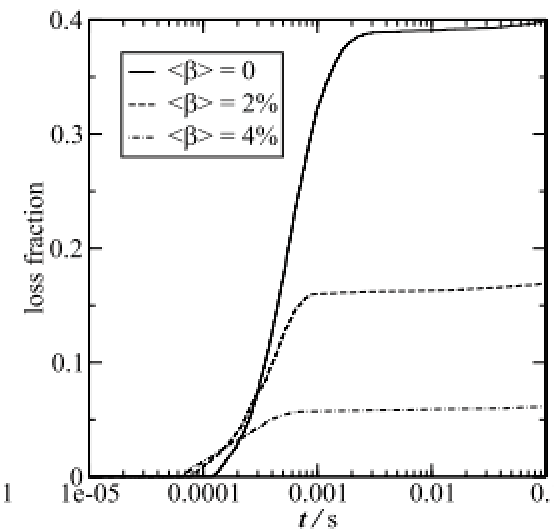

typical slowing down time: 0.1 s

M. Drevlak, Nucl. Fusion 54 (2014)

Summary

• renaissance of stellarator as possible reactor concept due to optimization

• in many subtle aspects different from tokamaks :

- three-dimensional coils (assembly, accuracy, forces)
- ambipolar electric field (electron and ion root)
- particle transport (pinches)
- impurity transport (accumulation)
- operation limits (MHD instabilities, pressure limit, radiation limit)
- heat and particle exhaust (island divertor)

• most of reactor relevant issues will be adressed in W7-X